

**The expression of polyspecific transporters in  
renal tumors and their role in  
chemotherapeutical treatment**

Dissertation

zur Erlangung des Doktorgrades

der Mathematisch-Naturwissenschaftlichen Fakultät

der Georg-August-Universität zu Göttingen

vorgelegt von

Volodymyr Shnitsar

aus Mostyska, Ukraine

Göttingen 2008

D7

Referent:

Dr. W. Kramer

Korreferent:

Prof. Dr. Sigrid Hoyer-Fender

Tag der mündlichen Prüfung:

16 Mai 2008

# CONTENT

<b>CONTENT .....</b>	<b>1</b>
<b>ABBREVIATION .....</b>	<b>5</b>
<b>ABSTRACT .....</b>	<b>7</b>
<b>ZUSAMMENFASSUNG .....</b>	<b>8</b>
<b>1. INTRODUCTION .....</b>	<b>9</b>
<b>1.1 Renal carcinoma cells.....</b>	<b>9</b>
<b>1.2 Transporter characterization.....</b>	<b>11</b>
1.2.1 <i>The SLC transporter superfamily.....</i>	11
1.2.1.1 <i>The amino acid transporter family SLC7 .....</i>	11
1.2.1.2 <i>The sodium dicarboxylate transporter family SLC13.....</i>	13
1.2.1.3 <i>The monocarboxylate transporter family SLC16 .....</i>	14
1.2.1.4 <i>The folate/thiamine transporter family SLC19 .....</i>	15
1.2.1.5 <i>The organic anion and peptide transporter family SLC21.....</i>	15
1.2.1.5.1 <i>OATP1 subfamily.....</i>	16
1.2.1.5.2 <i>OATP2 subfamily.....</i>	18
1.2.1.5.3 <i>OATP3 subfamily.....</i>	18
1.2.1.5.4 <i>OATP4 subfamily.....</i>	19
1.2.1.5.5 <i>OATP5 subfamily.....</i>	19
1.2.1.5.6 <i>OATP6 subfamily.....</i>	20
1.2.1.6 <i>The organic anion, cation, zwitterion family SLC22.....</i>	20
1.2.1.6.1 <i>The organic cation transporters.....</i>	21
1.2.1.6.1.1 <i>The organic cation transporter 1 (OCT1).....</i>	21
1.2.1.6.1.2 <i>The organic cation transporter 2 (OCT2).....</i>	21
1.2.1.6.1.3 <i>The organic cation transporter 3 (OCT3).....</i>	22
1.2.1.6.2 <i>The organic anion transporters.....</i>	23
1.2.1.6.2.1 <i>The organic anion transporter 1 (OAT1).....</i>	23
1.2.1.6.2.2 <i>The organic anion transporter 2 (OAT2).....</i>	23
1.2.1.6.2.3 <i>The organic anion transporter 3 (OAT3).....</i>	24
1.2.1.6.2.4 <i>The organic anion transporter 4 (OAT4).....</i>	24
1.2.1.7 <i>The concentrative nucleoside transporters family SLC28.....</i>	25
1.2.1.7.1 <i>The concentrative nucleoside transporter 1 (CNT1).....</i>	25
1.2.1.7.2 <i>The concentrative nucleoside transporter 2 (CNT2).....</i>	25
1.2.1.7.3 <i>The concentrative nucleoside transporter 3 (CNT3).....</i>	26

1.2.1.8 The equilibrative nucleoside transporter family SLC29.....	26
1.2.1.8.1 The equilibrative nucleoside transporter 1 (ENT1) .....	27
1.2.1.8.2 Equilibrative nucleoside transporter 2 (ENT2) .....	27
1.2.1.8.3 Equilibrative nucleoside transporter 3 (ENT3) .....	28
1.2.2 The ABC transporter superfamily .....	28
<b>1.3 Antitumor drug characteristics .....</b>	<b>29</b>
1.3.1 Cytostatics acting on DNA.....	30
1.3.1.1 Mustard analogs.....	30
1.3.1.2 Alkyl sulfonates.....	31
1.3.1.3 Platinum compounds .....	32
1.3.1.4 Cytostatic producing free radical .....	34
1.3.1.5 Antimetabolites .....	34
1.3.1.5.1 Folate analogs .....	35
1.3.1.5.2 Antimetabolite nucleoside analogs .....	36
1.3.1.6 Topoisomerase inhibitors .....	38
1.3.1.7 Antracycline cytostatics .....	39
1.3.2 Cytostatics disturbing the mitotic spindle.....	41
1.3.3 Substances acting on the estrogen receptor .....	42
<b>1.4 Aims.....</b>	<b>43</b>

## **2. MATERIALS AND METHODS..... 44**

<b>2.1. Materials.....</b>	<b>44</b>
2.1.1. Primers .....	44
2.1.2. Chemicals.....	49
2.1.3. Enzyme .....	49
2.1.4. Bacterial strains.....	50
2.1.5. Plasmid vector.....	50
2.1.6. Used kits.....	52
2.1.7 Software .....	52
2.1.8 Equipment.....	53
<b>2.2. Methods.....</b>	<b>55</b>
2.2.1. Renal cancer cell (RCC) lines.....	55
2.2.2. Cell culture .....	56
2.2.3. RNA preparation.....	57
2.2.4. cDNA synthesis .....	57
2.2.5. Polymerase chain reaction .....	58
2.2.6. Agarose gel electrophoresis .....	59
2.2.7. TA cloning .....	59
2.2.8. Bacterial plasmid DNA preparation.....	61
2.2.9. Plasmid DNA restriction.....	61
2.2.10. cRNA synthesis .....	61
2.2.11. DNA sequencing.....	62

2.2.12. Real-time PCR.....	63
2.2.13. Radioactive transport studies in CHO cell stably transfected with hOCT3 .....	64
2.2.14. [ <sup>3</sup> H]thymidine incorporation assay .....	64
2.2.15. BrdU incorporation method (ELISA) .....	65
2.2.16. MTT assay.....	66
2.2.17. Comet assay.....	67
2.2.18. Intracellular ATP concentration measurement.....	67
2.2.19. Expression of hOCT3 in <i>Xenopus laevis</i> oocytes .....	68
2.2.20. Preparation of <i>Xenopus laevis</i> oocytes .....	68
2.2.21. Oocyte injection.....	69
2.2.22. Oocyte uptake experiments.....	69
2.2.23. Two-electrode-voltage-clamp measurement in <i>Xenopus laevis</i> oocytes .....	70

### **3. RESULTS..... 72**

#### **3.1 RT-PCR analysis of transporter expression in kidney cancer-derived cell lines and tissue samples ..... 72**

3.1.1 The expression of organic anion and cation transporters (OATs and OCTs).....	74
3.1.1.1 OAT.....	74
3.1.1.2 OCT.....	74
3.1.2 The expression of organic anion-transporting polypeptide transporters (OATP).....	76
3.1.3 The expression of sodium-coupled nucleoside transporters and equilibrative nucleoside transporters (CNT and ENT) .....	77
3.1.4 The expression of L-amino acid transporters (LAT).....	78
3.1.5 The expression of monocarboxylate transporters (MCT).....	79
3.1.7 The expression of reduced folate and thiamine transporters.....	81
3.1.8 The expression of the ATP-binding cassette (ABC) transporter family....	82

#### **3.2 Quantification of the transporter expression levels in kidney tumor cells by real time PCR ..... 83**

3.2.1 The expression of the organic anion transporter 1 (OAT1).....	83
3.2.2 The expression of organic anion transporter 3 (OAT3).....	84
3.2.3 The expression of organic cation transporter 3 .....	86
3.2.4 The expression of equilibrative nucleoside transporters 1,2 and 3.....	87

#### **3.3 [<sup>3</sup>H]MPP uptake investigation in CHO-hOCT3 and RCC lines..... 89**

3.3.1 Inhibition of [ <sup>3</sup> H]MPP uptake by cationic substances.....	89
3.3.2 Inhibition of [ <sup>3</sup> H]MPP uptake by cytostatic substances .....	91
3.3.3 Dixon plot analysis for irinotecan, vincristine, and melphalan.....	92
3.3.4 [ <sup>3</sup> H]MPP uptake into <i>Xenopus laevis</i> oocytes injected with hOCT3 cRNA .....	94

<b>3.4. Inhibition of [<sup>3</sup>H]gemcitabine uptake by nucleoside analogs.....</b>	<b>95</b>
<b>3.5 Cytostatic sensitivity investigation.....</b>	<b>96</b>
3.4.1 <i>Evaluation of the cytotoxic activity of bendamustine and chlorambucil by the [<sup>3</sup>H]thymidine incorporation assay .....</i>	96
3.4.2 <i>Evaluation of the cytostatic activity of melphalan by [<sup>3</sup>H]thymidine incorporation assay. ....</i>	98
3.4.3 <i>Evaluation of cytostatic activity irinotecan and vincristine by the MTT assay.....</i>	102
3.4.4 <i>Evaluation of the cytostatic activity of gemcitabine by MTT assay. ....</i>	108
<b>4. DISCUSSION .....</b>	<b>110</b>
<b>4.1 Expression of uptake transporters of the SLC family in kidney tumour cells .....</b>	<b>110</b>
<b>4.2 Real-time PCR reinvestigation of SLC22 transporters in renal carcinoma cells .....</b>	<b>115</b>
<b>4.3 Investigation of OCT3 activity in renal carcinoma cell lines .....</b>	<b>116</b>
<b>4.4 Investigation the interaction of cytostatics with OCT3 .....</b>	<b>117</b>
<b>4.5 Investigation on the activity of ENTs in renal carcinoma cell lines ...</b>	<b>118</b>
<b>4.6 Transporter-mediated inhibition of thymidine incorporation by chlorambucil, bendamustin and melphalan.....</b>	<b>119</b>
<b>4.7 Transporter mediated-cytotoxic activity of irinotecan .....</b>	<b>121</b>
<b>4.8 Transporter mediated cytotoxic activity of vincristine .....</b>	<b>122</b>
<b>4.9 Conclusions and outlook.....</b>	<b>123</b>
<b>5. REFERENCES .....</b>	<b>125</b>
<b>ADDITION 1 .....</b>	<b>139</b>
<b>ACKNOWLEDGMENTS .....</b>	<b>142</b>
<b>LEBENS LAUF .....</b>	<b>143</b>

## Abbreviation

ATP	adenosine triphosphate
BSA	bovine serum albumin
BSP	bromosulfophthalein
°C	degrees Celsius
cDNA	complementary DNA
DHEA-S	dehydroepiandrosterone sulfate
DMSO	dimethyl sulfoxide
dNTP	deoxyribonucleotide phosphate
Fig.	figure
MPP	4-methyl-pyridinium iodide
h	hour
HEK-293	human embryonic kidney cell line 293
hOAT	human organic anion transporter
IC <sub>50</sub>	half maximal inhibitory concentration
k	kilo
K <sub>m</sub>	Michaelis-Menten constant
LB	Luria Bertani broth
M	molar (moles per liter)
μM	micromolar
ml	milliliter
mRNA	messenger RNA
MRP2	multiple drug resistance-associated protein 2
NBTI	6-[(4-Nitrobenzyl)thio]-9-β-D-ribofuranosylpurine

OAT	organic anion transporter
OCT	organic cation transporter
ORI	oocyte Ringer's solution
PAH	<i>para</i> -aminohippurate
PBS	phosphate-buffered saline
PCR	polymerase chain reaction
pmol	picomol
RNA	ribonucleic acid
RNase	ribonuclease
NaDC-1	sodium/dicarboxylate cotransporter
rpm	revolutions per minute
SEM	standard error of the mean
TAE	tris-acetate-EDTA
TBE	tris-borate-EDTA
TK	tyrosine kinase
TEA	tetraethylammonium
TLC	tauroolithocholate
TLC-S	sulfated tauroolithocholate
Tris	tris-(hydroxymethyl)-aminomethane
U	unit
UTR	untranslated region
UV	ultraviolet
V	volts



## Abstract

Renal cancer cell carcinoma (RCC) is usually chemoresistant. This chemoresistance would be overcome when a cytostatic is applied for which the RCC possesses an uptake transporter. In the present study I investigated the expression of solute carrier (SLC) transporters in different RCC samples and their ability to interact with chemotherapeutic drugs. I tested five RCC cancer lines as well as normal and tumor renal tissue for the expression of different SLC by RT-PCR and TaqMan real-time PCR. In two of five RCC lines, A498 and 786-O, I observed a highly significant expression of SLC22A3 (hOCT3). The uptake of the organic cation [<sup>3</sup>H]MPP (4-methyl-pyridinium iodide) into these cells and also into hOCT3 stably transfected CHO cells was inhibited by irinotecan, vincristine and melphalan. The K<sub>i</sub> values determined from Dixon plots for irinotecan and vincristine were 1.72±0.45 μM, 17±4.81 μM, and 366±51 μM, respectively. The cytotoxic activities of the selected drugs were tested by the [<sup>3</sup>H]thymidine incorporation and MTT assays on CHO-hOCT3, A498 (high expression of hOCT3) and ACHN cell lines (low expression of hOCT3). The growth of CHO-hOCT3 was inhibited by 20% more with irinotecan and by 50% more with vincristine compared to non-transfected CHO cells. Melphalan produced 20-30% more inhibition in hOCT3 expressing cells compared to non-expressing control cells. Similar results were obtained for A498 and ACHN cells. Thus, my data support the hypothesis that the sensitivity of tumor cells to chemotherapeutic treatment depends on the expression of transporter proteins mediating specific drug accumulation into the target cell.

## Zusammenfassung

Nierenzellkarzinome (RCC) sind normalerweise Chemotherapie-resistent. Diese Chemoresistenz kann durch Gabe von Zytostatika überwunden werden, für welches die Karzinomazellen einen Aufnahmetransporter exprimieren.

In der vorliegenden Arbeit wurde sowohl die Expression unterschiedlicher löslichen Carrier Transporter (SLC) in verschiedenen RCC-Proben als auch ihre Fähigkeit, mit verschiedenen Chemotherapeutika zu interagieren, untersucht. Dafür wurden fünf Nierenkarzinoma-Linien, gesundes Gewebe und Nierentumorgewebe mittels RT-PCR und TaqMan *real-time*-PCR analysiert. In zwei der untersuchten Zelllinien, A498 und 786-O, konnte eine signifikant erhöhte Expression von SLC22A3 (hOCT3) detektiert werden. Die Aufnahme des organischen Kations [<sup>3</sup>H]MPP (4-Methylpyrididinium-Iodid) in diese Zellen und in stabil transfizierte hOCT3-exprimierende CHO-Zellen (CHO-hOCT3) wurde durch die Agenzien Irinotekan, Vincristin und Mephalan inhibiert. Die durch Dixon-Plots bestimmten  $K_i$ -Werte für Irinotekan und Vincristin und Mephalan sind  $1,72 \pm 0,45 \mu\text{M}$ ,  $17,0 \pm 4,81 \mu\text{M}$  und  $366,0 \pm 51,0 \mu\text{M}$ . Die zytotoxischen Aktivitäten dieser Drogen wurden durch [<sup>3</sup>H]-Thymidin-Inkorporation und MTT-Assays in CHO-hOCT3, A498 (hohe Expression von hOCT3) und ACHN (niedrige Expression von hOCT3) Zellen überprüft. Das Wachstum der CHO-hOCT3 Zellen wurde im Vergleich zu nicht-transfizierten CHO Zellen durch Irinotekan um 20% und durch Vincristin um 50% inhibiert. Mephalan löste eine 20-30%ige Wachstumsinhibierung in hOCT3 transfizierten im Vergleich zu nicht-transfizierten Zellen aus. Ähnliche Ergebnisse wurden für A498 und ACHN Zellen erhalten. Damit unterstützen die in dieser Arbeit erhaltenen Daten die Hypothese, wonach die Sensitivität von Tumorzellen für Chemotherapeutika von der Expression von Transporter-Proteinen abhängig ist, welche die spezifische Akkumulation der Drogen in den Zielzellen vermitteln.

# 1. Introduction

## 1.1 Renal carcinoma cells

Renal cell carcinoma (RCC) are relatively rare tumors, amounting to approximately 3% of all neoplastic diseases, but their incidence is steadily increasing [1]. In 2001, 31,000 cases of RCC were diagnosed in the U.S., and 12,000 patients died of renal cancer [1, 2]. If locally restricted, the therapy of choice is surgical removal of the tumor-bearing kidney, leading to complete restoration of the patient. In the presence of metastases, however, surgery is no longer feasible. Unfortunately, most RCC and metastases are chemoresistant, i.e. they cannot be treated successfully by cytostatics [1]. One third up to one half of the patients has metastases at the time of diagnosis and, due to the chemoresistance, a mean survival time of 7 to 11 months only.

Seventy to eighty percent of RCC are clear cell carcinoma [3]. The name is based on the bright appearance of these glycogen-storing cells in the light microscope. Most of these cells show a mutation of the von Hippel-Lindau (vHL) gene. The vHL gene codes for a protein that leads to the faster degradation of hypoxia-induced factor HIF-1 $\alpha$  [4]. Loss-of-function mutations of the vHL gene cause an abnormally high activity of HIF-1 $\alpha$  which, among other effects, leads to a strong vascularisation of the tumor. Ten to fifteen percent of RCC are of the papillary type, five percent of the chromophobe type, and 3-5% are renal oncocytoma [3]. Clear cell carcinoma and papillary carcinoma are derived from proximal renal tubules.

The proximal tubules are the first segment of nephron, which is reached by the ultrafiltrate. In proximal tubules, all organic solutes such as glucose, amino acids, and mono- and dicarboxylates are reclaimed to avoid their loss which the urine. Two thirds of NaCl and water, i.e. 120 liters per day, are reabsorbed. In addition, proximal tubules secrete endogenous waste product as well as a large number of exogenous compounds such as drugs and toxins. It appears,

therefore, appropriate to state that proximal tubules are the “working horses” of the kidney.

To accomplish the secretion of anionic and cationic drugs and toxins, the epithelial cells of proximal tubules are equipped with a number of transporters in the basolateral and apical membranes [5]. The transporters in the basolateral membrane are involved in the first step of secretion, the uptake of organic anions and cations from the blood into the tubule cell. The transporters in the apical membrane release the organic anions and cations into the urine. The organic anion transporters 1 and 3 (OAT1 and OAT3) are located in the basolateral membrane of proximal tubule cells, and take up organic anions in exchange for intracellular  $\alpha$ -ketoglutarate. Many widely used drugs such as penicillines, diuretics, ACE inhibitors, analgetics, and uricosurics interact with OAT1 and OAT3. The organic cation transporters 1-3 (OCT1, OCT2, OCT3) are also located in the basolateral membrane and take up organic cations from blood into the proximal tubule cells [6]. Again, several widely used drugs are transported by the OCTs, such as histamine receptor blockers, adrenergic receptor agonist and antagonist, dopamine antagonists, and others. OATs and OCTs belong to the same transporter family, the solute carrier (SLC) family 22.

The apical (luminal, brush-border) membrane of proximal tubule cells is equipped with a number of transporters for the release or uptake of organic anions and cations [5]. The voltage-driven transporter OAT<sub>v</sub>1, the organic anions antiporter OAT4, and the ATP-driven multidrug resistance-related proteins MRP2 and MRP4 play a major role in organic anion release from the cells. Other transporters such as URAT1, OAT-K1 and OAT-K2 may be involved in organic anion absorption. The release of organic cations across the apical membrane occurs by exchange against luminal protons and is performed by the multidrug and extrusion transporter 1 (MATE1) [7]. Alternatively, organic cations can be transported out of proximal tubules cells by P-glycoprotein *alias* multidrug resistance transporter 1 (MDR1), an ATP-driven transporter residing in the apical membrane.

The expression of MDR1, MRP2 and MRP4 in cancer cells causes a resistance to several cytostatic drugs. Since most renal tumors originate from proximal tubule cells, they may have “inherited” these multidrug resistance transporters from their progenitor cells, rendering RCC and metastases chemoresistant. It is not known, whether RCC still express some other transporters typical of proximal tubule cells. Since the OAT and OCT transporters are polyspecific, i.e. they interact with a huge number of chemically unrelated compounds, it may well be that these transporters could be used to direct cytostatic drugs into the cancer cells. Indeed, some of the proximal tubular transporters interacted with methotrexate, nucleoside analogs, and cisplatin (for review see Table 1.1)

## **1.2 Transporter characterization**

### *1.2.1 The SLC transporter superfamily*

#### *1.2.1.1 The amino acid transporter family SLC7*

The SLC7 family is divided into two subgroups, the cationic amino acid transporter CAT (SLC7A1-4) and the glycoprotein-associated amino acid transporters graAT (SLC7A5-11). Structurally, glycoprotein-associated amino acid transporters consist of the heterodimeric amino acid transporter (HAT) or catalytic chain and the associated glycoprotein (heavy chain) 4F2hc (CD98) or rBAT. The heavy chain is covalently and hydrophobically associated with the catalytic chain [30]. Only upon association, activity is observed. The cationic amino acid transporter subfamilies have 14 transmembrane segments, some of which are glycosylated. The CAT subfamily transporters are 20% identical and 60% similar to those of the graAT subfamily [31].

Protein Name	Human Gene Name	Interaction with cytostatics	Reference
OAT1	SLC22A6	Methotrexate, Cisplatin	[8]
OAT2	SLC22A7	Methotrexate	[8]
OAT3	SLC22A8	Methotrexate	[8]
OAT4	SLC22A11	Methotrexate	[9, 10]
OCT2	SLC22A2	Cisplatin	[9, 11]
OCT6	SLC22A16	Doxorubicine, Epirubicine	[12]
OATP-A	SLC21A2	Bamet-UD2 and Bamet-R2	[9, 13, 14]
OATP-C	SLC21A6	Irinotekan metabolite	[9, 13-15]
OATP-D	SLCO21A11	Methotrexate	[10, 14, 16]
CNT1	SLC28A1	Gemcitabine, 5'-fluorouridine, Cytarabin	[17]
CNT2	SLC28A2	Anthracyclines Pirarubicin, Doxorubicine	[17-19]
CNT3	SLC28A3	Gemcitabine, Fludarabine, Cladribine	[17, 20]
ENT1	SLC29A1	Gemcitabine, Fludarabine, Cladribine, Cytarabine	[18, 21]
ENT2	SLC29A2	Gemcitabine, Fludarabine, Cladribine, Cytarabine	[18, 21]
LAT1	SLC7A5	Melphalan	[22-24]
MCT1	SLC16A1	lphosphamide	[25, 26]
MCT2	SLC16A2	lphosphamide	[25-27]
RFT	SLC19A1	Methotrexate	[28, 29]
ThTr	SLC19A2	Methotrexate	[28, 29]

Table 1.1 Interaction of SLC transporters with cytostatic drugs

Main substrates of CAT subfamily transporters are positively charged amino acid such as L-arginine, L-lysine, L-histidine etc. Cationic amino acid transporters mainly exchange cationic L-amino acids with intracellular amino acids such L-alanine, L-leucine, and the most pronounced trans-stimulation was observed for CAT-1 [32]. CAT transporters are expressed ubiquitously except for liver tissue. Their expression site is the basolateral membrane of epithelial cells [33]. The subfamily graAT transporters have 12 transmembrane segments, and the catalytic domain is not glycosylated [31]. The graAT transporters mainly function as exchangers, but the affinity to intracellular L-amino acids such L-leucine, L-cysteine is low. The main members of graAT transporters are the L-amino acid transporter 1 and 2 (SLC7A5, SLC7A8). The hLAT1 is widely expressed in human body, but the first cDNA was obtained from human leukocytes. LAT1 mainly functions as an exchanger with a ratio of 1:1, preferred efflux substrates of LAT1 are L-leucine, L-isoleucine, and L-methionine. For influx, LAT1 mostly uses aromatic amino acids [34]. LAT2 (SLC7A8) is ubiquitously expressed in the human body; main sites are kidney proximal tubules at the basolateral membrane. Functionally, LAT2 exchanges neutral L-amino acids across the basolateral membrane and equilibrates their concentration inside cells. LAT2 shows similar functional activities as LAT1. LAT1 and LAT2 were reported to interact with the mustard derivatives of L-phenylalanine, melphalan [35].

#### *1.2.1.2 The sodium dicarboxylate transporter family SLC13*

The SLC13 transporters include two major subgroups, Na<sup>+</sup>-sulphate co-transporter (NaS) and Na<sup>+</sup>-carboxylate (NaC) co-transporters. This transporters family is widely present in variety of organs. The members of the SLC13 group consist of 8-13 transmembrane helices and both subgroups have comparable amino acid sequences (similarity 66-70%) [36]. SLC13 group transporters

function as symporters using the  $\text{Na}^+$  ion gradient as energy. The ratio between  $\text{Na}^+$  ions and substrate is equal to 3:1. The subgroup of NaS includes NaS1 and NaS2 in humans. The main substrates are sulphate, thiosulphate, and selenate ions. The hNaS1 mRNA was detected in kidneys, ileum, duodenum/jejunum, and colon [37]. The hNaS2 is mainly present in placenta, heart, and testis [38]. The main function of NaS transporters is sulphate absorption. The second subgroup includes hNaC1 and hNaC3. Main substrates for this group are dicarboxylates such as  $\alpha$ -ketoglutarate, succinate, and citrate etc. hNaC1 is mainly expressed in kidneys and intestine [39]. hNaC3 is expressed in brain, kidneys, liver, and lung. The main function of hNaC1 and NaC3 is the transport of Krebs cycle intermediates. An other function of these transporters is to organize the dicarboxylate gradient in kidney tubule cells, which is used as energy source for other transporters (OATs) [8]. Interactions with cytostatics are not known for this transporter group.

### *1.2.1.3 The monocarboxylate transporter family SLC16*

The monocarboxylate co-transporter (MCT) includes 14 members, four of which (MCT1-4) show proton dependent monocarboxylate transport. Structurally, MCT transporters consist of 12 transmembrane helices. For expression of a functional protein at the plasma membrane, MCT1-4 need the monotopic ancillary protein CD147 [40]. Main substrates for MCT family transporters are monocarboxylate ions such as L-lactate, propionate, pyruvate, acetate etc. MCT1 (SLC16A1) and MCT2 (SLC16A7) are expressed ubiquitously, with a strong expression detected in muscle, heart, liver, and erythrocytes [41]. The main function is the exchange of monocarboxylates between cells and extracellular fluids in the human body. MCT transporters are tightly connected with the metabolism of glycogen. The monocarboxylate transporters mediate the transport of ifosphamide [25-27].



#### *1.2.1.4 The folate/thiamine transporter family SLC19*

The SLC19 transporter family includes three members: reduced folate transporter (RFT; SLC19A1) and two thiamine transporters ThTr1 (SLC19A2) and ThTr2 (SLC19A3) [28]. Structurally all three members are similar. They contain 12 transmembrane helices and one site for N-glycosylation. The SLC19A1 prefers as substrates folate analogs: N<sup>5</sup>-methyltetrahydrofolate, N<sup>5</sup>-formyltetrahydrofolate, and methotrexate. Most substrates of SLC19A1 exist as anions at physiological pH, and this transporter sensitive to probenecid. The mechanism of transport H<sup>+</sup> symport or folate OH<sup>-</sup> antiport [42]. Transport investigations have shown that SLC19A1 is electroneutral. Expression of SLC19A1 was detected ubiquitously, but high levels were observed in kidney, intestine, and placenta [43]. The main function of SLC19A1 is folate reabsorption. RFT plays also an important role in the sensitivity to methotrexate analogs [44].

The other member of SLC19 family, ThTr1 and 2, prefer as substrates thiamine and thiamine derivatives [45]. Transport activity investigations suggest that these transporters function as thiamine/H<sup>+</sup> antiporters. SLC19A2 and SLC19A3 are expressed ubiquitously in the human body [28]. The main function is the reabsorption of thiamine. An interaction with known cytostatic agents was not detected.

#### *1.2.1.5 The organic anion and peptide transporter family SLC21*

The SLC21 transporter family includes 36 members in humans. These members are divided in six families from OATP1 to 6. Structurally, SLC21 transporters are similar, they consist of 12 transmembrane helices and a large

extracellular domain between TM9 and 10 which contains many conserved cysteine residues. N-glycosylation sites were found in the extracellular loop 2 and 5. OATPs are sodium-independent transport systems. Their transport appears to be driven by antiport of negatively charged ions such as bicarbonate and glutathione-S-conjugates. The 36 member of SLC21 family are organized in 6 subfamilies from OATP1 to OATP6. Organic anion transport mediated by OATPs is pH dependent and electroneutral. Most of substrates which are transported by the OATP family are organic amphipathic anions.

#### *1.2.1.5.1 OATP1 subfamily*

To subfamily OATP1 belong three groups OATP1A, OATP1B, and OATP1C. OATP1A subfamily contains a single human member, OATP1A2 (SLC21A3). It is a glycoprotein with a molecular weight of 85 kDa and contains 670 residues [46]. OATP1A2 is expressed in liver, colon, and blood-brain barrier. In brain, the protein is not completely glycosylated and observed at a molecular weight of 60 kDa. The main substrates for OATP1A2 are bile salts, BSP (bromosulphophthalein), steroid hormones, thyroid hormones (T<sub>3</sub>,T<sub>4</sub>), prostaglandin E<sub>2</sub>, ouabain, etc. Human OATP1A2 has the widest range of substrates compared to the OATP superfamily. OATP1A2 plays an important role in blood-brain barrier transport and delivery neuroactive peptides to the brain. In hepatocytes, OATP1A2 is present at the basolateral membrane. The main function is extraction of bile acids from the blood. Localization and substrate specificity of OATP1A2 suggests its high importance for drug metabolism.

The OATP1B subfamily includes two members, OATP1B1 (SLC21A6) (OATP-C) and OATP1B3 (SLC21A8). The cDNA for OATP1B1 was cloned from human liver and encodes 691 residues. OATP1B1 is expressed in hepatocytes at the basolateral membrane [47]. The main suggested role for OATP1B1 is the

hepatic clearance from blood of amphipathic organic anions. The substrate specificity of OATP1B1 was investigated in *Xenopus laevis* oocytes and stably expressing HEK293 cells. Its spectrum of substrates contains bile salts, bilirubin, BSP (bromosulfophthalein), steroid conjugates, thyroid hormones, eicosanoids, cyclic peptides, drugs such as benzylpenicillin, methotrexate, pravastatin, and rifampicin [14]. Several polymorphisms were detected in OATP1B1 gene, some of which lead to functional inactivity. The cDNA of OATP1B3 was cloned from human liver and encodes a 120 kDa protein, consisting of 702 residues. Under normal conditions, OATP1B3 is expressed at the basolateral site of hepatocytes. Expression of OATP1B3 was observed also in cancer cell lines derived from stomach, colon, pancreas, lung, and brain. Substrate specificity for OATP1B3 was investigated in *Xenopus laevis* oocytes and stably expressing HEK293 cells. Its spectrum of substrates contains bile salts, bilirubin, BSP (bromosulfophthalein), steroid conjugates, thyroid hormones (T<sub>3</sub>,T<sub>4</sub>), eicosanoids, cyclic peptides, drugs such as benzpenicillin, methotrexate, pravastatin, rifampicine and also peptides like cholecystokinin 8 and deltorphin II. The main function of the OATP1B3 transporter is, like OATP1B1, blood clearance of amphipathic organic anions.

This group contains one member OATP1C1 (OATP-F). This transporter was cloned from a brain cDNA library, and contains 712 amino acid residues. At the mRNA level, expression of OATP1C1 was detected in brain and testis (Leydig cells) [47]. The substrate specificity of OATP1C1 is limited. Specific substrates are BSP, estradiol-17 $\beta$ -glucuronide, and estrone-3-sulfate. OATP1C1 possesses high affinity to T<sub>4</sub> and rT<sub>4</sub> (reverse tetra-iodothyronine) thyroid hormones. The main function of OATP1C1 could be the specific transport of thyroid hormones to the brain.

#### *1.2.1.5.2 OATP2 subfamily*

The subfamily OATP2 consists of two groups, OATP2A (SLC21A2) and OATP2B (SLC21A9) (OATP-B) with total of three individual genes in human.

The OATP2A group includes human OATPA1 (PGT) (SLC21A2). The protein contains 643 amino acids and was cloned from a kidney library. At the mRNA level, OATPA1 was detected in heart, skeletal muscle, and pancreas [47]. The main substrates for OATPA1 are different prostaglandins and tromboxane B<sub>2</sub>. The main function is the transport of derivatives of arachidonic acid.

The OATP2B (OATP-B) group was isolated from human brain. Expression was detected in liver, spleen, placenta, lung, kidneys, heart, ovary, small intestine, and brain [47]. In human liver, OATP2B is specifically expressed at the basolateral membrane of hepatocytes. The substrate specificity is similar to the OATP1 family. OATP2B transports BSP (bromosulphophthalein), estrone-3-sulfate, dehydroepiandrosterone-sulphate (DHEAS), and PGE<sub>2</sub>.

#### *1.2.1.5.3 OATP3 subfamily*

This subfamily consists of a single group (OATP3A) with one human gene. This group contains one human gene OATP3A1, which has been isolated from a human kidney library. OATP3A1 protein consists of 710 amino acid residues. This protein is 97% similar to mouse and rat protein. OATP3A1 is expressed ubiquitously [47]. Expression was also detected in several cancer cell lines. Transport activities of OATP3A1 were investigated poorly. OATP3A1 interacted with estrone-3-sulfate, PGE<sub>2</sub>, and benzylpenicillin [48]. Together with the wide expression and interspecies homology, OATP3A1 seems to be important, but its role is unclear due to limited characterization.

#### *1.2.1.5.4 OATP4 subfamily*

The subfamily OATP4 consists of three groups, of which two groups, OATP4A and OATP4C, contain two human genes.

The OATP4A group contains human OATP4A1 (SLC21A12) (OATP-E), which was cloned from kidney and brain as a 722 amino acid protein. Expression of OATP4A was detected at the mRNA level ubiquitously with strongest expression in liver, heart, placenta, and pancreas. Transport activities were investigated in *Xenopus laevis* oocytes and stably transfected HEK 293 cells. Main substrates include taurocholate and thyroid hormones T3 and T4 [49]. In addition, in stably transfected HEK293 cells the uptake of steroid conjugates, PGE<sub>2</sub>, and benzylpenicillin was observed.

The OATP4C group contains human OATP4C (OATP-H) (SLC21A20), the sequence of which was included in the database. Functional activities are under investigation.

#### *1.2.1.5.5 OATP5 subfamily*

OATP5 subfamily consist of a single group OATP5A with a single human gene.

This OATP5A group contains human OATP5A1 (OATP-J) (SLC21A15), which has been isolated and included in database [49]. The 848 amino acid residue protein has unknown transport activities.

#### *1.2.1.5.6 OATP6 subfamily*

The OATP6 subfamily contains four groups OATP6A, OATP6B, OATP6C, OATP6D, which contain genes of man, mouse and rat [14].

The OATP6A group contains human OATP6A1 (OATP-I) (SLC21A19), which has been isolated from human testis [50]. Any functional activities are not known.

The OATP6B group contains rat and mouse Oatp6b1 (Slc21a16). Rat Oatp6b1 was characterized as OATP related transporter which transports DHEAS [50]. Mouse Oatp6b1 is not yet characterized [51].

The OATP6C group contains the rat and mouse gonade-specific Oatp6c1 (Slc21a18) transporter. Oatp6b1 is not yet characterized [51].

The OATP6D group contains a single mouse member, Oatp6d1 (Slc21a17). This gene was identified as OATP related protein, but a function is not known [51].

#### *1.2.1.6 The organic anion, cation, zwitterion family SLC22*

This family of transporter proteins has affinity to organic anions, cations and zwitterions. Structurally, these proteins contain 12 transmembrane  $\alpha$ -helical domains and a large extracellular loop between helix 1 and 2. SLC22 transporter family proteins are mainly expressed in kidneys, intestine, and liver. In these organs they perform important transport of endogenous and exogenous substances. The SLC22 transporter family can use different energy sources for transport. Mostly they function as antiporters and can exchange organic ions.

### *1.2.1.6.1 The organic cation transporters*

#### *1.2.1.6.1.1 The organic cation transporter 1 (OCT1)*

The active form of OCT1 (SLC22A1) has been isolated from rat, mouse, man and rabbit. In man and rat, different splice variants were detected [52]. In all species OCT1 showed a strong expression in liver. In rodents it also was detected in kidneys and intestine. The main site of OCT1 expression in liver is the basolateral membrane of hepatocytes. Preferred substances of OCT1 are cationic substances such as tetraethylammonium (TEA), N-methylquinine, 1-methyl-4-phenilpyridinium (MPP), drug such as desipramine, acyclovir, ganciclovir, metformin, endogenous compound such as serotonin, and prostaglandin E<sub>2</sub> [53]. This substrate specificity is similar to two other members of SLC22 family, OCT2 and OCT3, but the affinities are a different. OCT1 transport activity can be regulated by phosphorylation, e.g. stimulated by PKC and PKA. The main physiological role of OCT1 is the primary excretion of cationic xenobiotics and drugs into bile. OCT1 interacted with cytostatic agents: mitoxantron, and cis-platinum derivates such as carboplatin, etc [54].

#### *1.2.1.6.1.2 The organic cation transporter 2 (OCT2)*

The organic cation transporter 2 (SLC22A2) was isolated from rat, human, mouse, and pig. The main site of expression is in kidney, but has also been detected in human placenta and central nervous system (CNS) [55]. In rat and human, OCT2 is expressed at the basolateral membrane of renal proximal tubule cells [56]. The expression of OCT2 is dependent on the gender and different short-term stimuli. It was shown that hOCT2 is constitutively activated by the Ca<sup>2+</sup>/calmodulin complex and inhibited by the muscarinic receptor agonist carbachol. OCT2 shows a similar substrate specificity as OCT1, but with different affinities in some cases. Well characterized substrates for OCT2

are: TEA, MPP, choline, dopamine, histamine, norepinephrine, serotonin, amantadine, and cimetidine [57]. A change in membrane potential was detected in *Xenopus laevis* oocytes expressed rat OCT2 after perfusion with choline. The function of rat OCT2 can be characterized as a cation antiporter. Some studies on *Xenopus laevis* oocytes show bidirectional transport of cations [58]. The main role for OCT2 is the clearance of cationic xenobiotics from blood in kidneys. OCT2 plays also an important role in transport of neuroactive cationic substances in CNS [59]. OCT2 can interact with cationic cytostatics such as cisplatin and cisplatin derivatives, and with mitoxantron [54]. Main side effects of cisplatin are connected with OCT2 expression sites [60].

#### 1.2.1.6.1.3 *The organic cation transporter 3 (OCT3)*

The organic cation transporter 3 (SLC22A3) was isolated from rat, human, and mouse. In human body, OCT3 is mainly expressed in kidneys, skeletal muscle, brain, liver, placenta, and heart [59]. In brain, OCT3 was detected by *in situ* hybridization in hippocampal and cerebellar neurons [61]. The substrate specificity for OCT3 is similar to that of for other members of the OCT family, but with different affinities for some substances. For example, OCT3 transports TEA, MPP, guanidine, dopamine, norepinephrine and histamine [59]. hOCT3 is involved in cationic drug excretion in liver and also in monoamine neurotransmitter transport in CNS, heart, and peripheral ganglia. For hOCT3 an interaction with cisplatin derivatives such as carboplatin, oxaliplatin was shown [60].



### 1.2.1.6.2 *The organic anion transporters*

#### 1.2.1.6.2.1 *The organic anion transporter 1 (OAT1)*

The organic anion transporter 1 (SLC22A8) was isolated from the human, rat, and flounder kidneys [8]. Differently sized transcripts were detected also in skeletal muscle, placenta and brain. Immunohistochemical investigation of OAT1 expression in human and rat kidneys revealed a strong signal at the basolateral membrane of renal proximal tubule cells [62, 63]. The substrate specificity for OAT1 isolated from different species demonstrated a wide selectivity for endogenous organic anions, such as cyclic nucleotides, prostaglandins, uric acid, as well as for drug compounds: antibiotics, non-steroidal anti-inflammatory drugs, diuretics, cytostatics, and uricosurics drugs [64]. The main substrate which can be used to characterize OAT1 is p-aminohippurat (PAH). The OAT1 is acting as organic anion antiporter. PAH uptake mediated by OAT1 was increased by intracellular  $\alpha$ -ketoglutarate or glutarate [8]. The main function of OAT1 is the excretion of organic anions and xenobiotics from blood into the urine through kidney proximal tubule cells. The hOAT1 interacted with different antiviral drugs and methotrexate [65].

#### 1.2.1.6.2.2 *The organic anion transporter 2 (OAT2)*

The organic anion transporter 2 (SLC22A7) was cloned as NLT in 1994 [66]. In 1998, after re-cloning and expressing in *Xenopus laevis* oocytes the transporter specificity was analyzed [67]. The hOAT2 is expressed mainly in liver and kidney. In humans, OAT2 is expressed at the basolateral membrane of proximal tubule cells [68]. Rat OAT2 expressed in *Xenopus laevis* oocytes showed affinity to PAH, dicarboxylates, PGE<sub>2</sub>, salicylate and acetylsalicylate [67]. The main function of hOAT2 is uptake of organic anions into the liver cells, where

they may be metabolized and excreted into bile. The interaction of OAT2 with cytostatics is unclear.

#### *1.2.1.6.2.3 The organic anion transporter 3 (OAT3)*

The organic anion transporter 3 (SLC22A8) has been cloned from human, rat, and mouse [69]. Human OAT3 is strongly expressed in kidneys, brain, and skeletal muscle. In kidneys hOAT3 is located at the basolateral membrane of proximal tubule cells [8]. The driving force for organic anion uptake mediated by hOAT3 is the efflux of dicarboxylates, such as  $\alpha$ -ketoglutarate. hOAT3 can transport different anionic substrates, such as PAH, estrone-3-sulfate, but also the weak base cimetidine [8]. The main function of OAT3 is the excretion of organic anions from blood into urine through kidney proximal tubule cells. The hOAT3 can interact with different antiviral drugs and methotrexate [65].

#### *1.2.1.6.2.4 The organic anion transporter 4 (OAT4)*

The organic anion transporter 4 (SLC22A11) was cloned from human kidney [70]. The main sites of expression were detected in placenta and kidneys. In kidneys, OAT4 is located at the apical side of proximal tubule cells. Known substrates which interact with human OAT4, are estrone-3-sulfate, DEAS, ochratoxin A, prostaglandin E<sub>2</sub> and F<sub>2 $\alpha$</sub> . The main physiological function of OAT4 is the re-absorption of prostaglandins, anionic drugs and xenobiotics in proximal tubule cells. In placenta, OAT4 can excrete organic anions from fetal to maternal circulation. The OAT4 can interact with methotrexate.

### *1.2.1.7 The concentrative nucleoside transporters family SLC28*

The SLC28 transporter family includes three subtypes of sodium-dependent concentrative nucleoside transporters, CNT1 (SLC28A1), CNT2 (SLC28A2), and CNT3 (SLC28A3). These transporters specifically transport nucleosides and their analogs. The transporter family is divided into subfamilies by their substrate specificity: CNT1 transports only pyrimidine nucleosides, CNT2 is specialized on purine nucleosides, and CNT3 prefers both pyrimidine and purine nucleosides [71]. CNT1 is mainly expressed in epithelia. CNT2 and CNT3 are expressed ubiquitously. The SLC28 and SLC29 families play a crucial role in nucleoside transport and of nucleoside-analogs .

#### *1.2.1.7.1 The concentrative nucleoside transporter 1 (CNT1)*

The concentrative nucleoside transporter 1 (SLC28A1) is mainly expressed in epithelial tissues such as kidneys, liver, and small intestine [72]. CNT1 is mainly located at the apical side of epithelial cells. For transport CNT1 uses the Na<sup>+</sup> ion gradient [73]. CNT1 transports natural pyrimidine nucleosides. CNT1 also transports a broad spectrum of pharmaceutical nucleoside analogs such zidovudine, lamivudine, zalcitabine, and the cytotoxic cytidine analogs: cytarabine and gemcitabine [71]. The main function of CNT1 is absorption of pyrimidine nucleosides in small intestine and primary urine in kidney.

#### *1.2.1.7.2 The concentrative nucleoside transporter 2 (CNT2)*

The concentrative nucleoside transporter 2 (SLC28A2) was isolated from human, rat, mouse, and rabbit [74]. The human transporter is 81% similar to rat, but has differences in substrate specificity and tissue distribution. Human CNT2

expression was detected in kidneys, liver, placenta, heart, brain, pancreas, skeletal muscle, colon, rectum, duodenum, jejunum, and ileum [75]. Rat CNT2 expression was not detected in kidneys. CNT2 mainly transports purine analogs and uridine. There are few antiviral drugs transported by hCNT2, such as dideoxyguanosine, used for HIV treatment, and ribavirin, used for hepatitis C treatment [71]. The CNT2 plays an important role in purine absorption in kidney and intestine. Interaction between hCNT2 and cytostatic nucleoside analogs was not shown.

#### *1.2.1.7.3 The concentrative nucleoside transporter 3 (CNT3)*

The broadly-selective concentrative nucleoside transporter 3 (SLC28A3) was isolated from human, and mouse. Human and mouse CNT3 are 73% similar at the protein level [76]. High expression of hCNT2 was found in pancreas, trachea, bone marrow, and mammary gland; lower levels were found in intestine, lung, placenta, prostate, testis, and liver. CNT3 transports a broad range of nucleoside analogs in a Na<sup>+</sup>-dependent manner. It was shown that CNT3 transports a number of anticancer nucleoside drugs including: cladribine, gemcitabine, FdU, 5-fluorouridine, fludarabine [71]. The main role of CNT3 is transport of nucleosides into cells and their absorption in kidney and intestine.

#### *1.2.1.8 The equilibrative nucleoside transporter family SLC29*

The equilibrative nucleoside family consists of four members ENT1, ENT2, ENT3, and ENT4. The best characterized are ENT1 and ENT2. All members exhibit the possibility to exchange nucleosides. They influence many physiological processes depending on nucleotides.

#### *1.2.1.8.1 The equilibrative nucleoside transporter 1 (ENT1)*

The ENT1 (SLC29A1) was isolated from human and mouse. The human ENT1 is 79% similar to the mouse protein [77]. ENT1 is widely expressed in human body. High expression levels were found in brain cortex and kidneys [78, 79]. In kidneys, ENT1 is present at the basolateral membrane of tubule cells. ENT1 possesses a broad-specificity to nucleoside analogs. It was shown that ENT1 can transport purine and pyrimidine nucleotide analogs, but was unable to transport uridine. ENT1 was strongly inhibited by nitrobenzylthioinosine (NBTI) and nitrobenzylmercaptapurine (NBMPR) ( $K_i = 5$  nM) [80]. Among them, ENT1 can interact with the coronary vasodilator drugs dipyridamole, dilazep and lidoflazine. It has a poor ability to transport the antiviral drugs 2',3'-dideoxycytidine (ddC) and 2',3'-dideoxyinosine (ddI) [81]. Among cytostatics, ENT1 mediated transport of gemcitabine, cladribine, cytarabine, fludarabine, capecitabine [82].

#### *1.2.1.8.2 Equilibrative nucleoside transporter 2 (ENT2)*

The ENT2 (SLC29A2) is a 456 amino acid residue protein cloned from human, mouse and rat. Human ENT2 is 46% identical to hENT1 [83]. There are two splice variants of hENT2. The first is a 326 amino acid residues truncated protein which lacks exon 4 [84]. The second splice variant has a 40 nucleotides deletion in exon 9 [85]. Both splice variants are coding for a non-active transporter. ENT2 mRNA was detected in a wide range of tissues including brain, heart, placenta, thymus, pancreas, prostate, and kidneys, but in skeletal muscle ENT2 was not present [85]. ENT2 transports a broad range of purine and pyrimidine nucleosides, except of inosine [83]. In comparison to ENT1, ENT2 has lower affinities and turnover for the some nucleoside substrates. With regards to drugs, ENT2 show high affinity to AZT, ddI, and ddC [81]. From

cytostatics ENT2 transports gemcitabine, cladribine, cytarabine, fludarabine, and capecitabine [82].

#### *1.2.1.8.3 Equilibrative nucleoside transporter 3 (ENT3)*

Human ENT3 (SLC29A3) is a 475 amino acid residue protein with 29% similarity in sequence to hENT1 [86]. hENT3 has a 51 hydrophobic amino acid residues long N-terminus, which is absent in ENT1 and 2. This N-terminal tail consists of two leucine motifs which respond for protein sorting in the Golgi apparatus [86]. ENT3 is present also in the cell membrane. Functionally ENT3 is characterized poorly. ENT3 mRNA was detected in a wide range of tissues, but particularly abundant in placenta [86].

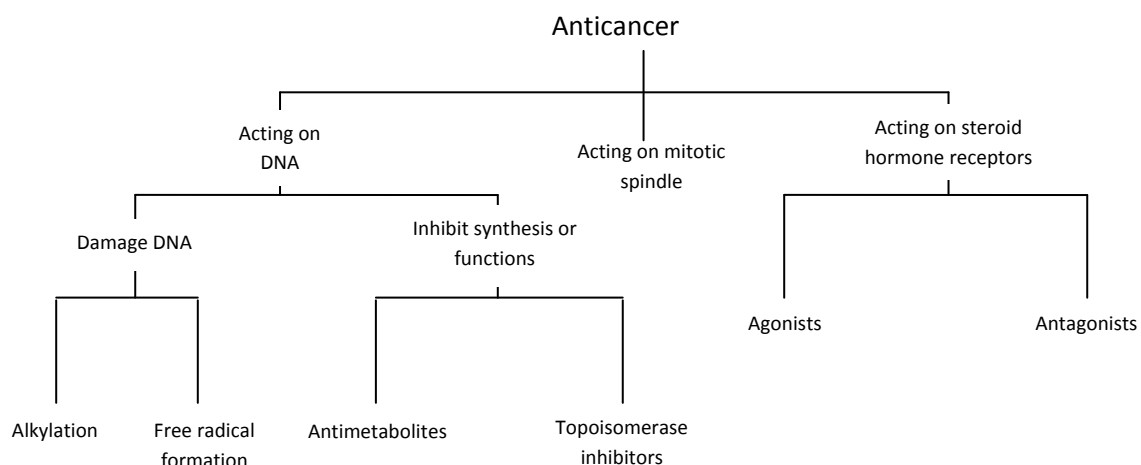
#### *1.2.2 The ABC transporter superfamily*

The ABC transporter superfamily proteins are widely present in living world. The coding sequences with similar structures were isolated from many organisms: bacteria, yeasts, fungi, insects, and vertebrata. They transport structurally different chemical substances, nutrients, and waste. The characteristic structural element of ABC transporters is the ATP binding cassette. The structure of most of members consists of two ABC domains. These domains play an important role in recognition of ATP. For their function, ABC transporters undergo conformational changes supported by the energy of the hydrolysis of the  $\gamma$ -phosphate ATP. This gives some advantages: transport can be provided against a concentrative gradient of substrate, and it is not dependent on membrane potential. In human body, ABC transporters are mainly used for xenobiotic excretion. The ABC transporters are an important object in pharmacology, because of their interaction with many drugs and influence on their activity. In oncology, ABC transporters are a opposition

chemotherapy. Information about expression and substrate specificity for ABC transporters expressed in human body is presented in Table 1.2 (Addition 1) [87].

### 1.3 Antitumor drug characteristics

Historically, the usages of harmful chemical substances as treatment for cancer disease start almost half a century ago. In Bari, an accident with mustard gas happened in 1943. The investigation of exposed civilians showed drastical changes in blood count: the white cells were decreased. This finding forced investigators to use mustard gas as a treatment of Hodgkin's lymphoma. In nowadays chemotherapy the list of drugs includes around 100 different cytostatic agents. In scheme 1.1 is presented a short classification of cytostatic drugs by their biological activities.



Scheme 1.1 Classification of cytostatic drugs by their biological activities

### 1.3.1 Cytostatics acting on DNA

#### 1.3.1.1 Mustard analogs

Mustard analogs as primary acting structure have a group of mechlorethamine (Figure 1.1A). This group has nucleophilic activities and attacks chemical groups with condensed negative charge such as  $-NH_2$  or  $-SH$ . The observed wide spectrum of activities of mustard analogs can be explained by their high potency to generate double strand adducts between  $N^7$ -amino groups of guanine. New substances such chlorambucil, bendamustin, melphalan, cyclophosphamide (Figure 1.1 B, C, D, E) were introduced in clinical practice. Mustard cytostatics are mainly used for the treatment of blood cancers. Short characteristic are listed in Table 1.3.

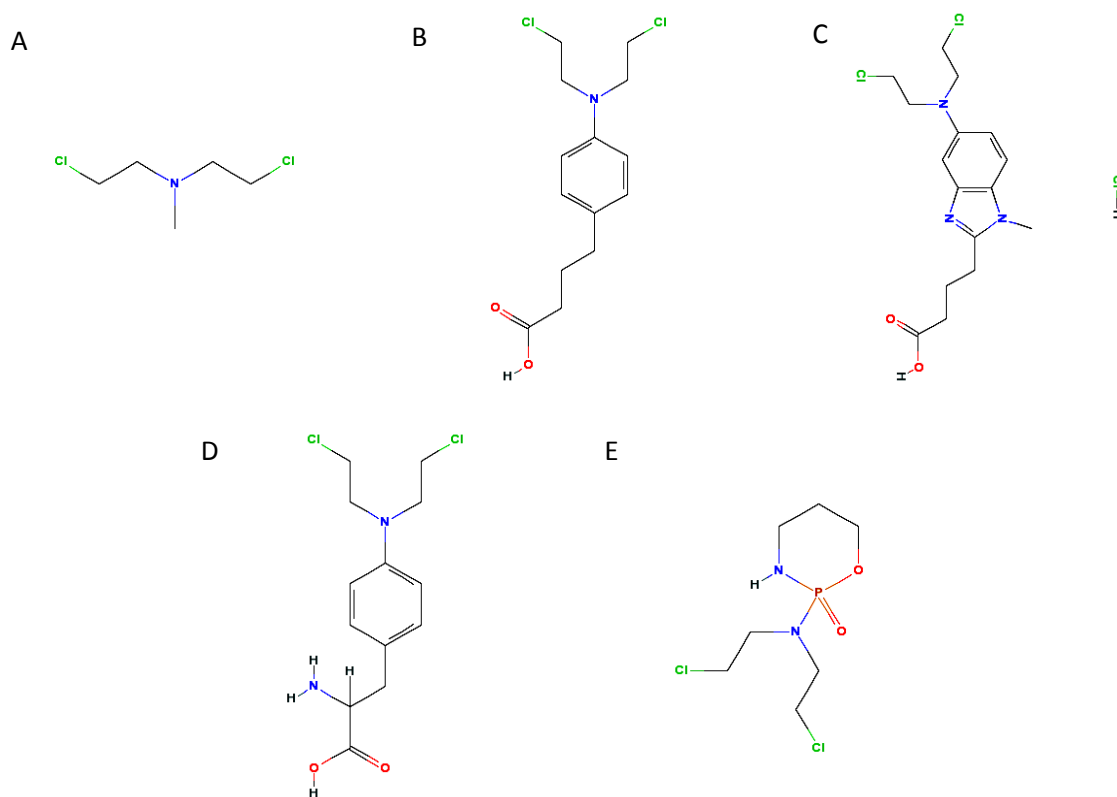


Figure 1.1 Structure of cytostatics based on the mustard group: A - mechlorethamine, B - chlorambucil, C - bendamustin, D - melphalan, E - cyclophosphamide



Name	Treated disease	Transporter type	Side effects
Chlorambucil	non-Hodgkin lymphoma, Waldenström macroglobulinemia, polycythemia vera, trophoblastic neoplasms, ovarian carcinoma	Not identified	nausea, vomiting, diarrhea, seizures, tremors, muscular twitching, confusion, agitation, ataxia, hallucinations, hepatotoxicity Infertility
Bendamustin	multiple myeloma, ovarian cancer	Not identified	nausea, vomiting, diarrhea, seizures, tremors, muscular twitching, confusion, agitation, ataxia,
Melphalan	multiple myeloma, ovarian cancer, melanoma	LAT1 [24], OCT3	nausea, vomiting, bone marrow suppression, hair loss, rash, itching
Cyclophosphamide	Lymphomas, leukemia, antirheumatic drugs	Not identified	bone marrow suppression, stomach ache, diarrhea
Ifosfamide	testicular cancer, breast cancer, lymphoma, lung cancer, cervical cancer, ovarian cancer, bone cancer	MCT1 [25-27]	bone marrow suppression, stomach ache, diarrhea

Table 1.3 Characteristic of mustard based cytostatic

### 1.3.1.2 Alkyl sulfonates

This class of alkylating substances is presented by busulfan (Figure 1.2). The main biological activity is based on the production of cross-links in the DNA. Busulfan is used for the treatment of chronic myeloid leukemia (CML), chronic lymphocytic leukemia (CLL), and for inhibition of bone marrow before transplantation. Side effects of busulfan treatment may include interstitial

pulmonary fibrosis, hyperpigmentation, seizures, hepatic (veno-occlusive disease) and wasting syndrome. Interaction with transporters have not been investigated.

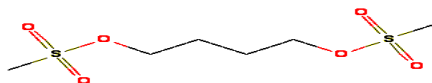
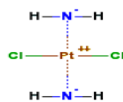


Figure 1.2 Structure formula of busulphan

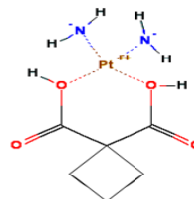
### 1.3.1.3 Platinum compounds

Cytostatic compounds containing platinum were discovered as toxins which occurred during electrolysis with platinum electrodes. The first member of the platinum compound family was cisplatin (Figure 1.3 A)

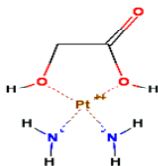
A



B



C



D



Figure 1.3 Structural formula of platinum cytostatics: A - cisplatin, B - carboplatin, C - nedaplatin, D - oxaliplatin

The mechanism of action is a classical nucleophilic attack at electron-dense enriched groups such as  $-NH_2$ ,  $-SH$ . Cisplatin shows affinity to DNA and RNA. After reaction of DNA with cisplatin, N<sup>7</sup>-guanosine and cytosine adducts are obtained. After cisplatin treatment, DNA loses its biological functions. Platinum adducts can be removed by excising repair. This kind of repair produces double stranded breaks and can include changes in nucleotide sequence. Many proliferative cells are very sensitive to DNA break. Treatment of such cells with cisplatin leads to apoptosis. Cisplatin is also used as pretreatment of radiation therapy of cancer diseases. The effect of X-ray radiation is amplified by cisplatin treatment. This effect is based on producing superoxide radicals by platinum ions when they meet an X-ray photon. In clinical practice, other platinum analogs such carboplatin, nedaplatin, and oxaliplatin are widely used (Figure 1.3 B, C, D). These substances produce fewer side effects in comparison to cisplatin. It was shown that cisplatin can be transported by OCT2 [11]. Carboplatin had a high affinity to OCT1 and OCT2 [54]. The usage of platinum compounds and their side effects are summarized in table 1.4.

Name	Treated disease	Transporter type	Side effects
Cisplatin	small cell lung cancer, and ovarian cancer, lymphomas	OCT2 [11]	Nephrotoxicity, neurotoxicity, nausea, vomiting, ototoxicity, alopecia
Carboplatin	ovarian carcinoma, lung, head, neck cancers	OCT1, OCT2 [54]	Nephrotoxicity, neurotoxicity, nausea, vomiting, ototoxicity,
Nedaplatin	ovarian carcinoma, lung, head, neck cancers, lymphomas	Not identified	nausea, vomiting, bone marrow suppression, hair loss, rash, nephrotoxicity, neurotoxicity
Oxaliplatin	colorectal cancer	Not identified	bone marrow suppression, stomach ache, diarrhea, nephrotoxicity, neurotoxicity, nausea

Table 1.4 Characteristic of platinum based compounds

#### 1.3.1.4 Cytostatic producing free radical

This group encounters one member – bleomycin. The structural formula is presented in figure 1.4. Bleomycin cleave DNA in the presence of a metal ion. It was suggested that bleomycin chelates metal ions and generates free radicals which cleave DNA molecules [88]. The mechanism of action is not completely clear. Bleomycin is used for the treatment of Hodgkin lymphoma, squamous cell carcinomas, and testicular cancer. The most prominent side effects of bleomycin is pulmonary fibrosis. Other side effects include fever, rash, hyperpigmentation, alopecia, Raynaud's phenomenon, and ototoxicity [89].

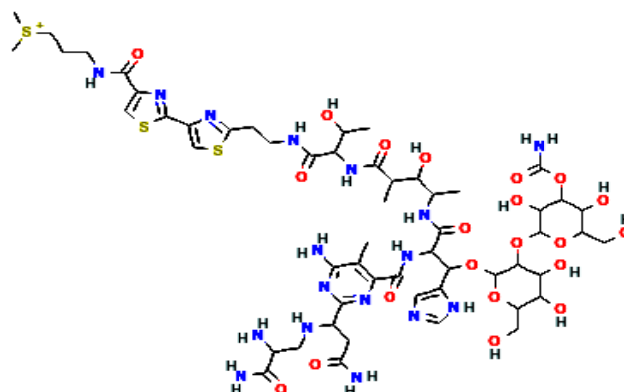


Figure 1.4 Structural formula of bleomycin

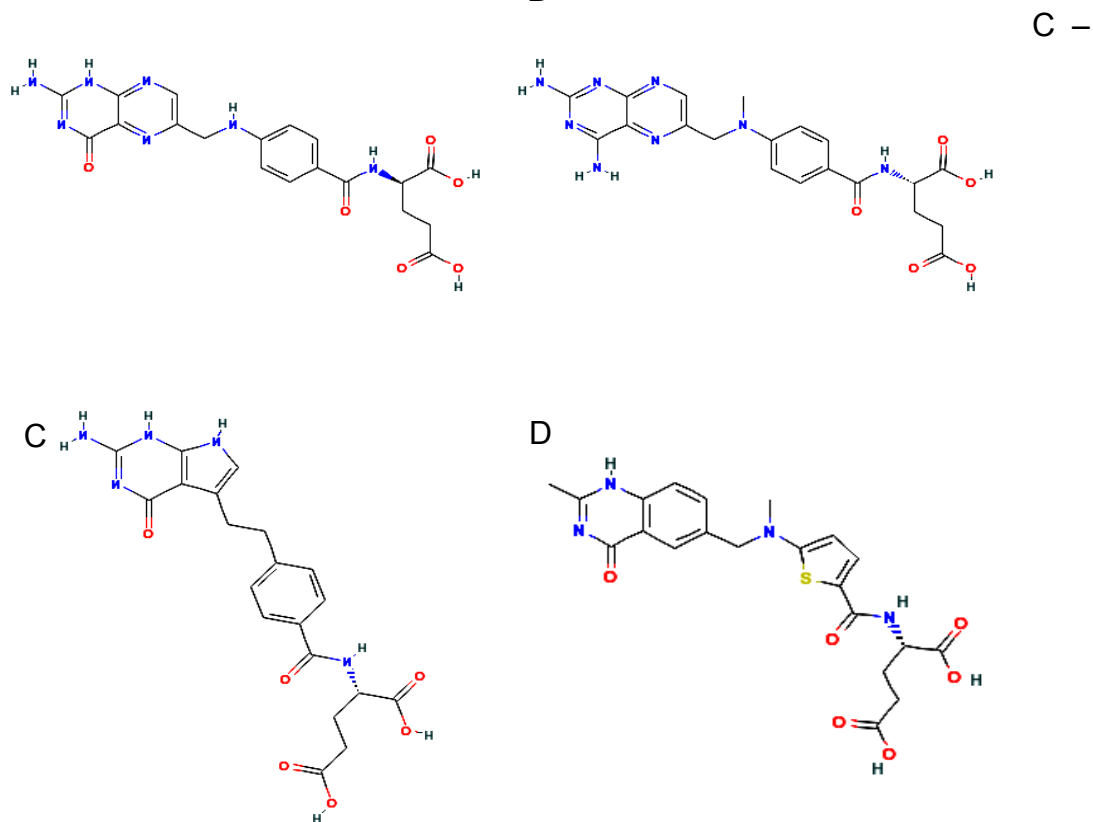
#### 1.3.1.5 Antimetabolites

This class of cytostatic compounds is divided in two groups, folate analogs and nucleoside analogs. The main mechanism of action of antimetabolites is disturbing normal metabolite exchanges by enzyme inhibition.

### 1.3.1.5.1 Folate analogs

This group of compounds is including analogs of folic acid (Figure 1.5 A). Methotrexate is the most prominent member of the antifolate group and is used for treatment of leukemia in children. Methotrexate reversibly and competitively inhibits dehydrofolate reductase (DHFR) Fig. 1.5B [90]. The deficit of reduced folate leads to the inhibition of nucleoside and protein synthesis and cell, may undergo apoptosis. This mode of action is exhibited by all members of the antifolate group. In clinical practice are used pemetrexate and raltitrexed (Figure 1.5 C, D). The usage of antifolate compounds and their side effects are summarized in table 1.5.

Figure 1.5 Structural formulas of antifolate drugs: A - folic acid, B -methotrexate,



pemetrexate, D - raltitrexed

Name	Treated disease	Transporter type	Side effects
------	-----------------	------------------	--------------

Methotrexate	acute lymphoblastic leukemia, Crohn's disease, psoriasis, psoriatic arthritis [91]	OAT1, 3, 4 [8]	Anemia, neutropenia, bruising, nausea, hepatitis
Pemetrexate	pleural mesothelioma, non-small cell lung cancer [92]	Not identified	Anemia, neutropenia, bruising, nausea, hepatitis
Raltitrexed	Different types of cancer, inhibitor thymidine synthetase [44]	Not identified	Anemia, neutropenia, bruising, nausea, hepatitis

Table 1.5 Characteristic of antifolate compounds

### 1.3.1.5.2 Antimetabolite nucleoside analogs

Nucleoside cytostatics mainly block enzymes involved in nucleotide metabolism. There exist many antitumor active nucleoside substances. Most frequently used in clinical practice are fludarabine, mercaptopurine, capecitabine, fluorouracil, and gemcitabine (Figure 1.6 A, B, C, D, E). The usage of nucleoside cytostatics and their side effects are summarized in table 1.6.

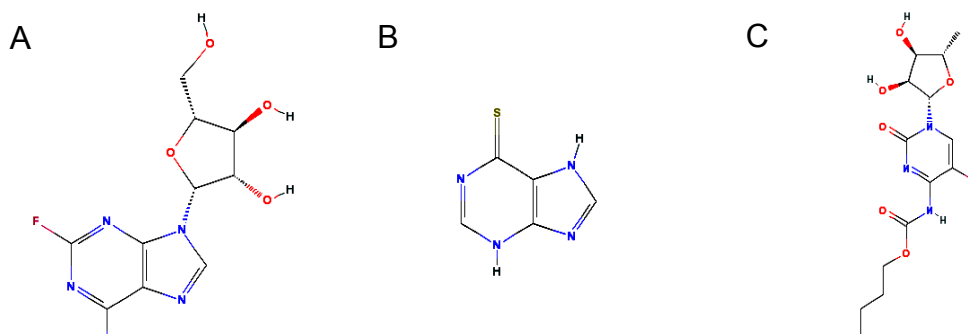


Figure 1.6 Structural formulas of nucleoside cytostatics: A- fludarabine, B- mercaptopurine, C- capecitabine, D- fluorouracil, E- gemcitabine

Name	Treated disease	Transporter type	Side effects
Fludarabine	Blood cancers [18]	ENT1, 2	opportunistic infections, neutropenia
Mercaptopurine	non-Hodgkin's lymphoma, polycythemia vera, psoriatic arthritis [93]	GLUT-1, ENT1	Anemia, neutropenia, myelosuppression
Capecitabine	breast and colorectal cancers	ENT1, 2	myocardial infarction, angina, nausea, stomatitis, anemia, thrombocytopenia
Fluorouracil	Colorectal cancer, pancreatic cancer	ENT1, 2	myelosuppression, mucositis, dermatitis
Gemcitabine	Lung cancer, pancreatic cancer, bladder cancer	ENT1, 2	Anemia, neutropenia, myelosuppression

Table 1.6 Characterization of nucleoside cytostatics

### 1.3.1.6 Topoisomerase inhibitors

This group of cytostatics was mainly isolated from plants as alkaloids. This group can be divided by their affinities into topoisomerase I inhibitors and topoisomerase II inhibitors. Topoisomerases play an important role in cell cycle. Topoisomerases are acting on secondary and tertiary structures in DNA. Topoisomerase I is present as a single protein molecule [94]. To release DNA concatamers, topoisomerase does not use ATP energy. A potent inhibitor of topoisomerase I is camptotecin, a cytotoxic quinoline alkaloid isolated from *Camptotheca acuminata* [95]. Other camptotecin analogs are irinotecan and topotecan presented in Figure 1.7.

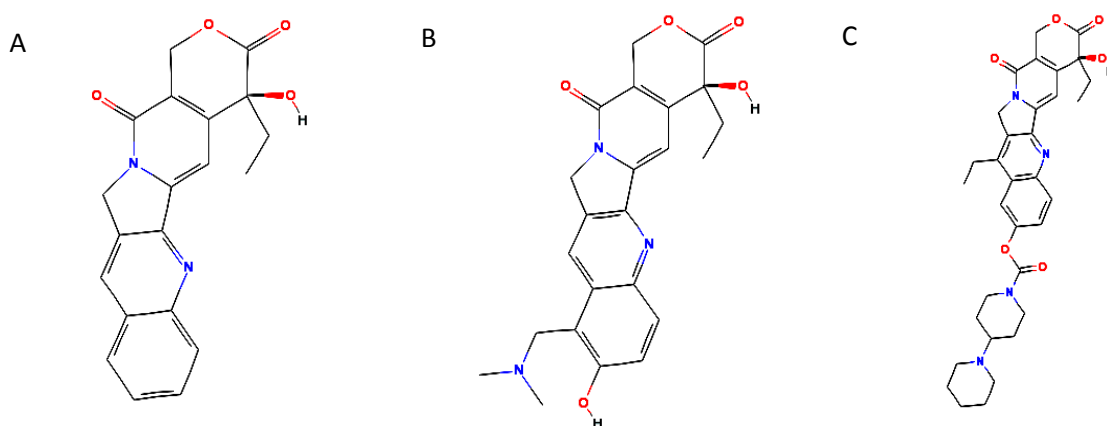


Figure 1.7 Structural formulas of topoisomerase I inhibitors: A - camptotecin, B - topotecan, C - irinotecan

The second enzyme topoisomerase II, has two subunits and uses ATP as energy source for their action. It is a high fidelity enzyme included in the mammalian DNA polymerase complex. Inhibitors of topoisomerase II are based on podofilotoxin isolated from *Podophyllum peltatum* [96]. In clinical practice etoposide and teniposide are used (Figure 1.8). The usage of topoisomerase inhibitors and their side effects are summarized in table 1.7.



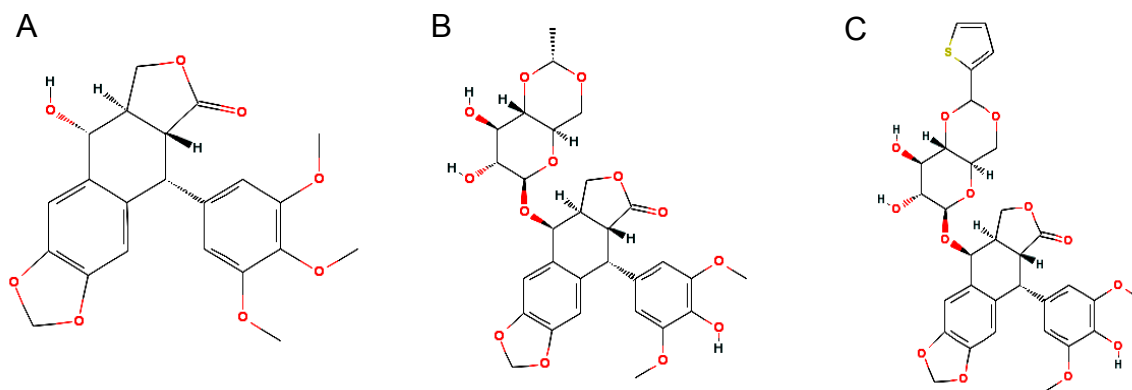


Figure 1.8 Structural formulas topoisomerase II inhibitors: A - podofilotoxin, B - etoposide, C - teniposide

Name	Treated disease	Transporter type	Side effects
Irinotecan	colon cancer[97]	Not identified	Diarrhea, neutropenia
Topotecan	ovarian cancer, lung cancer	Not identified	Diarrhea, anemia, susceptibility to infection
Etoposide	lung cancer, testicular cancer, lymphoma, non-lymphocytic leukemia, head and neck cancer [98]	Not identified	low blood pressure, hair loss, diarrhea
Teniposide	acute lymphocytic leukemia	Not identified	nausea, vomiting, diarrhea

Table 1.7 Characterization of topoisomerase I and II inhibitors

### 1.3.1.7 Anthracycline cytostatics

Anthracycline antibiotics are wide range activity cytostatics primarily isolated from *Streptomyces peucetius* [99]. The distinctive feature this group of drugs is the presence of an anthracycline ring. The mechanism of action of anthracyclins is not clear. A high potency to DNA intercalation and inhibition of RNA translation was

demonstrated. Doxorubicin was reported acting as inhibitor of topoisomerase II[100]. The structural formulas of most popular anthracyclines are mentioned in figure 1.9. The usage of anthracycline cytostatics and their side effects are summarized in table 1.8

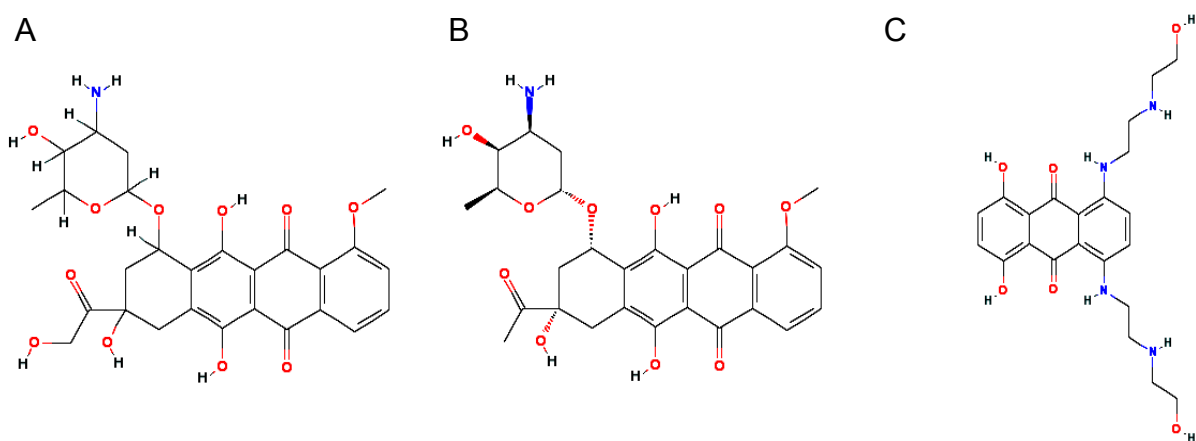


Figure 1.9 Structural formulas of anthracycline cytostatics: A - doxorubicin, B - daunorubicin, C - mitoxantron

Name	Treated disease	Transporter type	Side effects
Doxorubicin	leukemias, Hodgkin's lymphoma, bladder, breast, stomach, lung, ovaries, thyroid cancers, soft tissue sarcoma	Not identified	arrhythmias, neutropenia, bruising, nausea, alopecia
Daunorubicin	AML, neuroblastoma, chronic myeloid leukemia	Not identified	arrhythmias, neutropenia, bruising, nausea, alopecia
Mitoxantron	metastatic breast cancer, acute myeloid leukemia, and non-Hodgkin's lymphoma	Not identified	nausea, vomiting, hair loss, heart damage

Table 1.8 Characterization of anthracycline cytostatics

### 1.3.2 Cytostatics disturbing the mitotic spindle

This group of cytostatic agents can be divided into two groups acting in an opposite way and obtained from different sources. The first group taxol derived substances docetaxel and paclitaxel (Figure 1.10). These substances acting on the microtubules and stabilizes their structure [101]. After treatment cell lose the ability to change microtubule structure and to divide. The second group of mitotic spindle acting cytostatics comprises vinca alkaloids. These substances also interact with cytoskeletal microfilaments, but their mode of action in the disruption of the microtubular net. Clinically used are vinblastine, vincristine (Figure 1.10) [101]. The use of taxenes, vinca derivatives and their side effects are summarized in table 1.9.

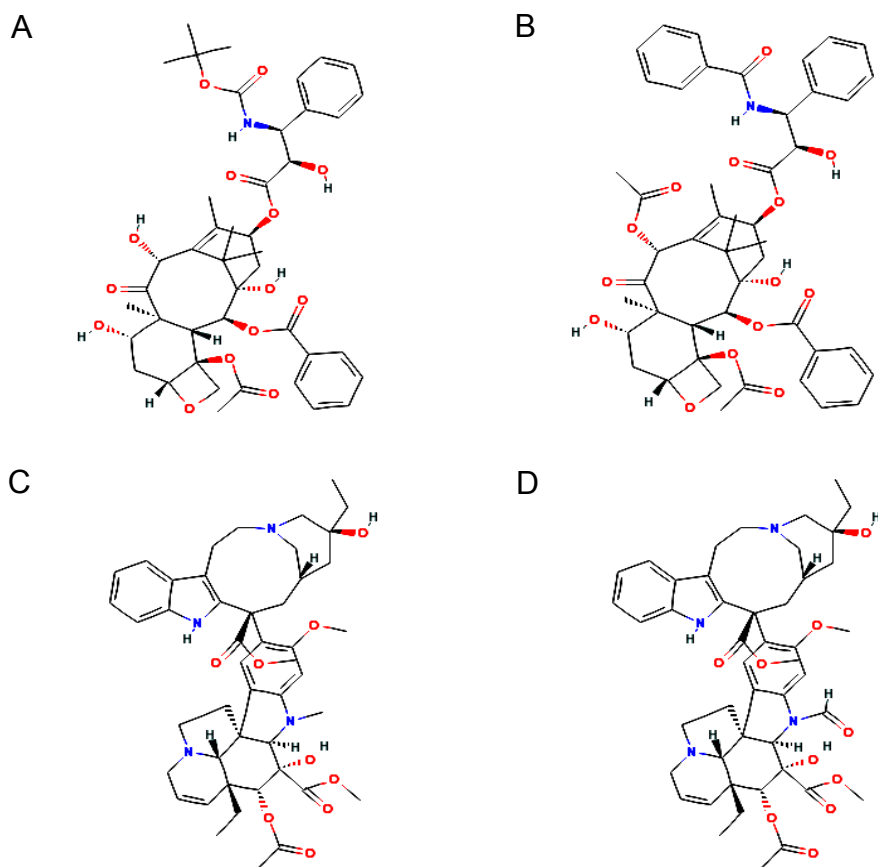


Figure 1.10 Structure formulas of anti-mitotic drugs: A - docetaxel, B - paclitaxel, C - vinblastine, D - vincristine

Name	Treated disease	Transporter type	Side effects
Docetaxel	Breast, non small-cell lung cancer	Not identified	Neutropenia, anaemia, liver dysfunction
Paclitaxel	lung, ovarian, breast cancer, head and neck cancer, advanced forms of Kaposi's sarcoma	Not identified	Nausea, vomiting, skin rash,
Vinblastine	Hodgkin's lymphoma, non-small cell lung cancer, breast cancer and testicular cancer	Not identified	peripheral neuropathy, hyponatremia, constipation and hair loss
Vincristine	non-Hodgkin's lymphoma, Hodgkin's lymphoma, acute lymphoblastic leukemia, thrombotic thrombocytopenic purpura	Not identified	peripheral neuropathy, hyponatremia, constipation and hair loss

Table 1.9 Characterization of anti-mitotic cytostatics

### 1.3.3 Substances acting on the estrogen receptor

This group includes substances which modulate the activities of the estrogen receptor. Estrogen receptors mediate expression of many oncogenes. Proliferations of 60% of breast cancers are driven by the estrogen receptor. Estrogen receptor positive breast cancer is treated with tamoxifen. Tamoxifen is acting as antagonist of the estrogen receptor. The active form of tamoxifen is produced after hydroxylation to 4-hydroxytamoxifen by CYP2D6 (Figure.1.11). In clinical practice, tamoxifen is widely used for correction of reproductive dysfunctions in men and women. As mentioned previously, breast cancer and prostate cancer are treated with tamoxifen. In 10-15% of the patients a total remission is observed after tamoxifen treatment [102]. In comparison to other cytostatics, tamoxifen therapy has weak side effects and has an increased risk of thromboembolism, and fatty liver.

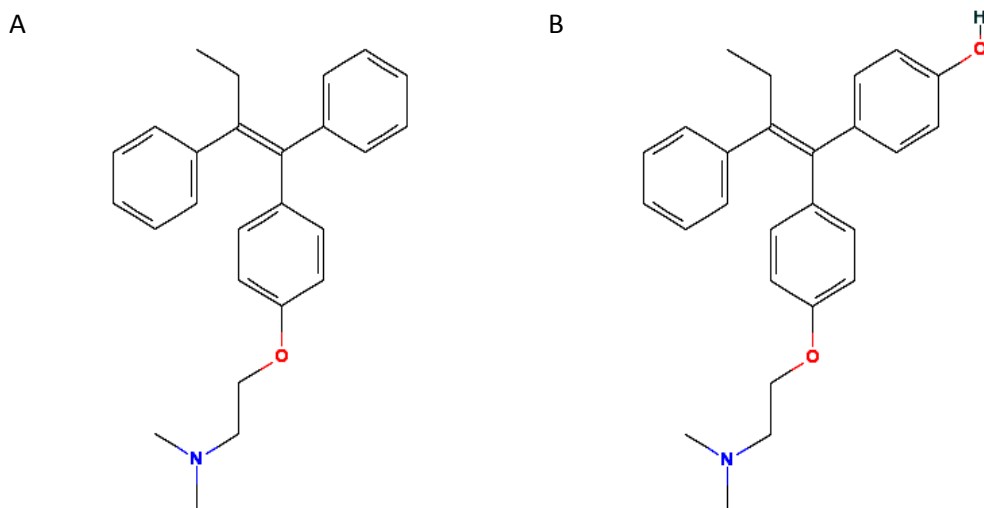


Figure 1.11 Structural formulas of tamoxifen (A) and his active product 4-hydroxytamoxifen (B)

## 1.4 Aims

Active transport of drugs in cells is an important factor for the cytostatic action. The first aim of our work was to find which transporters demonstrate significant expression levels in malignant renal cells. The second aim was to characterize the activity of expressed transporters. The third aim was to find cytostatic substances which can be delivered to tumor cells with a help of specific transporters. The fourth aim was to investigate how sensitivity of tumor cells to certain cytostatic drug depends on their ability to deliver it inside with a help of specific transporter.

## 2. Materials and methods

### 2.1. Materials

#### 2.1.1. Primers

Specific primers for RT-PCR study were obtained from MWG Biotech AG (Martinsried, Germany). All used primers are presented in tables 2.1-2.8.

Transporter family name	Name	Sequence 5'-3'	Product Size bp	Annealing Temp.C°
SLC22A6 (OAT1)	hOAT1_933 for	gggcaccttgattggctatgtc	502	58
	hOAT1_1434 rev	gatgacaaggaagcccacaagc		
SLC22A7 (OAT2)	hOAT2_835 for	tctgcacgctggcttctgac	552	59,4
	hOAT2_1386 rev	tgtctgtctgagaccgtaggg		
SLC22A8 (OAT3)	hOAT3_871 for	cttctatcatcctggtggac	549	53,6
	hOAT3_1419 rev	tagaggaagaggcagctgaag		
SLC22A12 (OAT4)	hOAT4_130 for	catggcggttctcgaagctc	593	54
	hOAT4_722 rev	cgcagtagatgacgaatgttg		

SLC22A1 (OCT1)	OCT1_115 for	gtggatgacattctggagca	485	53,6
	OCT1_599 rev	ccgagagagccaaacaaga		
SLC22A2 (OCT2)	OCT2_2199 for	accaagagtgaaccctaagc	606	54,2
	OCT2_2803 rev	tagaccaggaatggcgtga		
SLC22A3 (OCT3)	OCT3_1293 for	tgtcactgcttctaccag	433	54,3
	OCT3_1725 rev	tccttcttctgtcttctgctgg		
SCL22A16 (OCT6)	OCT6_1466 for	ctgtggtgctgttatggtgat	224	54,1
	OCT6_1689 rev	tccaaatgctgctgaggtc		

Table 2.1. Characteristics of primer pairs which were used for PCR screening of the expression level of the SLC22A family transporters.

Transporter family name	Name	Sequence 5'-3'	Product Size bp	Annealing Temp.C°
SLC21A3 (OATP-A)	hOATP-A_831for	caggagttaacgtgctcactg	460	55,3
	hOATP-A_1413rev	gatggacagttgcaatccac		
SLC21A9 (OATP-B)	hOATP-B_382for	cctaaagagctccatctccac	443	56,5
	hOATP-B_956rev	ctggcatctggtaatgtcc		
SLC21A6 (OATP-C)	hOATP-C_662for	tcattggctttaccctgggatc	551	52,6
	hOATP-C_1224rev	ggcaattccaacgggtgtcag		
SLC21A12 (OATP-E)	hOATP-E_524for	atgccagctcctacgacattg	513	54,5
	hOATP-E_1073rev	gggaacggcgggtaagaaag		

Table 2.2. Characteristics of primers pairs which were used for PCR screening of the expression level of the SLC21A family transporters.

Transporter family name	Name	Sequence 5'-3'	Product Size bp	Annealing Temp.C°
SLC28A1 (CNT1)	CNT1_1146for	tctttgtgagccagaccgag	460	55,3
	CNT1_1605rev	aggatgtaggagcagatgagc		
SLC28A2 (CNT2)	CNT2_1068for	atgactggagggttgccac	443	56,5
	CNT2_1510rev	accatctcagccaccattgg		
SLC28A3 (CNT3)	CNT3_171for	gagaacgagaacacatcagg	551	52,6
	CNT3_721rev	tacattatgagcccaccgaa		
SLC29A1 (ENT1)	ENT1_1114for	tgaggtaagtcagcatcg	462	55,9
	ENT1_1575rev	caggcagtccttctgtccat		
SLC29A2 (ENT2)	ENT2_723for	gctcctccagtctgatgaga	513	54,5
	ENT2_1235rev	accaggtagccattagaaacg		
SLC29A3 (ENT3)	ENT3_470for	actggtgaaggtggacact	513	54,1
	ENT3_987rev	ggtagatgaggctggtgatga		

Table 2.3. Characteristics of primer pairs which were used for PCR screening of the expression level of the SLC28A and SLC29A family transporters.



Transporter family name	Name	Sequence 5'-3'	Product Size bp	Annealing Temp.C°
SLC16A1 (MCT1)	MCT1_1183for	gtatttctttgCGGcttccggtg	512	57,6
	MCT1_1694rev	agactggacttctctctccttg		
SLC16A7 (MCT2)	MCT2_334for	ggttgattgtggttgagc	564	55,7
	MCT2_897rev	cttagaagtggttgattgggtcc		
SLC16A3 (MCT3)	MCT4_864for	accatcctgggcttcattgac	450	56,7
	MCT4_1313rev	tggctctttgggcttcttcta		

Table 2.5. Characteristics of primer pairs which were used for PCR screening of the expression level of the SLC16A family transporters.

Transporter family name	Name	Sequence 5'-3'	Product Size bp	Annealing Temp.C°
SLC7A5 (LAT1)	LAT1_1001for	cgtggacttcggaactatcac	558	57,2
	LAT1_1558rev	ttctgacacaggacgggtcgt		
SLC7A8 (LAT2)	LAT2_976for	agccctctgctatgctgaac	454	55,9
	LAT2_1429rev	ctgaaggaaagccagtgcca		

Table 2.4. Characteristics of primer pairs which were used for PCR screening of the expression level of the SLC7A family transporters.

Transporter family name	Name	Sequence 5'-3'	Product Size bp	Annealing Temp.C°
SLC13A3 (NaDC3)	NADC3_1422for	tgctgctcatcactgtggt	619	54,7
	NADC3_2040rev	gagagatacctgggctttgaac		

Table 2.6. Characteristics of primer pairs which were used for PCR screening of the expression level of the SLC13A3 transporter.

Transporter family name	Name	Sequence 5'-3'	Product Size bp	Annealing Temp.C°
SLC19A1 (RFT)	RFT_886for	tctgggggtcttcaactcg	486	55,6
	RFT_1372rev	aactggaactgcttgcgga		
SLC19A2 (ThTr1)	ThTr1_1241for	ctgtgggtaacattgggtgtg	481	55,1
	ThTr1_1721rev	tagtcaagtggtgctgtgaag		

Table 2.7. Characteristics of primer pairs which were used for PCR screening of the expression level of the SLC19A family transporters.

Transporter family name	Name	Sequence 5'-3'	Product Size bp	Annealing Temp.C°
ABCC1 (MRP1)	MRP1_4421 for20	aaggacttcgtgtcagccct	476	57,2
	MRP1_4897 rev22	tttggttcagtggtggaggc		
ABCC2 (MRP2)	MRP2_3831 for19	acattgtggctgttgagcg	504	55,2
	MRP2_4334 rev21	cctctgtcacttcgtgggata		
ABCC4 (MRP4)	MRP4_1812 for20	atgcggaaggttagcagacac	518	53,6
	MRP4_2329 rev21	ccagtatgaaagccaccaatc		
ABCB1 (MDR1)	MDR1_1854for	cctgtattgttgcaccacg	595	56,3
	MDR1_2428rev	atccacggacactcctacga		

Table 2.8. Characteristics of primer pairs which were used for PCR screening of the expression level of the ABC family transporters.

### 2.1.2. Chemicals

Chemicals were bought from Sigma-Aldrich (Hamburg, Germany), Applichem (Darmstadt, Germany) Merck (Darmstadt, German) and Calbiochem (Gibbstown, USA). Radioactive chemicals were bought from Amersham Bioscience (Freiburg, Germany).

### 2.1.3. Enzyme

Taq polymerase was purchased from Promega GmbH (Göttingen, Germany). Restriction endonuclease were purchased from New England Biolabs<sup>®</sup> Inc (Beverly, MA, USA) or MBI Fermentas (Vilnius, Lithuania). T4 DNA ligase was

purchased from Boehringer Mannheim (Mannheim, Germany). Collagenase CLS II was purchased from Biochrom KG (Berlin, Germany).

#### 2.1.4. Bacterial strains

Strain name	Company	Genotype
JM109	Promega GmbH	endA1, recA1, gyrA96, thi, hsdR17 (rk-, mk+), relA1, supE44, Δ( lac-proAB), (F' traD36, proAB, laqlqZΔM15).
TOP 10F'	Invitrogene	F' {lac <sup>q</sup> Tn10(Tet <sup>R</sup> )}, mcrA, Δ(mrr-hsdRMS-mcrBC), o80lac ZΔM15, ΔlacX74, recA1, araD139, Δ(ara-leu)7697, gal U, gal K, rps L (Str <sup>R</sup> ) endA1, nupG

Table 2.9 Bacterial strains used in this study

#### 2.1.5. Plasmid vector

For TA cloning the pGEM®-T Easy vector from Promega GmbH (Göttingen, Germany) was used. It includes a multiple cloning site (polylinker), containing sites for different restriction endonucleases, and primer sequences (universal and reverse primers) necessary for DNA sequencing. The PCR products can be inserted in the linearized vector between part of *LacZ* gene, which has single, overlapping deoxythymidine (T) residues. The pGEM®-T Easy vector map is presented in Figure 2.1. For cRNA preparation the pSPORT1 vector with hOCT3 cloned in 5' Sall and 3' NotI sites was used. The pSPORT1 vector map is present in Figure 2.2.

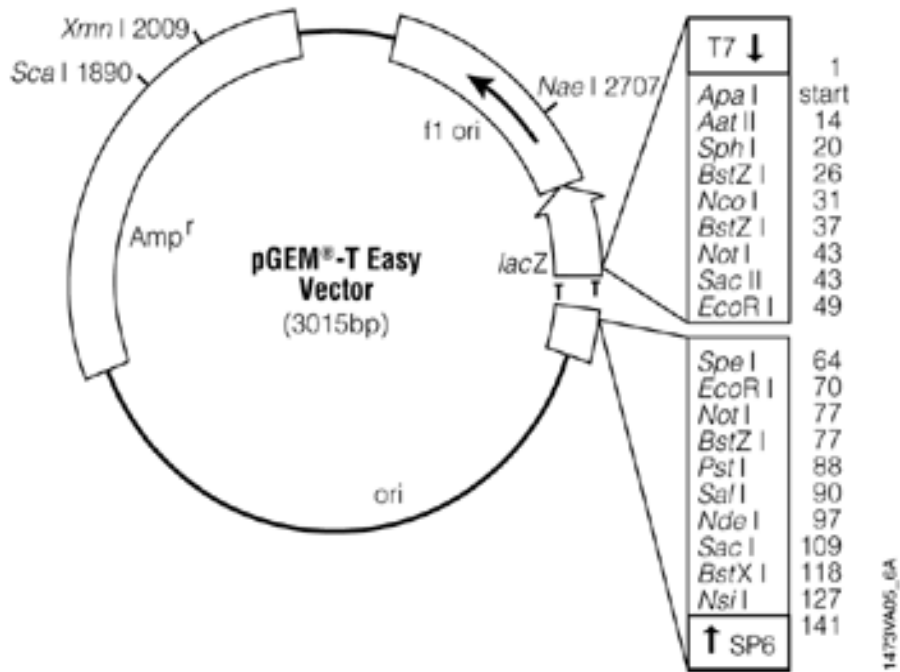


Figure.2.1 Structure map of the pGEM-T Easy vector.

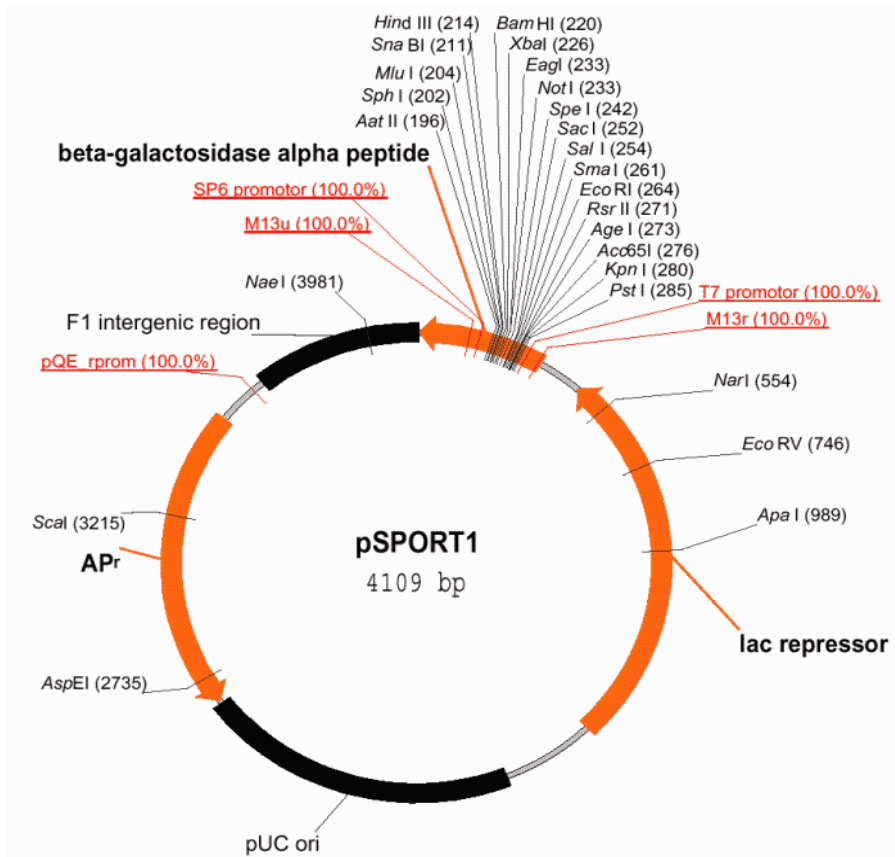


Figure 2.2 Structure map of pSPORT1 vector

### 2.1.6. Used kits

Application	Kit	Manufacturer
Bacterial plasmid purification	NucleoSpin Plasmid Kit	Macherey-Nagel
PCR product purification	NucleoSpin Extract Kit	Macherey-Nagel
TA cloning	pGEM®-T Easy Vector System II	Promega corporation
cRNA synthesis	mMASSEGE mMACHINE® T7	Ambion
ATP amount measurement	ATP Kit SL	Biothema

Table 2.10 Kits used in this work

### 2.1.7 Software

Program	Usage	Reference
Chromas	Sequence reading program	Technesium Pty Ltd
DNAMAN	Primer design	Lynnon Ltd
Microsoft Excel	Evaluation of uptake and sensitivity experiments	Microsoft Corporation
Sigma Plot	Graphic preparation	Jandel Corporation
EndNote	Managing of bibliographic references	Wintertree Software Inc.
Vector NTI	DNA alignment, cloning	Invitrogene Corp.

Table 2.11 Installed software

Online used software		
Program	Usage	Reference
Entrez Browser	Sequence retrieval, paper searching	<a href="http://www.ncbi.nlm.nih.gov/Entrez/">http://www.ncbi.nlm.nih.gov/Entrez/</a>
Blast	Sequence alignment	<a href="http://www.ncbi.nlm.nih.gov/blast/Blast.cgi">http://www.ncbi.nlm.nih.gov/blast/Blast.cgi</a>
Nebcutter	Restriction enzyme test	<a href="http://tools.neb.com/NEBcutter2/index.php">http://tools.neb.com/NEBcutter2/index.php</a>

Table 2.12 Software available on-line

### 2.1.8 Equipment

Real-time PCR amplifcator	Abi Prism 7000	Applied Biosystems (Laguna Beach CA,USA)
Centrifuges	Biofuge fresco	Heraeus (Osterode, Germany)
Circulating water baths	D8	Haake (Karlsruhe, Germany)
Dissection microscope	Stemi1000	Zeiss (Jena, Germany)
Gel chamber	Midi	MWG-Biotech (Ebersberg, Germany)
Gel documentation	Gel Print 2000 I	Biophotonics (Ann Arbor, MI, USA)
Electroporator	Easyject	Equibio (Monchelsea, England)
Microwave	Privileg 8017	Quelle Schikedanz (Fürth, Germany)

Nanoliter injector		World Precision Instruments (SarasotaFL, USA)
pH meter	pH-Meter 611	Orion Research Inc (Beverly MA, USA)
Power pack	P24	Biometra (Göttingen, Germany)
	LKBBromma2297	Pharmacia (Uppsala, Sweden)
Scintillation counter	1500 Tri-Carb	Packard Instrument Co (Meriden CT,USA)
	2100 TR	Packard Instrument Co (Meriden CT,USA)
Shaking incubator	3031	GFL (Burgwedel, Germany)
Spectrophotometer	GeneQuant II	Pharmacia (Uppsala, Sweden)
Speed vacuum concentrator	SVC 100E	Savant (Holbrook NY, USA)
Thermocycler	PTC-200	MJ Research (Watertown MI, USA)
UV transilluminator	TM40	UVP Inc (Upland, CA, USA)
Vortexer	MS1	IKA (Staufen, Germany)
Multi-plate reader	Mithras LB 940	Berthold (Wildbad, Germany)
Microscope	Wild M3C	Leica Microsystems (Wetzlar, Germany)
Electro measurement unit	Model OC 725-C	Warner instruments corporation, (Hamden, USA)
Two channel paper plotter	model BD 112	Kipp & Zonnen(Delft, Netherlands)

Table 2.13 Equipment used for work



## 2.2. Methods

### 2.1.1. Renal cancer cell (RCC) lines.

#### **A498 cell lines (Renal epithelial cell carcinoma cell line)**

ATCC Number	HTB-44 <sup>TM</sup>
Organism	Homo sapiens (Human female 52 years)
Source	Kidney
Disease	Carcinoma
Growth properties	Adherent
Morphology	Epithelial

#### **LN 78 (Clear renal cell carcinoma)**

Organism	Homo sapiens (Human female 73 years)
Source	Kidney
Disease	clear renal cell carcinoma
Growth properties	Adherent
Morphology	Epithelial

#### **786-O (renal cell adenocarcinoma cell line)**

ATCC Number	CRL-1932
Organism	Homo sapiens (Human Caucasian male 58 years)
Source	Kidney
Disease	renal cell adenocarcinoma
Growth properties	Adherent
Morphology	Epithelial

### **ACHN (renal cell adenocarcinoma cell line)**

ATCC Number	CRL-16112
Organism (years)	Homo sapiens (Human caucasian male 22 years)
Source	Kidney
Disease	renal cell adenocarcinoma (derived from metastatic site: pleural effusion)
Growth properties	Adherent
Morphology	Epithelial

### **RCCNG1**

Primary cell culture

#### *2.2.2. Cell culture*

For the expression studies of uptake transporters, 5 cell lines derived from kidney tumor tissue were used: A498, ACHN, LN78, RCCNG1 and 786-O. All cell lines were kindly provided by Dr. Hassan Dihazi and Prof. Dr. Gerhard A. Müller, Dept. of Nephrology, Uni-Klinikum, Göttingen. To investigate the interaction of anionic cytostatics with the organic anion transporters we used HEK-293 cells stably transfected with OAT1 or OAT3.

The cells were cultivated in Quantum 263 (RPMI 1640 based medium supplemented with chelated iron and growth factors) or Trex (High glucose DMEM medium, 10% fetal bovine serum, 5 µg/ml blascitidine, 2 mM L-glutamine) medium at 37°C, and 5% CO<sub>2</sub>. The media were supplemented with 100 U/ml penicillin and 100 µg/ml streptomycin. For harvesting, the cells were washed with PBS (140 mM NaCl, 8 mM Na<sub>2</sub>HPO<sub>4</sub>, 1 mM KH<sub>2</sub>PO<sub>4</sub>, 1 mM KCl) and incubated 5 -10 min with Medium C (1 mM EGTA, 85 mM NaCl, 17,5 mM NaHCO<sub>3</sub>, 3,9 mM KCl, 0,8 mM KH<sub>2</sub>PO<sub>4</sub> and 10 mM glucose). After the incubation the cells were intensively mixed with medium for detaching from the

plastic dish. The cell suspension was transferred to 15 ml falcon tubes. After the centrifugation for 5 min at 1000 rpm the cells pellet was resuspended in medium and seeded in culture dish, 24 well plates or used for RNA extraction.

### *2.2.3. RNA preparation*

For the RNA preparation the cells were harvested at 90 -100% of confluence and the total-RNA extraction was carried out by an RNA isolation kit (Promega). The RNA isolation was performed according to the manufacturer's protocol. Briefly, the pellet of  $1 \times 10^6$  cells was resuspended in 175  $\mu$ l of Lysis Buffer. The suspension was diluted with Dilution Buffer and heated for 3 min at 70 ° C and centrifuged for 10 min at 14,000 rpm. The supernatant was transferred to a new tube and after addition 200  $\mu$ l of 95% ethanol the samples were mixed by intensive pipetting. To separate nucleic acids from solution the silica spin column was used. Nucleic acid bound to the spin column was washed once with Wash Buffer. After the washing, bound DNA contaminants were removed by treatment with a DNase mix for 15 min at room temperature. The reaction was stopped by addition of 200  $\mu$ l DNase Stop Solution. Spin column was washed twice with Washing Solution, dried by centrifugation for 2 min at 14,000 rpm. Bound total RNA was eluted with 30 -100  $\mu$ l of nuclease-free water. The amount and quality of total RNA was measured with spectrophotometer.

### *2.2.4. cDNA synthesis*

Total RNA was used for the preparation of cDNA. For this purpose, Promega Reverse Transcription MuLV reverse polymerase RNase H (-) point mutant was used. The reaction mix consisted of: RT reaction buffer 5 x (100 mM Tris-HCl (pH 9.0 at 25°C), 500 mM KCl, 1% Triton® X-100), dNTP 500  $\mu$ M of each,

MuLV polymerase 200 U, random primer N<sub>6</sub> 2,5 µg/µl, total RNA 2 µg, and nuclease free water up to the volume of 20 µl. The reaction mixture was divided into two mix parts: the first containing total RNA, random primer, water, and the second mix with buffer, dNTP and MuLV polymerase. The first mix was heated to 70° for 5 min to denature the RNA, and then cooled down on ice for 2 min. Then, the second mix was added and the reaction was carried out for 60 min at 37°C. After the incubation, the mixture was incubated for 10 min at 70°C in order to deactivate the MuLV polymerase. Prepared cDNA stock was diluted at a ratio of 1:3 with nuclease-free H<sub>2</sub>O and stored at -20°C.

#### *2.2.5. Polymerase chain reaction*

To evaluate the expression level of the uptake transporters, the polymerase chain reaction (PCR) was performed on the obtained cDNA samples. The PCR components were mixed as follows: Master Mix to 50 µl total volume: 10x Buffer (10 mM Tris-HCl (pH 9.0 at 25°C), 50 mM KCl and 0.1% Triton® X-100 ), 200 µM dNTP of each, reverse and forward primer 20 pmol of each, nuclease free water till 50 µl. Then the tubes with reaction mixture were placed in a thermocycler, and the following PCR program was used: initial denaturation for 3 min at 94°C, then 35 to 40 cycles at 94°C and 40 sec denaturation, 50 sec of annealing at the temperature specific for each pair of primers (Table 2), and 60 sec at 72°C for elongation. The total PCR reaction was finished with 5 min of elongation at 72°C. To avoid nonspecific reactions, the annealing temperature was tested for each primer pair prior to the expression studies. For the testing, the plasmids containing the DNA sequences of relevant transporters were used.

### *2.2.6. Agarose gel electrophoresis*

For the visualization of PCR fragments (300-600 bp), 1% agarose gels were used. Gels were prepared from solid agarose that was boiled in 1 x TBE (Tris 0.89M, EDTA-Na<sub>2</sub> 20 mM, 0.89 M H<sub>3</sub>BO<sub>3</sub>) buffer. After the complete dilution, the solution was cooled down to 70° C and EtBr (ethidium bromide) was added to a final concentration of 0.5 µg/ml. The solution was then immediately poured into the mold. After the agarose polymerization (30 min) the samples were run for 1-1.5 h at 80-120V. The results were visualized and photo-documented by a Dual Intensity Ultraviolet Transilluminator. Before the PCR of target gene the cDNA amounts used for reaction were equilibrated in accordance to the amount of signal obtained from the PCR analysis of the GAPDH, housekeeping gene in the corresponding sample.

### *2.2.7. TA cloning*

The verification of PCR product was provided by sequencing. Before the sequencing procedure the PCR product was cloned into the pGEM T Easy vector with the use of the pGEM®-T Easy Vector System II kit. The desired PCR product was purified from the agarose gel with the use of DNA NucleoSpin® Extraction II kit (the piece of the agarose gel containing the relevant band was cut and then melted in NT buffer). Then the PCR product was bound to NucleoSpin® Extract II column and washed once with NT3 buffer. After that, the DNA was eluted from the column with Elution Buffer and the amount and quality of DNA were measured with a spectrophotometer.

After cleaning of PCR fragment the ligase reaction was set up as follows: Ligase buffer 2x (60 mM Tris-HCl (pH 7.8 at 25°C), 20 mM MgCl<sub>2</sub>, 20 mM DTT and 2 mM ATP), pGEM-T vector 5 ng/µl, PCR product in the relevant amount,

nuclease free H<sub>2</sub>O to 10 µl of the end volume. The amount of the PCR product used for ligase reaction was calculated according to the formula:

$$\frac{ng(vector) \times Kb(insert\ size)}{Kb(vector\ size)} \times \frac{insert}{vector} (molar\ ratio) = ng(insert)$$

The ligation reaction was performed at 4° for 16 h. The products of the ligase reaction were further used for the transformation of the *E.coli* JM109 strain. For this purpose, the chemically competent JM109 *E.coli* cells were thawed on ice. Then, 1-2 µl of ligase reaction was added to the vial containing 50 µl of bacterial cell pellet and incubated for 30 min on ice. After the incubation the vial was transferred to water bath and heat shocked for 45 s at 42° C. For the heat shock, the vial was transferred on ice for 2 min and then the pellet was resuspended in 800 µl of pre-warmed LB medium and incubated for 1h at 37°C with vigorous shaking. During this process, only the transformed bacterial cells gained antibiotic resistance and were able to grow on Petri dishes with 1,5% agar containing 100 µg/ml ampicillin. Thus, the bacteria were spread on the agar plate and incubated for 16-24 h for white-blue screening.

As the target gene insertion in the vector occurred in the β-galactosidase sequence, the bacteria containing the vector with insertion lost their capability to gain a blue color when growing on X-gal (5-Bromo-4-chloro-3-indolyl β-D-galactopyranoside) and IPTG (isopropyl β-D-1-thiogalactopyranoside) containing medium. Thus, after incubation on ampicillin-X-gal-IPTG containing plate, only white ones were selected. Then, the colonies were transferred to LB medium with 100 ng/ml of ampicillin and incubated at 37°C with vigorous shaking over night. Small drops of bacterial biomass were used for the PCR-test, after which the positive clones were selected for plasmid DNA preparation.

### *2.2.8. Bacterial plasmid DNA preparation*

For plasmid DNA preparation the NucleoSpin® Plasmid kit based on the alkali lysis principle was used. Bacterial pellet was mixed with 250 µl of buffer A1 containing RNase A. After 5 min of incubation 250 µl of buffer A2 was added and the bacterial cells were lysed by gentle mixing. For precipitation of proteins and genomic DNA, 300 µl of buffer A3 was used with further centrifugation for 10 min at 14,000 rpm. The supernatant was transferred to NucleoSpin® silica column and after the binding the plasmid DNA was washed once with 500 µl of AW buffer to avoid contamination with protein and once with 600 µl of A4 buffer. Then, the plasmid DNA was eluted with the use of Elution buffer and DNA amount and quality were measured with a spectrophotometer.

### *2.2.9. Plasmid DNA restriction*

For restriction reaction the following reaction mixture was prepared: 5 µl 10× reaction buffer (type depend from desired restriction enzyme), 0.5 µl 100× BSA solution, 10 µg plasmid DNA, 5-25 U restriction enzyme. The reaction runs for 3-4 h at 37°C. After 0.5-1 µl of reaction mixture was analyzed on an agarose gel. When the digestion was proven the reaction mixture was purified by NucleoSpin Extract Kit as described previously.

### *2.2.10. cRNA synthesis*

For oocyte transport experiments, specific hOCT3 cRNA was synthesized. All specific reagents and enzymes were obtained from the Ambion mMASSEGE mMACHINE® T7 Kit. pSPORT1 plasmid DNA with cloned hOCT3 cDNA was

used for synthesis. Plasmid DNA before reaction was treated by BamHI endonuclease where digest site on 3'-end of hOCT3 cDNA insert to produce a linear plasmid structure. The reaction mixture was prepared by Ambion mMASSEGE mMACHINE® T7 Kit reagent: 10 µl (2× NTP mix), (2 µl 10× reaction buffer contain T7 primer), 2 µl (10× enzyme mix contain T7 RNA polymerase), 1 µg plasmid DNA, nuclease free water till 20 µl end volume. The reaction mixture was incubated for 1,5-2 h at 37°C. After incubation plasmid DNA was degrade by 1 U TURBO DNase for 15 min at 37°C. Before usage, the cRNA was purified. To the reaction mixture was added 15 µl of 5 M ammonium acetate, 115 µl nuclease free water and 150 µl 2-propanol. For sedimentation of the cRNA reaction, the mixture was centrifugated for 45 min at 13,000 rpm. The resul precipitate was washed twice with 70% ethanol and dried for 15 min at RT. Dried cRNA was dissolved in 15 µl nuclease-free water. Concentration and quality was measured with a spectrophotometer at  $\lambda=260\text{nm}$  and the amount was calculated by the formula  $C = 40 \times OD$  were 40 is the coefficient for RNA. Quality was calculated by the formula  $R = \frac{OD_{\lambda=260}}{OD_{\lambda=280}}$ .

### *2.2.11. DNA sequencing*

The sequencing of target DNA was performed by the dye terminator cycle sequencing method (Applied Biosystems) at the Department of the Biochemistry, Göttingen University. The sequencing PCR mixture was prepared as follows: Reaction setup: 6 x SeqMix, 5x Buffer, 10 pmol primer, 300 ng of plasmid DNA, HPLC grade H<sub>2</sub>O to 10 µl of end reaction volume. One of the system component sequence MIX included four types of ddNTP labeled with four different fluorescent dyes and unlabeled dNTPs. In each amplification cycle thermostable polymerase produced casual length ssDNA product with has at the 3'-prime end one of the fluorescently labeled ddNTP. After the reaction, newly synthesized DNA was transferred into a clean tube. For DNA



precipitation, 50 µl of 100% ethanol with 1 µl of 3 M Na acetate, 1 µl of 125 mM EDTA were added and incubated for 5 min. After the precipitation, DNA was sedimented by centrifugation for 20 min at 14,000 rpm. DNA pellet was washed once with 70% ethanol, dried on air for 10 min, resuspended in 30 µl of HPLC grade water and sent to the Biochemistry Department. The obtained sequences were analyzed by ClustalW <http://bioweb.pasteur.fr/seqanal/interfaces/clustalw.html> or Blast <http://www.ncbi.nlm.nih.gov/BLAST/> online software.

### *2.2.12. Real-time PCR*

For the quantification of the target gene expression levels we used the real-time PCR. Two approaches in real-time PCR were used: SYBR Green I and TaqMan based methods as described before [103]. For the TaqMan based PCR the reaction mix included 2 x reaction buffer, 20x TaqMan probe, 5 µl of cDNA, nuclease free H<sub>2</sub>O till the volume of 25 µl. The thermocycler was programmed as follows: 2 min at 52°, 10 min at 95° and 40 cycles, including 15 s at 95° and 1 min at 61°C. The SYBR Green I reaction setup included: reaction buffer 2x, forward primer and reverse primer 10 mM of each, cDNA 5 µl from RT-mixture, nuclease free H<sub>2</sub>O till 25 µl. The thermocycler was programmed as previously described for TaqMan.

In order to evaluate the expression levels of the target gene, two approaches were used, which were appropriate for SYBR Green and TaqMan based PCR. To evaluate the results of SYBR Green based real-time PCR we used the same target DNA sequence, obtained via TA-cloning, which was added to the reaction mix in a known copy number. The expression level was then estimated by the comparison of signals from the cloned DNA with the signals from the studied samples, in a way previously described [104]. Additionally, for the verification of the SYBR Green based real-time PCR results we analyzed the

melting curves of an obtained product. For the analysis of TaqMan based real-time PCR data  $\Delta C_t$  evaluation method was used as described before [105].

#### *2.2.13. Radioactive transport studies in CHO cell stably transfected with hOCT3*

The cells were cultured in 24 well plates and grown until they reached 90 -100% of confluence. After that, the cells were washed three times with Mammalian Ringer solution (130 mM NaCl, 4 mM KCl, 1 mM CaCl<sub>2</sub>, 1 mM MgSO<sub>4</sub>, 20 mM HEPES, 1 mM NaH<sub>2</sub>PO<sub>4</sub>, 18 mM Glucose). The radioactive substrates were diluted for desired final concentration (e.g. 1  $\mu$ M [<sup>3</sup>H]MPP) in Mammalian Ringer Solution, transferred to each well and incubated for 15 min. After the incubation, the plate was washed with ice cold PBS solution and the cells were lysed by addition of 500  $\mu$ l 1N NaOH for 20 min. After the lysis the solution was neutralized with 1N HCl and transferred to scintillator vial. Upon the addition of 2,5 ml of Lumasafe scintillation solution the results were obtained after 5 min of radioactivity counting in a scintillation counter (TriCarb 1500 Packard).

#### *2.2.14. [<sup>3</sup>H]thymidine incorporation assay*

The cells were incubated for 1 h with cytostatic drugs at different concentrations. After the incubation the cells were washed twice with medium. The radioactive thymidine was diluted with the medium to the final activity of 0.2-1  $\mu$ Ci/ml. After 30 min incubation at 37°C, the cells were fixed with 5% trichloroacetic acid for 30 min at 4°C. The plate was then washed twice with 500  $\mu$ l of ice cold PBS and once with 500  $\mu$ l of ice cold 95% ethanol. For the full solubilisation of genomic DNA, the plate was incubated with 500  $\mu$ l of 1N NaOH overnight. After the incubation, the solution was neutralized with 500  $\mu$ l of 1N

HCl and then transferred to scintillator vials together with 2.5 ml of Lumasafe scintillation fluid. The results of the experiment were obtained after 5 min of the counting of incorporated radioactivity in the scintillation counter (TriCarb 1500 Packard).

#### *2.2.15. BrdU incorporation method (ELISA)*

The amount of 10000 cells was seeded into 96 well plates and grown until reaching 50-70% confluence. The cells were then incubated for 1 h with the desired cytostatics and washed 2 times with the medium. After that, BrdU (Bromo-deoxyuridine) in the final concentration of 10  $\mu$ M was added and incubated for 1 h. The cells were fixed with 70% ethanol for 30 min and washed 3 times with PBS. To denature double-stranded DNA, cells were incubated for 30 min with the solution containing 4N HCl and 0,5% Triton X-100. After incubation, the solution was washed out and the DNA mixture was neutralized with 0.1N  $\text{Na}_3\text{BO}_3$  solution for 5 min and washed with PBS 3 times. For blocking of non-specific binding sites, the plate was incubated with 5% non fat milk, 0.1% Tween 20 for 3 h. After the blocking step, the plate was incubated with anti-BrdU antibody coupled with horse raddish peroxidase (Abcam) diluted 1:500 in blocking solution for 3 h. At the end, non-bound antibodies were removed by washing 3 times with 0.1% Tween 20.

Evaluation of BrdU incorporation was provided by the visualization of peroxidase reaction with the use of specific substrate TMB (3,3',5,5'-Tetramethylbenzidine) in the solution including: 50 mM phosphate-citrate buffer, 0.1mg/ml of TMB, 0.006%  $\text{H}_2\text{O}_2$ ). The plates were incubated with TMB-solution from 10 to 20 min, until a deep blue color was obtained. Then the reaction was stopped with 0.1 M  $\text{H}_2\text{SO}_4$  and the measurements were performed on  $\lambda=570$  nm using Multi-plate reader Mithras LB 940 (Berthold).

### 2.2.16. MTT assay

Cells in an amount of  $2 \times 10^4$  were seeded on 96 well plates and grown 24h till reaching 50-70% of confluence. Then the plate was incubated with the desired cytostatics of different concentrations. After incubation, cells were incubated in normal medium for addition of 24 h.

Surviving was evaluated by incubation with 7.5  $\mu\text{g/ml}$  MTT ((3-(4,5-Dimethylthiazol-2-yl)-2,5-diphenyltetrazolium bromide, a tetrazole) dissolved in normal medium. The chemical reaction is shown schematically in Figure 2.3.

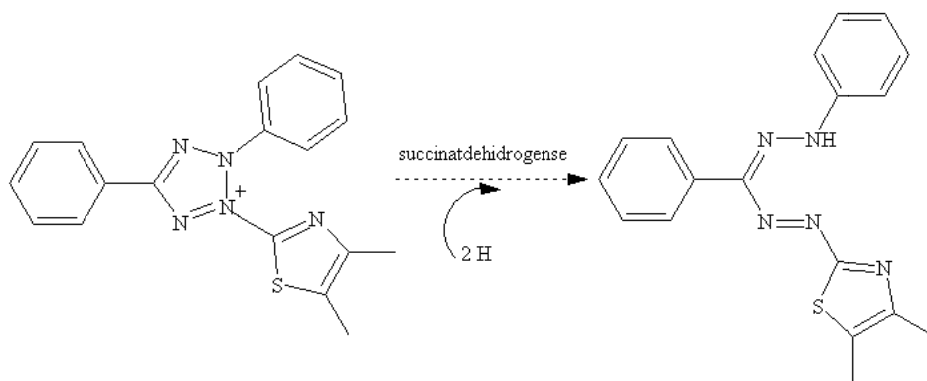


Figure 2.3 Reduction of MTT to formazan blue

To obtain blue crystals of MTT formazan, a 4 h incubation was provided. To dissolve MTT crystals 1:1,5 w/w acidified isopropanol (96% isopropanol, 4% 1n. HCl w/w) was added to the medium. Absorbance measurement was performed using the Multi-plate reader Mithras LB 940 (Berthold) and calculated by formula the  $D = D^{\lambda=620} - D^{\lambda=595}$ .

### 2.2.17. Comet assay

For investigation of cytotoxic activity of topoisomerase I inhibitors, the alkaline single cell gel electrophoresis (Comet assay) was used.  $2 \times 10^5$  cells were transferred onto 24 well plates and grown till 80-90% confluence. After cytostatic treatment,  $1 \times 10^4$  cells were mixed with 85  $\mu$ l 0.5% low-melting agarose and transferred on cover slips covered by 300  $\mu$ l 0,6% normal melted agarose. Cover slips were cooled down in ice bath for 30 min. For release of DNA from cells, cover slips with agarose slices were incubated in lysis buffer (10 mM tris-HCl pH 10, 2,5 M NaCl, 100 mM EDTA, 1% Triton X-100, 10% DMSO) 1 h at 4°C. After lysis, cover slips were transferred into an electrophoresis chamber and covered by electrophoresis buffer (300 mM NaOH, 1 mM EDTA pH 13). Electrophoresis was performed at 25V, 300 mA (0,66 V/cm), for 30 min. To neutralize agarose, slices were washed 3 $\times$  in neutralization buffer (Tris-HCl 400 mM pH7.4). Released DNA was stained by 60  $\mu$ l EtBr solution for 10 min. Cover slips were examined on fluorescent microscope 400 $\times$  with excitation filter at  $\lambda=510-590$ .

### 2.2.18. Intracellular ATP concentration measurement

ATP level was measured using the ATP Kit SL with modification. Cells were grown in 96 well plates till 50-60% confluence. After treating with cytostatics and incubating in normal medium for 24-48 h, the ATP level was measured. Cells were lysed in lysis buffer (20 mM Tris-HCl pH 8.0, 150 mM NaCl, 1 mM EDTA pH 8.0, 0.5% Triton X-100) for 15 min at RT. Therefore, cell extracts were diluted 1:20 with lysis buffer. 5  $\mu$ l of sample was transferred into the reaction mix (160  $\mu$ l Tris-EDTA buffer, 40  $\mu$ l SL-reagent). Luminescence was measurement using the Multi-plate reader Mithras LB 940 (Berthold). To reaction mix containing sample 10 $\mu$ l diluted ATP standard was added, and

luminescence measuring was repeated. The amount of ATP was calculated using the formula  $ATP_{smp} = \frac{10^{-7} \times I_{smp}}{(I_{smp+std} - I_{smp})}$  where  $I_{smp}$  is the sample luminescence,  $I_{smp+std}$  is the sample luminescence after adding the ATP standard,  $10^{-7}$  concentration of ATP standard (mol/l).

#### 2.2.19. Expression of hOCT3 in *Xenopus laevis* oocytes

*Xenopus laevis* oocytes were used as expressing system for hOCT3 protein. Oocytes were injected with cRNA from the full clone of hOCT3. After 3 days of expression, oocytes were used for [<sup>3</sup>H]MPP uptake and electrophysiological investigation.

#### 2.2.20. Preparation of *Xenopus laevis* oocytes

Individual stage V-VI oocytes were defolliculated by collagenase treatment. This procedure involved an overnight incubation of several ovarian lobes in 20 ml Barth's solution (88 mM NaCl, 1 mM KCl, 0.3 mM Ca(NO<sub>3</sub>)<sub>2</sub>, 0.41 mM CaCl<sub>2</sub>, 0.82 mM MgSO<sub>4</sub>, 15 mM HEPES, 12 µg/ml gentamycin, pH set to 7.4) containing 0.5 mg/ml collagenase (Type CLSII, Biochrom KG) at 18°C. On the following day, oocytes were washed several times with oocyte Ringer's solution (ORI) (90 mM NaCl, 3 mM KCl, 2 mM CaCl<sub>2</sub>, 1mM MgCl<sub>2</sub>, 5 mM HEPES, pH was set to 7.4 ), incubated for 10 min in Ca<sup>2+</sup> free medium and then washed again 2-3 times with ORI solution. Oocytes were sorted and the "healthy" looking oocytes were used for the cRNA injection.

### *2.2.21. Oocyte injection*

cRNA was injected into the oocyte using a nanoliter microinjector with glass capillaries (Word Precision Instruments). In each oocyte 5-20 ng of cRNA in 22-50 nl volume was injected. As negative control, oocytes injected by water were used. For injection oocytes were mechanically fixed in a microwell on a plastic chamber filled with ORI solution. After cRNA injection oocytes were transferred into 24 well cell culture plates with Barth's solution. For expression injected oocytes were incubated 3 days at 18°C. Barth's solution was changed every 24 h and damaged oocytes were separated from healthy ones.

### *2.2.22. Oocyte uptake experiments*

Surviving oocytes were divided into groups containing 8-11 oocytes. Groups were transferred into 24 well plates which contained ORI uptake medium. For preparing of ORI uptake medium, [<sup>3</sup>H]MPP 0.25 µCi/ml (4-methyl-pyridinium acetate 80 Ci/mmol) was used. For inhibition studies inhibitors were dissolved in uptake ORI solution. Oocytes were incubated for 30-60 min at RT and transferred to ice-cold ORI solution to stop uptake process. To eliminate contamination from uptake solution, oocytes were washed 3 times. Then single oocytes were isolated from groups and transferred individually to the scintillation vial. To dissolve oocytes, 250 µl of 1N NaOH was added to the scintillation vial. After 2h incubation with shaking, alkali solution was neutralized by 250 µl 1N HCl. Upon the addition 2.5 ml of Lumasafe scintillation solution radioactivity was counted in the scintillation counter (TriCarb 1500 Packard).

### 2.2.23. Two-electrode-voltage-clamp measurement in *Xenopus laevis* oocytes

This method is based on the measurement of transport-mediated current at fixed membrane potential. Figure 2.4 shows schematically the setup.

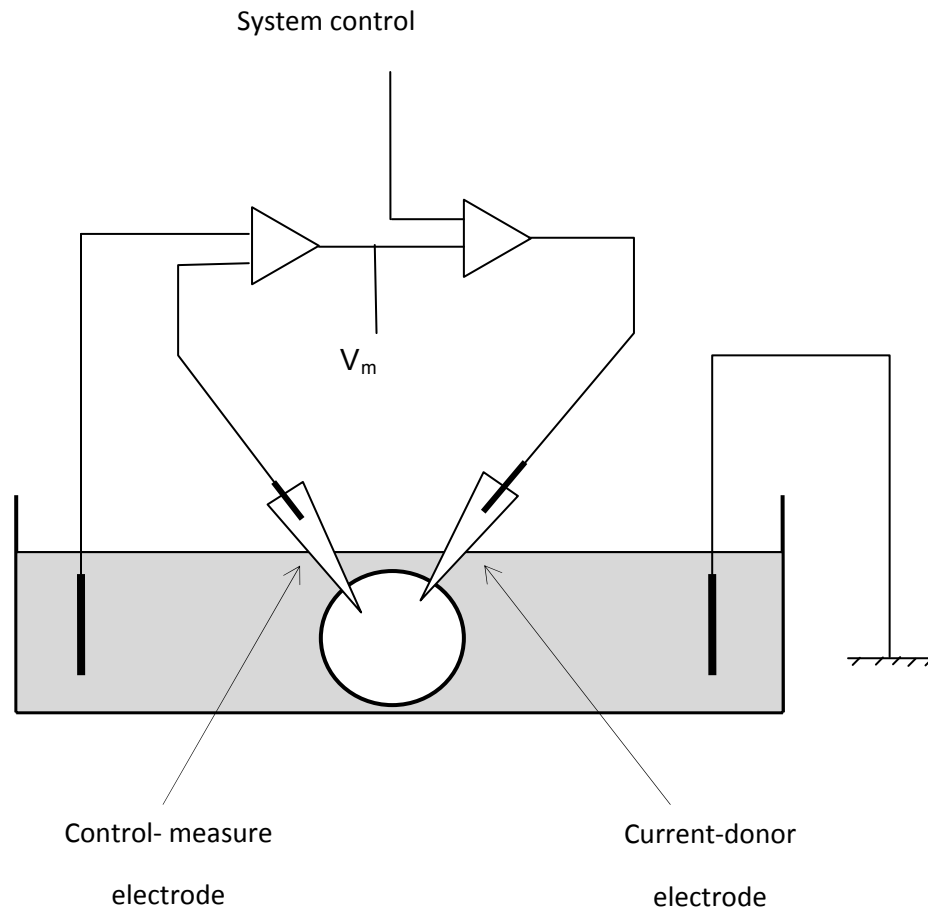


Figure 2.4 Principle scheme for current measuring.

After 3 days expression, oocytes were washed in ORI solution. Each oocyte was transferred into a plastic perfusion chamber. Before manipulation, glass electrodes (Borosilicate glass, Hihgenberg) were filled with 3M KCl solution. The chamber was connected to ground. In first control electrode was impaled into the oocyte. Therefore, the oocyte was transferred into the second position



in chamber and the current-donor electrode was introduced. Then, the oocyte was fixed and perfusion was started (4ml/min). Intracellular voltage was observed at the central control unit (Model OC 725-C, Warner instruments corporation, Hamden, USA). The usual voltage level for healthy oocyte was observed at -29 to -37mV. For stabilization, the oocyte was perfused for 10-20 min and the voltage level was controlled. In a stable oocyte, voltage did not change more than 2-3 mV. Therefore, the oocyte voltage level was clamped to -60 mV. Perfusion was prolonged for additional 10 min to observe the oocyte's current stability. For experimental procedure, different test substances were dissolved in ORI solution. Measurement was performed by perfusion of the clamped oocyte by different concentrations of test substances. Current changes were recorded on paper by a two channel paper plotter.

## 3. Results

### 3.1 RT-PCR analysis of transporter expression in kidney cancer-derived cell lines and tissue samples

To explore the expression level of the uptake transporters in the tumor cells we performed a semi-quantitative RT-PCR for selected transporter proteins. The sequence data were obtained from the NCBI database ([www.ncbi.nih.gov](http://www.ncbi.nih.gov)) and the primers were designed with the use of NCBI online software. The cell lines were obtained from the Dept. of Nephrology, and the kidney tumor as well as the normal kidney tissues from the same patient was kindly provided by the Dept. Pathology of the Universität klinikum, Göttingen, respectively.

The results of PCR screening are shown in the following tables. They are presented as semi-quantitative estimation from the agarose gel. We evaluated our data by Gel Pro Analyser. Gels were saved as picture file in .jpg format. The program counted white pixels in marked bands. Expression of single genes was divided by expression of GAPDH in the same sample. After evaluation of gene expression, ratio numbers were estimated. If the ratio of gene/GAPDH was  $<2$ , expression was counted as +,  $<3 = ++$ ,  $<4 = +++$ ,  $<5 = ++++$  (Figure 3.1, Table 3.1). The results were additionally proven by sequencing of each PCR fragment and further sequencing analysis with a data bank (CrustalW software).

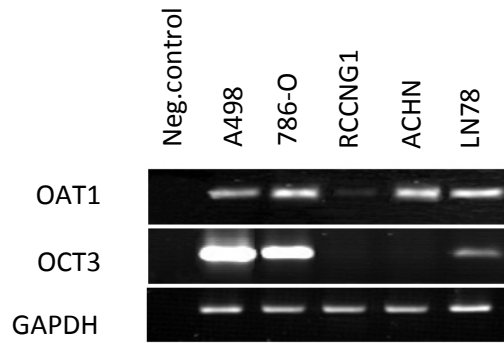


Figure 1.1 Representative gel for gene expression evaluation

Cell line		A498	786-O	RCCNG1	ACHN	LN78
Transporter						
Ratio	OAT1	0,57	0,99	0,23	1,13	1,03
Gene/GAPDH	OCT3	5,42	4,01	0	0	1,16
Evaluation	OAT1	+	+	+	+	+
	OCT3	++++	+++	-	-	+

Table 3.1 Example of gene expression evaluation

### *3.1.1 The expression of organic anion and cation transporters (OATs and OCTs)*

#### *3.1.1.1 OAT*

The first transporter family screened with RT-PCR included organic anion transporters SLC22A6 (OAT1), SLC22A7 (OAT2), SLC22A8 (OAT3) and SLC22A11 (OAT4). Our data showed considerable variations in the mRNA levels for OATs in tumor tissue U675599T compared with normal tissue U675599N. In cell lines (786-O, A498, LN78) a medium expression level of OAT1 was observed. The cell lines RCCNG1 and ACHN had low expression levels in comparison to normal tissue. The OAT2 was detected at a low level only in the 786-O cell line. The expression of OAT2, OAT3 and OAT4 was otherwise not detected by RT-PCR in cancer cell lines.

#### *3.1.1.2 OCT*

The SLC22 organic cation transporter transporters OCT2 and OCT3 were highly expressed in the normal kidney tissue. In the tumor tissue and kidney tumor-derived cell lines 786-O and A498 SLC22A3 (OCT3) was expressed at a level similar to or higher than that in normal tissue. In RCCNG1, LN78 and ACHN cells, no or a low expression of OCT3 was found. Except normal kidney tissue and the ACHN cell line, the expression of SLC22A1 (OCT1) was not detectable with RT-PCR. The expression of SLC22A2 (OCT2) was absent in all tumor cell lines. A low expression of SLC22A16 (OCT6) was observed in A498, ACHN, tumor tissue, and normal tissue.

### The organic cation/anion/zwitterion family SLC22

Cell Trans porters	786-O	RCCNG1	A498	LN78	ACHN	U675599T	U675599N
OAT1	+	+	+	+	+	+	+++
OAT2	+	-	-	-	-	-	+++
OAT3	-	-	-	-	-	+	+++
OAT4	-	-	-	-	-	+	+
OCT1	-	-	-	-	+	-	+
OCT2	-	-	-	-	-	+++	+++
OCT3	++++	-	++++	+	-	+++	+++
OCT6	-	-	+	-	+	+	+

Table 3.2. The results of RT-PCR screening of kidney tumor cell and tissue samples for the SLC22A family. The normal tissue is marked by yellow color, and malignantly transformed tissue by blue (- no amplification, + low amplification, ++ medium amplification, +++ high amplification, ++++ very high amplification)

### 3.1.2 The expression of organic anion-transporting polypeptide transporters (OATP)

SLC21/SLCO21 proteins were shown to be functionally close to SLC22A transporter family. The RT-PCR data presented in Table 3.3 demonstrate an expression of all five types of OATPs in the cell lines 786-O and A498. The cell lines RCCNG1, ACHN, and tumor and normal kidney tissue did not express OATP-C. The OATP-A, OATP-B and OATP-E had different levels of expression in these cell lines. From the SLC21/SLCO family only OATP-B and OATP-E were expressed at high level in A498 and LN78 cells respectively. The other transporters of SLC21/SLCO family were present in the cell lines as well, but at lower levels in comparison with OATP-B and OATP-E.

#### The organic anion transporter family SLC21/SLCO

Cell Trans porters	786-O	RCCNG1	A498	LN78	ACHN	U675599T	U675599N
OATP-A	+	+	+	++	+	+++	+
OATP-B	++	+	++++	-	+	+++	+++
OATP-C	+	-	+	-	-	-	-
OATP-E	+	+	+	+++	+	+	+

Table 3.3. The results of RT-PCR screening of kidney tumor cell and tissue samples for the SLC22A family. The normal tissue is marked by yellow color, and malignantly transformed tissue by blue (- no amplification, + low amplification, ++ medium amplification, +++ high amplification, ++++ very high amplification)

### 3.1.3 The expression of sodium-coupled nucleoside transporters and equilibrative nucleoside transporters (CNT and ENT)

The nucleoside transporters are presented by two families, namely SLC 28 (sodium coupled nucleoside transporters, CNT) and SLC29 (equilibrative nucleoside transporters, ENT). The data obtained from RT-PCR analysis indicated that most of SLC28 transporters were not present in the selected cell lines. However, the A498 cell line showed a low expression of SLC28A1 (CNT1) (Table 3.4). In contrast to SLC28, the SLC29 family demonstrated high expression levels. A very high expression of SLC29A1 (ENT1) was found in all five kidney cancer cell lines. The SLC29A2 (ENT2) was expressed in almost all cell lines at different levels. The A498 did not show any expression of this transporter. The SLC29A3 (ENT3) appeared in all cell lines at a low level (Table 3.5).

**The sodium-coupled nucleoside transporter family SLC28**

Cell Trans porters	786-O	RCCNG1	A498	LN78	ACHN	U675599T	U675599N
CNT1	-	-	+	-	-	++	++
CNT2	-	-	-	-	-	-	-
CNT3	-	-	-	-	-	+	-

Table 3.4. The results of RT-PCR screening of kidney tumor cell and tissue samples for the SLC28 family. The normal tissue is marked by yellow color, and malignantly transformed tissue by blue (- no amplification, + low amplification, ++ medium amplification, +++ high amplification, ++++ very high amplification)

### The nucleoside transporter family SLC29

Cell	786-O	RCCNG1	A498	LN78	ACHN	U675599T	U675599N
Trans porters							
ENT1	++++	++++	+	++++	++++	++++	++++
ENT2	++	++	+	++++	+++	+	+
ENT3	+	+	+	+	+	+	+

Table 3.5. The results of RT-PCR screening of kidney tumor cell and tissue samples for the SLC29 family. The normal tissue is marked by yellow color, and malignantly transformed tissue by blue (- no amplification, + low amplification, ++ medium amplification, +++ high amplification, ++++ very high amplification)

#### 3.1.4 The expression of L-amino acid transporters (LAT)

The transporters LAT1 and LAT2, demonstrated a high or very high expression level in cancer cells and normal tissues. In general, SLC7A8 (LAT2) appeared to be expressed more than SLC7A5 (LAT1). The results are presented in Table 3.6.



**The cationic amino acid and glycoprotein-associated amino acid transporter family SLC7**

Cell Trans porters	786-O	RCCNG1	A498	LN78	ACHN	U675599T	U675599N
LAT1	+++	+++	+++	+++	+++	+++	+++
LAT2	+	+	+	-	+	++++	++++

Table 3.6. The results of RT-PCR screening of kidney tumor cell and tissue samples for the SLC7 family. The normal tissue is marked by yellow color, and malignantly transformed tissue by blue (- no amplification, + low amplification, ++ medium amplification, +++ high amplification, +++++ very high amplification)

*3.1.5 The expression of monocarboxylate transporters (MCT)*

The monocarboxylate transporters showed high expression levels in kidney cancer cells (Table 3.7). Among the members of the MCT family the highest expression was observed for SLC16A1 (MCT1), while SLC16A2 (MCT2), and SLC16A4 (MCT4) demonstrated less expression. In addition, the expression of SLC16A4 (MCT4) was not found in 786-O cells.

### The monocarboxylate transporter family SLC16

Cell	786-O	RCCNG1	A498	LN78	ACHN	U675599T	U675599N
Trans porters							
MCT1	++++	++++	++++	++++	++++	++++	++++
MCT2	+++	+++	+++	+++	+++	+++	+++
MTC4	-	+++	+++	+++	+++	+++	+++

Table 3.7. The results of RT-PCR screening of kidney tumor cell and tissue samples for the SLC16 family expression. The normal tissue is marked by yellow color, and malignantly transformed tissue by blue (- no amplification, + low amplification, ++ medium amplification, +++ high amplification, ++++ very high)

#### 3.1.6. The expression of sodium dicarboxylate transporters (NaDC/SLC13)

In Table 3.8 the expression levels of SLC13A3 is shown. Most of cell lines and normal tissue demonstrated the same expression level of SLC13A3 (NaDC 3). However, LN78 cells had a low expression.

### The human Na<sup>+</sup>-sulfate/carboxylate cotransporter family SLC13A3

Cell	786-O	RCCNG1	A498	LN78	ACHN	U675599T	U675599N
Trans porters							
NaDC3	+++	+++	+++	+	+++	+++	++++

Table 3.8. The results of RT-PCR screening of kidney tumor cell and tissue samples for the SLC 13 family. The normal tissue is marked by yellow color, and malignantly transformed tissue by blue (- no amplification, + very low amplification, ++ medium amplification, +++ high amplification, ++++ very high amplification)

#### 3.1.7 The expression of reduced folate and thiamine transporters

The SLC19 folate and thiamine transporter expression levels were studied in the cancer cell lines (Table 3.9). The thiamine transporter ThTr had the same level of expression as in normal tissues in all type of tested cell lines. The reduced folate transporter (RFT) expression level was higher in 786-O, LN78, ACHN, and lower in RCCNG1 and A498 cells.

### The folate/thiamine transporter family SLC19

Cell	786-O	RCCNG1	A498	LN78	ACHN	U675599T	U675599N
Trans porters							
ThTr	+++	+++	+++	+++	+++	+++	+++
RFT	++	+	+	++	++	+++	+++

Table 3.9. The results of RT-PCR screening of kidney tumor cell and tissue samples for the SLC 19 family. The normal tissue is marked by yellow color, and malignantly transformed tissue by blue (- no amplification, + low amplification, ++ medium amplification, +++ high amplification, ++++ very high amplification)

#### 3.1.8 The expression of the ATP-binding cassette (ABC) transporter family

All investigated members of ABC family (MRP1, MRP2, MRP4, and MDR1) were shown to be present in kidney malignantly transformed tissue at the same relatively high or very high level as in normal tissue (Table 3.10). Different expression levels were observed in the MDR1 transporter. The 786-O and A498 cell lines had a very high expression level even comparison to tissue samples and the cell lines ACHN and LN78 showed low expression. The RCCNG1 did not show any expression of MDR1.

### The human ATP-Binding Cassette (ABC) Transporter Superfamily

Cell	786-O	RCCNG1	A498	LN78	ACHN	U675599T	U675599N
Trans porters							
MRP1	+++	+++	+++	+++	+++	+++	+++
MRP2	++++	++++	++++	++++	++++	+++	+++
MRP4	++++	++++	++++	++++	++++	++++	++++
MDR1	++++	-	++++	+	++	+++	+++

Table 3.10. The results of RT-PCR screening of kidney tumor cell and tissue samples for the SLC 19 family. The normal tissue is marked by yellow color, and malignantly transformed tissue by blue (- no amplification, + low amplification, ++ medium amplification, +++ high amplification, +++++ very high amplification)

## 3.2 Quantification of the transporter expression levels in kidney tumor cells by real time PCR

### 3.2.1 The expression of the organic anion transporter 1 (OAT1)

After screening the expression level of the SLC transporter family in several kidney tumor cells by semi-quantitative RT-PCR, we performed real-time PCR experiments to evaluate and quantify the expression of the organic anion transporter 1 (OAT1). The real-time PCR experiments were performed using the SYBR Green I method. Figure 3.2 illustrates the results of the real-time PCR

analysis of OAT1 expression level in kidney tumor cell lines and in tumor and normal tissue. The OAT1 expression level in normal tissue is 14 times higher than in tumor tissue and 44-50 times higher than in cancer cell lines. Among all analyzed samples, the highest level of the expression (around 2500 copies) was detected in A498 and a newly added cell line, SKRC17 cells. The second place according to OAT1 expression levels is taken by LN78 and 786-O cells with around 1800 copies. The cell lines ACHN and RCCNG1 have around 800 copies.

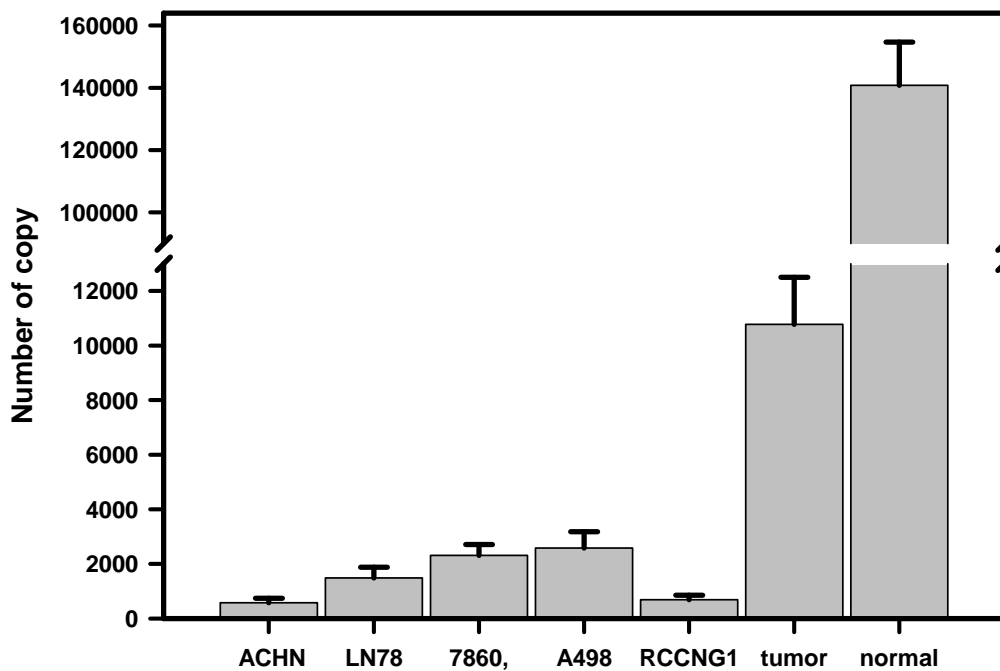


Figure 3.2. The expression level of OAT1mRNA in kidney cancer cells and tumor and normal tissues. The hOAT1 expression was equilibrated by comparison with hGAPDH and hHPRT. Means  $\pm$  SEM were calculated from three independent experiments with three repeats each.

### 3.2.2 The expression of organic anion transporter 3 (OAT3)

Figure 3.2 demonstrates the data on OAT3 expression in cancer cell lines, normal and tumor tissues. In normal tissue the levels of OAT3 expression was 3000 times higher than in malignantly transformed tissue, and 12000 times higher than in cancer cell lines. The expression levels in tumor cell lines were at the lower border of detection. Thus, the highest level of expression detected in cancer cell lines was around 600 copies per sample in SKRC17cells. The LN78 and RCCNG1 (not shown in Figure 3.3) cells had even lower expression levels, around 300 copies per sample. The cell lines 786-O and A498 contained approximately 200 copies per sample, while in ACHN the OAT3 expression was not detected.

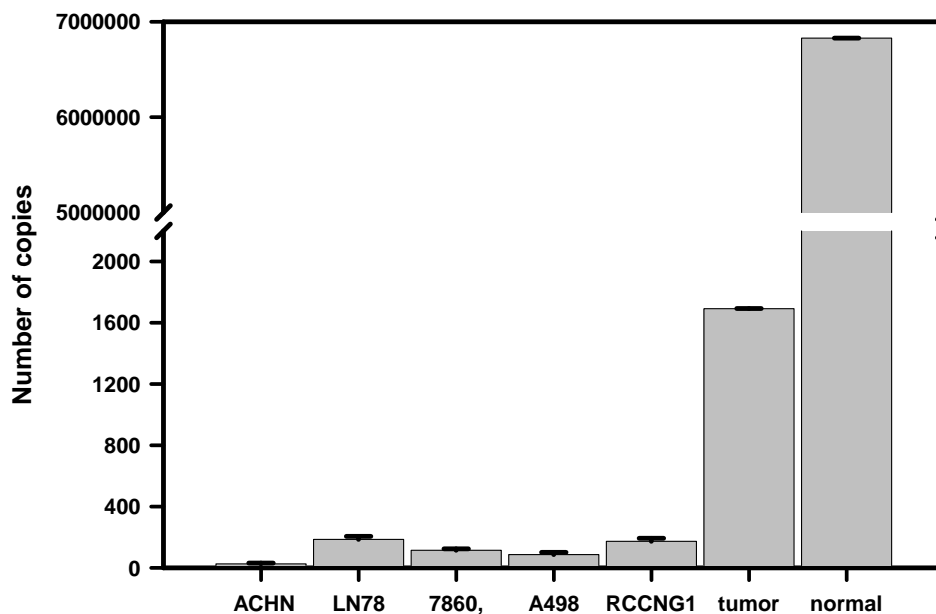


Figure 3.3. The expression level of mRNA OAT3 in kidney cancer cells and tumor and normal tissue. The hOAT3 expression was equilibrated by comparison with hGAPDH and hHPRT. Means  $\pm$  SEM was calculated from three independent experiments with three repeats each.

The comparison of obtained data for OAT1 and OAT3 expression is illustrated in figure 3.4. In normal tissue the expression of OAT3 was 10 times higher than that of OAT1. At the same time, in tumor tissue and cancer cell lines the expression levels of OAT1 were 5-6 times higher than that of OAT3.

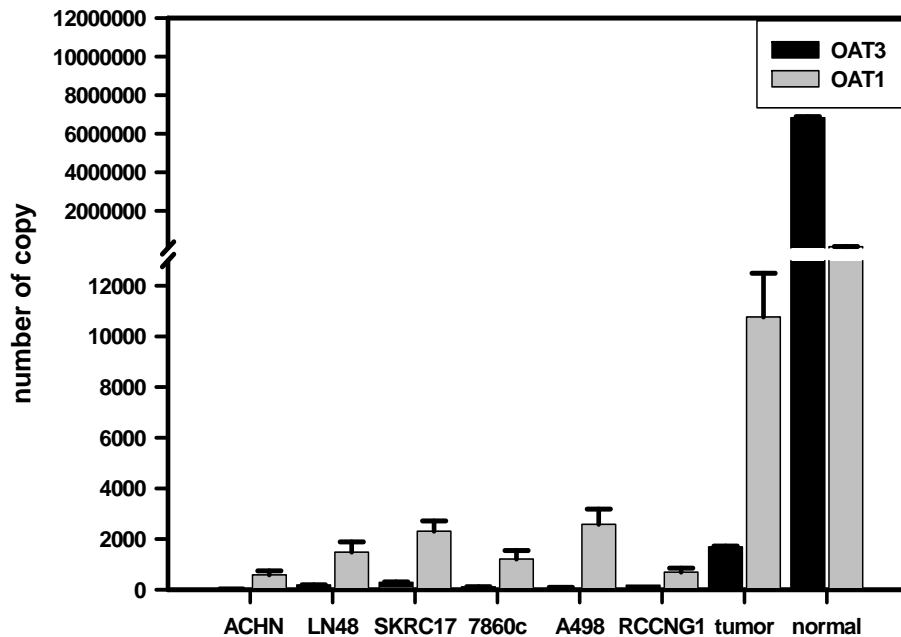


Figure 3.4 Comparison of expression levels of OAT1 and OAT3 mRNA in kidney cancer cells and tumor and normal tissue. The hOAT1 and hOAT1 expression was equilibrated by comparison with hGAPDH and hHPRT. Means  $\pm$ SEM was calculated from three independent experiments with three repeats each.

### 3.2.3 The expression of organic cation transporter 3

To more deeply study the expression of hOCT3 (SLC22A3) in RCC lines we chose five renal carcinoma cell lines, namely A498, ACHN, 786-O, RCCNG1 and LN78. Upon the RNA isolation and reverse transcription, hOCT3 expression was evaluated by TaqMan real-time PCR. The results of the real-time PCR are summarized in Figure 3.5. We demonstrate that A498 and 786-O



RCC lines have the highest hOCT3 expression levels (12.5 and 6 cycles difference compared to ACHN and RCCNG1 cells). Medium expression levels of hOCT3 were observed in LN78 (4-5 cycles differences with ACHN and RCCNG1 cells). Therefore, for the next experiments we selected A498 as highly hOCT3 expressing cells and ACHN as a cell line with very low levels of OCT3.

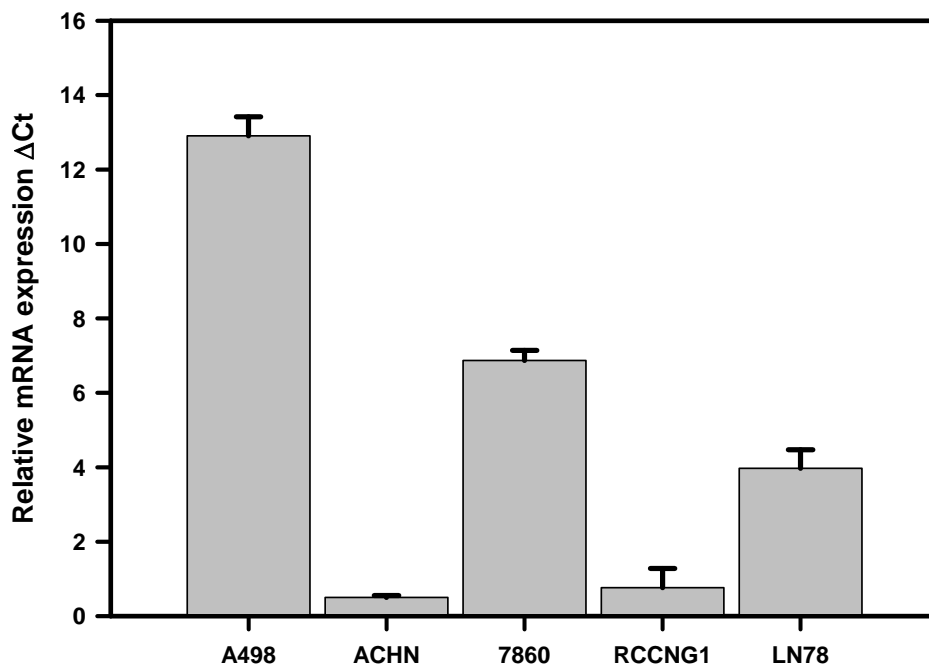


Fig. 3.5 TaqMan real-time PCR hOCT3 examination of total RNA extracted from renal carcinoma cell lines. The hOCT3 expression was equilibrated by comparison with hGAPDH and hHPRT. Data means difference between lowest expression member (ACHN) and other tested RCC lines. Means  $\pm$ SEM was calculated from three independent experiments with three repeats each.

### 3.2.4 The expression of equilibrative nucleoside transporters 1,2 and 3

The RT-PCR analysis demonstrated the expression of equilibrative nucleoside transporters in all RCC lines. To compare the ENT expression levels in more

detail the real-time TaqMan was applied. In the result it was demonstrated that in all RCC lines ENT3 had low expression, while ENT1 and 2 were expressed at different levels with an exception of A498 cells, where all the ENTs were poorly presented. ENT1 expression was 16.51 and 15.71 cycles higher in LN78 and ACHN cells respectively compared to A498 cells. In RCCNG1 and 786-O ENT1 expression was detected respectively 14.53 and 10.73 cycles earlier in comparison with A498 cells. For the expression of ENT2 these numbers were relatively moderate and comprise 10.11 cycles, 11.65 cycles, 10.5 cycles and 5.95 cycles more for ACHN, LN78, RCCNG1 and 786-O cells respectively. For the expression of ENT2 these numbers were relatively moderate and comprise 10.11 cycles, 11.65 cycles, 10.5 cycles and 5.95 cycles more for ACHN, LN78, RCCNG1 and 786-O cells respectively.

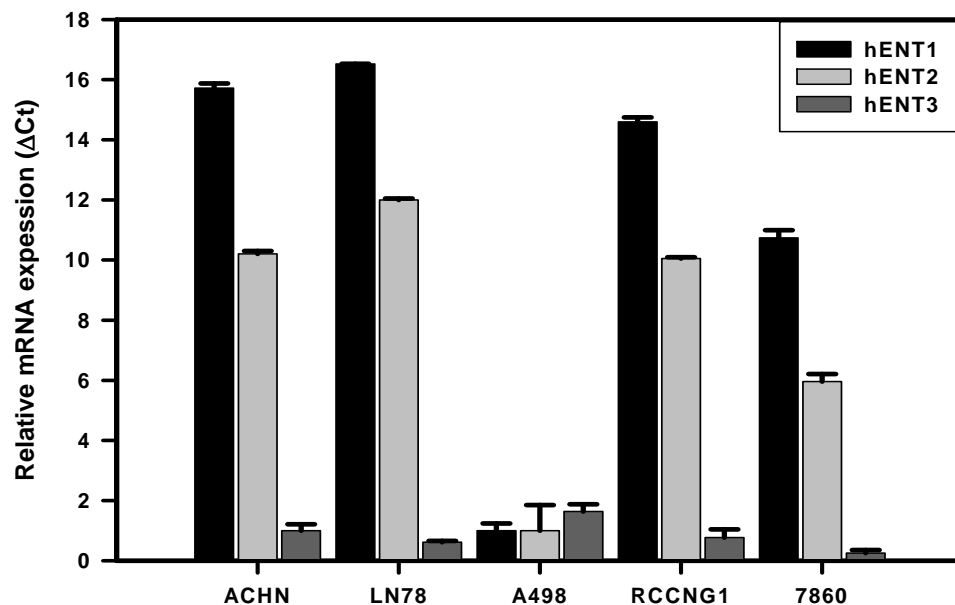


Fig. 3.6 TaqMan real-time PCR hENT1,2,3 examination of total RNA extracted from renal carcinoma cell lines. The hENT1,2,3 expressions were equilibrated by comparison with hGAPDH and hHPRT. Data means difference between lowest expression member (A498) and other tested RCC lines. Means  $\pm$  SEM were calculated from three independent experiments with three repeats each.

### 3.3 [<sup>3</sup>H]MPP uptake investigation in CHO-hOCT3 and RCC lines

#### 3.3.1 Inhibition of [<sup>3</sup>H]MPP uptake by cationic substances

MPP is known as a substance specifically transported by OCTs. As ACHN and A498 cell lines did not show any expression of other OCTs (unpublished data), MPP uptake is mainly mediated by hOCT3. Thus, to investigate the activity of hOCT3, A498 and ACHN cells were tested for [<sup>3</sup>H]MPP uptake. The results were compared with hOCT3-stably transfected CHO and control CHO cells. The data are presented in Figure 3.7. The uptake of [<sup>3</sup>H]MPP in CHO-hOCT3 was  $3.5 \pm 0.01$  pmol/5 min, which was 11 fold higher compared to CHO cells ( $0.2 \pm 0.01$  pmol/5 min,  $P < 0.00001$ ). hOCT3 mediated [<sup>3</sup>H]MPP uptake was significantly inhibited by 100  $\mu$ M quinine ( $0.55 \pm 0.02$  pmol/5 min,  $P < 0.00001$ ) and 500  $\mu$ M unlabeled MPP ( $0.47 \pm 0.05$  pmol/5 min,  $P < 0.00001$ ). Tetraethylammonium (TEA) at a concentration of 1 mM inhibited [<sup>3</sup>H]MPP uptake only partially ( $1.32 \pm 0.04$  pmol/5min,  $P < 0.00001$ ). Non-transfected CHO cells did not show significant [<sup>3</sup>H]MPP uptake. In A498 cells the uptake of [<sup>3</sup>H]MPP was 10 fold higher compared to ACHN cells. The [<sup>3</sup>H]MPP uptake in A498 cells was also inhibited by 100  $\mu$ M quinine ( $0.3 \pm 0.003$  pmol/5min  $P < 0.00001$ ) and 500  $\mu$ M unlabeled MPP ( $0.31 \pm 0.01$  pmol/5min  $P < 0.00001$ ). Inhibition by 1 mM TEA caused 2 fold decreases in [<sup>3</sup>H]MPP uptake compared to untreated cells (Figure 3.8).

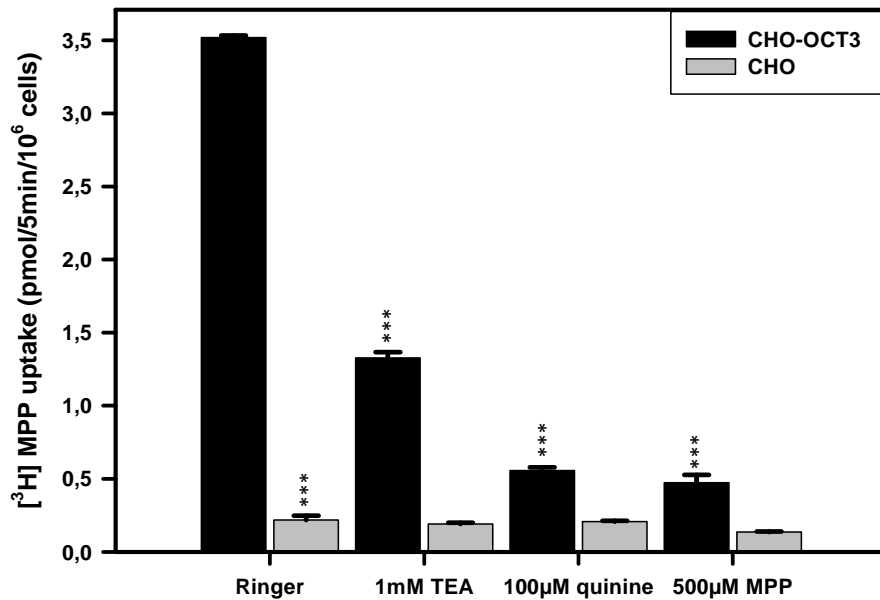


Fig. 3.7 Inhibition by known hOCT3 inhibitor of [<sup>3</sup>H]MPP uptake into CHO-hOCT3. [<sup>3</sup>H]MPP uptake into stably transfected hOCT3-CHO cells and CHO. ■ hOCT3 expressing cells, □ mock cells. Data are means ± SEM of three independent experiments with four repeats each. \*\*\* P<0.0001

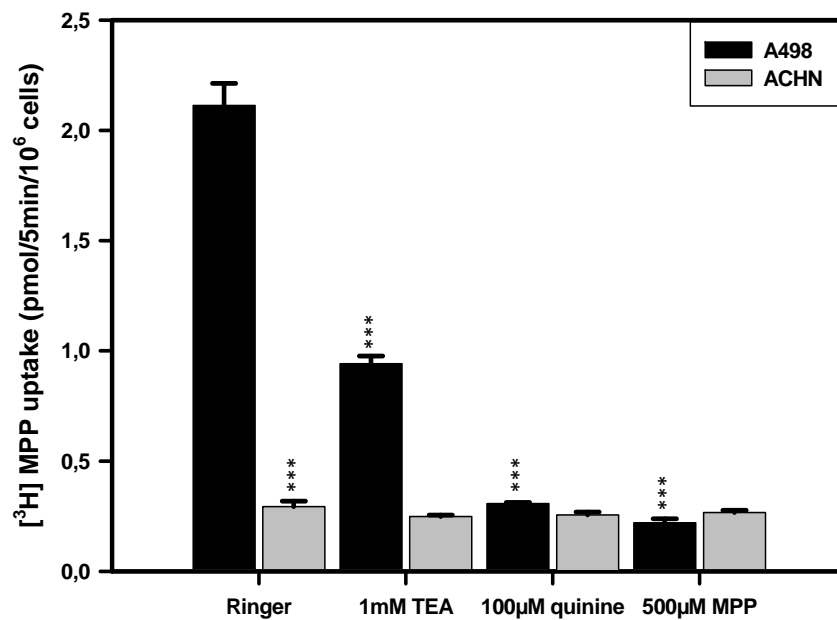


Fig. 3.8 Inhibition by known hOCT3 inhibitor of [<sup>3</sup>H]MPP uptake into RCC lines. [<sup>3</sup>H]MPP uptake into high expressing A498 and low expressing ACHN cells. ■ hOCT3 expressing cells, □ mock cells. Data are means ± SEM of three independent experiments with four repeats each. \*\*\* P<0.0001

### 3.3.2 Inhibition of [<sup>3</sup>H]MPP uptake by cytostatic substances

The interaction of cytostatic substances with hOCT3 was estimated by inhibition of [<sup>3</sup>H] MPP uptake. For our investigation we selected a range of widely used cytostatic agents and the results are summarized (Figure 3.9). Several independent experiments with quadruplicate determinations showed that [<sup>3</sup>H]MPP uptake was significantly inhibited to 100 μM of melphalan by 40.5 ± 0.7% (P<0.0001) of the uptake into untreated cells, prednisone to 64.1 ± 4.1% (P<0.01), vincristine to 29.5 ± 1.7% (P<0.0001), irinotecan to 19.6 ± 0.7% (P<0.0001). Other substances like doxorubicin, methotrexate, fluoroadenine and cyclophosphamide exceeded slight not significant inhibition (P<0.05) of [<sup>3</sup>H]MPP uptake, to 82.2 ± 3.5%, 90.1 ± 3.1%, 77.9 ± 3.1% and 84.5 ± 1.4%, respectively, of uptake into untreated cells. Other tested substances such as cytarabine and busulfan have no interaction with hOCT3.

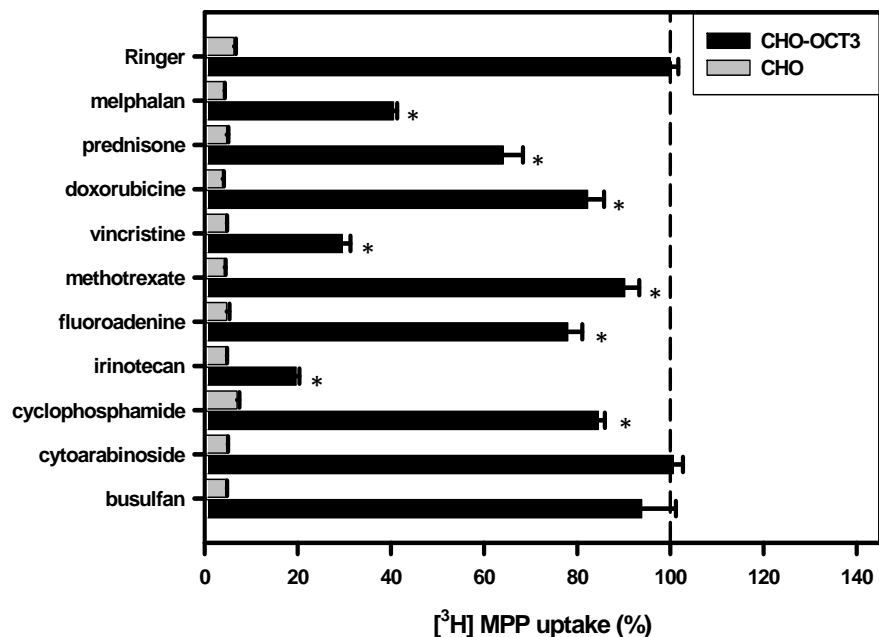


Fig 3.9 Inhibition of [<sup>3</sup>H]MPP uptake by different cytostatic agents(100 μM each) . □ mock cells, ■ hOCT3 –expressing cells. All experiments were standardized by setting the control (without inhibitor) of each experiment to 100%. Data are means ±SEM of three independent experiments with four repeats each. \* P<0.05, \*\* P<0.01, \*\*\* P<0.0001

### 3.3.3 Dixon plot analysis for irinotecan, vincristine, and melphalan

To investigate the type of interaction, selected cytostatic inhibitors (vincristine, irinotecan, and melphalan) of [<sup>3</sup>H]MPP uptake were analyzed by Dixon plots. Three experiments were performed for each substance, and shown in Figures 3.10, 3.11, and 3.12. The Dixon plot analysis showed that all tested compounds interact with hOCT3 in an uncompetitive manner. The K<sub>i</sub> values for melphalan, irinotecan, and vincristine are 366 ± 51 μM, 1.75 ± 0.45 μM, and 17 ± 4.5 μM respectively.

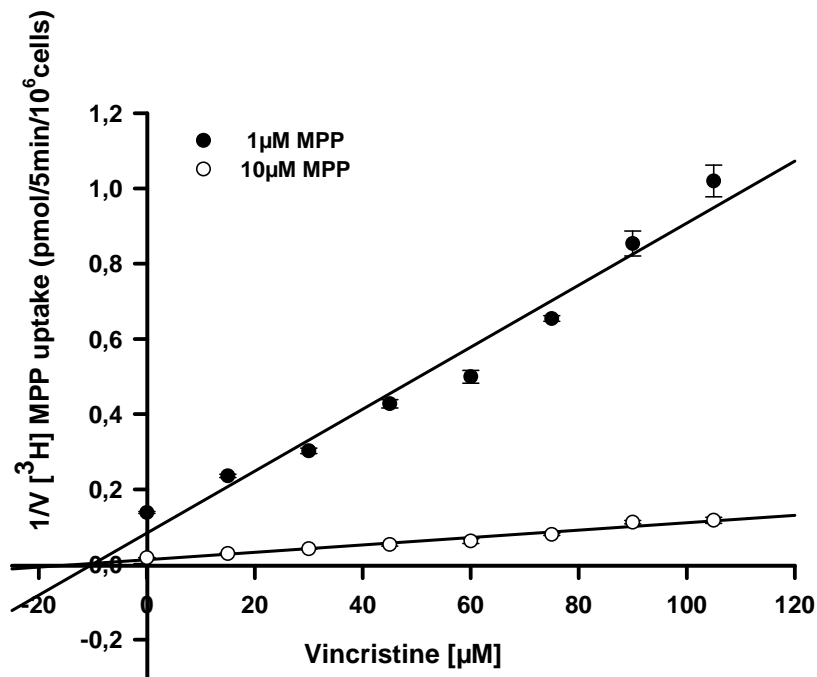


Figure 3.10 Kinetic analysis inhibition of hOCT3 by vincristine. Uptake experiment with ● 1 μM and ○ 10 μM [<sup>3</sup>H]MPP (20 nM [<sup>3</sup>H]MPP+980 nM MPP or 9980 nM MPP) concentrations were performed with different concentration of vincristine. Data are presented as Dixon plots. Data are means ± SEM of three repeats. The K<sub>i</sub> was calculated from these plots.

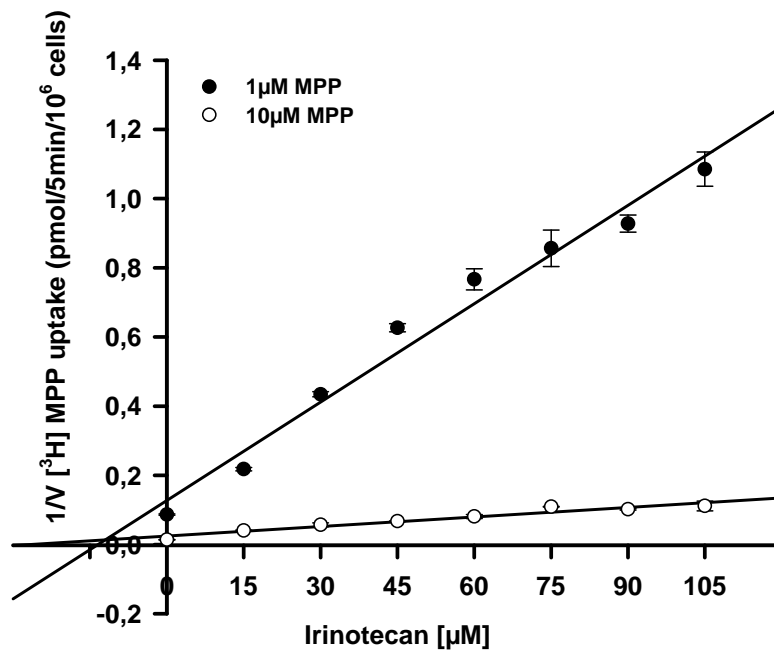


Figure 3.11 Kinetic analysis inhibition of hOCT3 for irinotecan. Uptake experiment with  $\bullet$  1  $\mu\text{M}$  and  $\circ$  10  $\mu\text{M}$  [ $^3\text{H}$ ]MPP (20 nM [ $^3\text{H}$ ]MPP+980 nM MPP or 9980 nM MPP) concentrations were performed with different concentration of irinotecan. Data are presented as Dixon plots. Data are means  $\pm$  SEM of three repeats. The  $K_i$  was calculated from these plots.

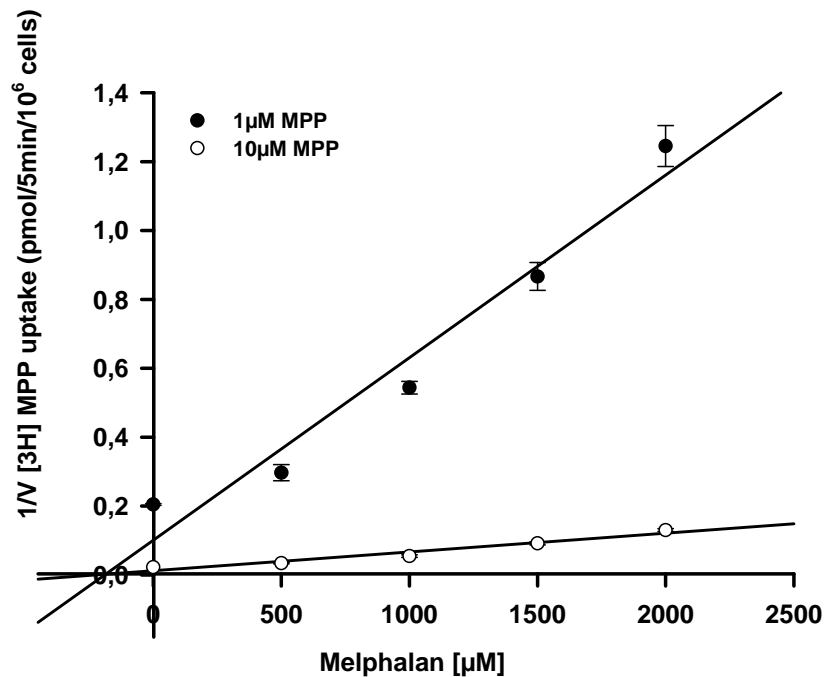


Figure 3.12 Kinetic analysis inhibition of hOCT3 for melphalan. Uptake experiment with  $\bullet$  1  $\mu\text{M}$  and  $\circ$  10  $\mu\text{M}$  [ $^3\text{H}$ ]MPP (20 nM [ $^3\text{H}$ ]MPP+980 nM MPP or 9980 nM MPP) concentrations were performed with different concentration of melphalan. Data are presented as Dixon plots. Data are means  $\pm$  SEM of three repeats. The  $K_i$  was calculated from these plots.

### 3.3.4 [<sup>3</sup>H]MPP uptake into *Xenopus laevis* oocytes injected with hOCT3 cRNA

For further investigation of hOCT3 mediated cytosolic transport *Xenopus laevis* oocytes were injected with hOCT3 cRNA. The quality of expression of hOCT3 was tested by [<sup>3</sup>H]MPP uptake (Figure 3.13). Injected oocytes took up  $1.68 \pm 0.21$  pmol [<sup>3</sup>H]MPP/30min/oocyte. This level was 3 times higher than in H<sub>2</sub>O injected oocytes:  $0.56 \pm 0.06$  pmol [<sup>3</sup>H]MPP/30min/oocyte ( $P < 0.001$ ). [<sup>3</sup>H]MPP uptake into hOCT3 injected oocytes was inhibited by 100  $\mu$ M quinine down to a level comparable to H<sub>2</sub>O injected oocytes. Oocytes from the same batch were also tested in electrophysiological experiments to show MPP uptake-dependent current. However, no currents could be recorded in response to MPP uptake (data not shown).

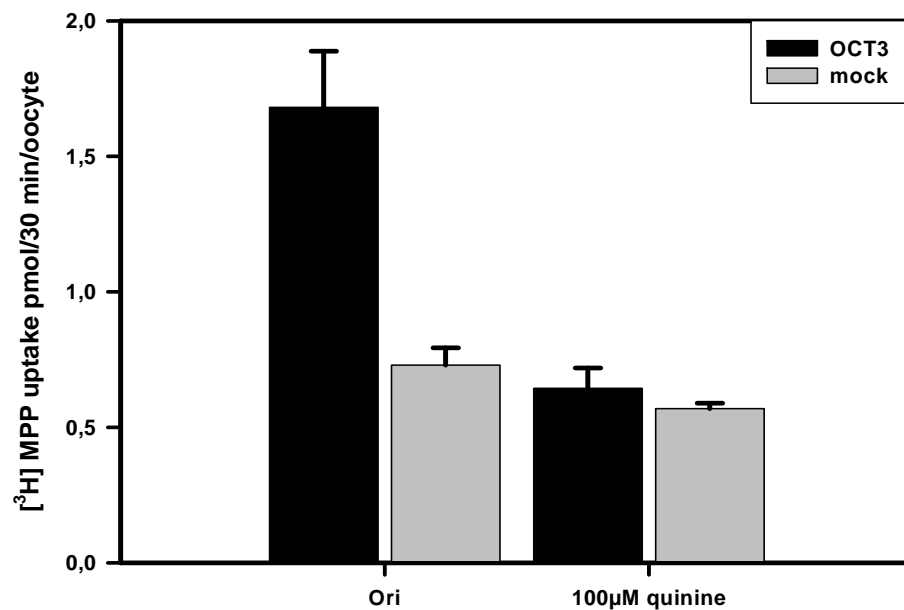


Figure 3.13 [<sup>3</sup>H]MPP uptake into *Xenopus laevis* oocytes. ■ hOCT3 injected oocytes, □ H<sub>2</sub>O injected oocytes. Data are means  $\pm$  SEM of three repeats



### 3.4. Inhibition of [<sup>3</sup>H]gemcitabine uptake by nucleoside analogs.

For investigation of [<sup>3</sup>H]gemcitabine uptake in RCC lines we selected the LN78 cell line with high expression of hENT1 and hENT2, and the A498 cell line with low expression. The [<sup>3</sup>H]gemcitabine uptakes were inhibited by known nucleoside compounds which interact with hENT1 and hENT2 (Figure 3.13). LN78 cells showed an almost 3.5 times higher [<sup>3</sup>H]gemcitabine uptake ( $359.83 \pm 11.3$  fmol/5min/ $10^6$  cells) a A498 cells ( $102.56 \pm 6.51$  fmol/5min/ $10^6$  cells). The [<sup>3</sup>H]gemcitabine uptake in LN78 cell line was significantly inhibited by 1 mM thymidine to  $65.71 \pm 14.41$  fmol/5min/ $10^6$  cells, 1 mM cytidine to  $92.47 \pm 13.74$  fmol/5min/ $10^6$  cells, 1  $\mu$ M NBTI to  $41.35 \pm 4.08$  fmol/5min/ $10^6$  cells, and 1 mM gemcitabine to  $40.21 \pm 1.02$  fmol/5min/ $10^6$  cells of the uptake in the absence of added compound. A similar behavior was observed for A498 cells: 1 mM thymidine inhibited to  $33.90 \pm 0.91$  fmol/5min/ $10^6$  cells, 1 mM cytidine to  $35.68 \pm 3.16$  fmol/5min/ $10^6$  cells, 1  $\mu$ M NBTI to  $17.98 \pm 2.91$  fmol/5min/ $10^6$  cells, and 1 mM gemcitabine to  $18.46 \pm 0.60$  fmol/5min/ $10^6$  cells of the uptake in the absence of added compound.

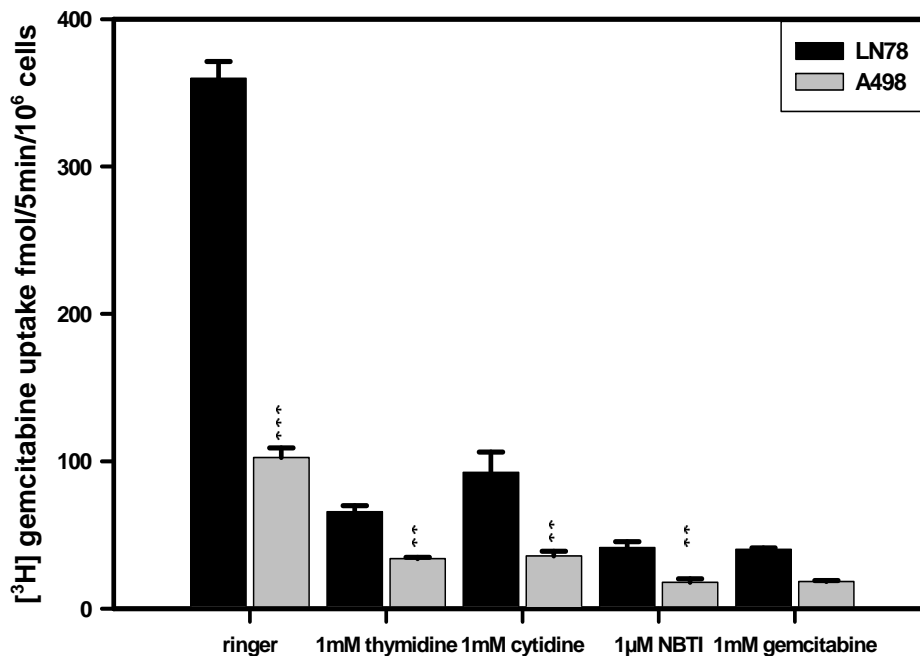


Fig. 3.14 Inhibition of [<sup>3</sup>H]gemcitabine uptake into RCC lines by known hENT's inhibitors. [<sup>3</sup>H]gemcitabine uptake into low expressing A498 and high expressing LN78 cells. ■ LN78 cell line, □ mean A498 cell line. Data are means  $\pm$  SEM of three independent experiments with four repeats each. \*\*

### 3.5 Cytostatic sensitivity investigation

#### 3.4.1 Evaluation of the cytotoxic activity of bendamustine and chlorambucil by the [<sup>3</sup>H]thymidine incorporation assay

For the better understanding of the role of OAT1 and OAT3 in the uptake of cytostatics and the effects of these drugs on cell proliferation, we performed a thymidine incorporation assay in HEK-293 cells stably expressing OAT1 or OAT3. For this test, chlorambucil and bendamustine were selected as cytostatics because of their structural similarity to specific OAT1 and OAT3 substrates like *p*-aminohippurate and estron-3-sulfate, respectively. The most important intracellular target of chlorambucil and bendamustine is double-stranded DNA. Figures 3.15 and 3.16 demonstrate the incorporation of radioactive thymidine after 30 min of cytostatic treatment. The result revealed that chlorambucil, which is specifically delivered by OAT1, inhibited the thymidine incorporation in OAT1 expressing cells with a higher efficiency than in OAT3 expressing cells or non-transfected HEK-293 cells. HEK-OAT1 cells treated with 10  $\mu$ M chlorambucil showed a decrease in [<sup>3</sup>H]thymidine incorporation by  $30 \pm 6\%$ , whereas non-expressing HEK cells and HEK-OAT3 cells exhibited a smaller decrease by  $21 \pm 5$  ( $P=0.01$ ). For 50  $\mu$ M and 100  $\mu$ M chlorambucil, inhibition of [<sup>3</sup>H]thymidine incorporation was  $45 \pm 5\%$  and  $40 \pm 5\%$  ( $P<0.05$ ) in HEK-OAT1. In mock cells and HEK-OAT3 [<sup>3</sup>H]thymidine incorporation was inhibited  $20 \pm 5\%$ . When we compared mock and HEK-OAT3 cells to HEK-OAT1 after chlorambucil treatment, [<sup>3</sup>H]thymidine incorporation was decreased by  $25\pm 5\%$  ( $P<0.05$ ). Bendamustine treatment of OAT3 expressing cells render a higher inhibition of [<sup>3</sup>H]thymidine incorporation as compared to OAT1 expressing or non-transfected cells. At 10  $\mu$ M concentration HEK-OAT3 cells are by  $29\pm 5\%$  ( $P<0.05$ ) more sensitive than non-treated cells.

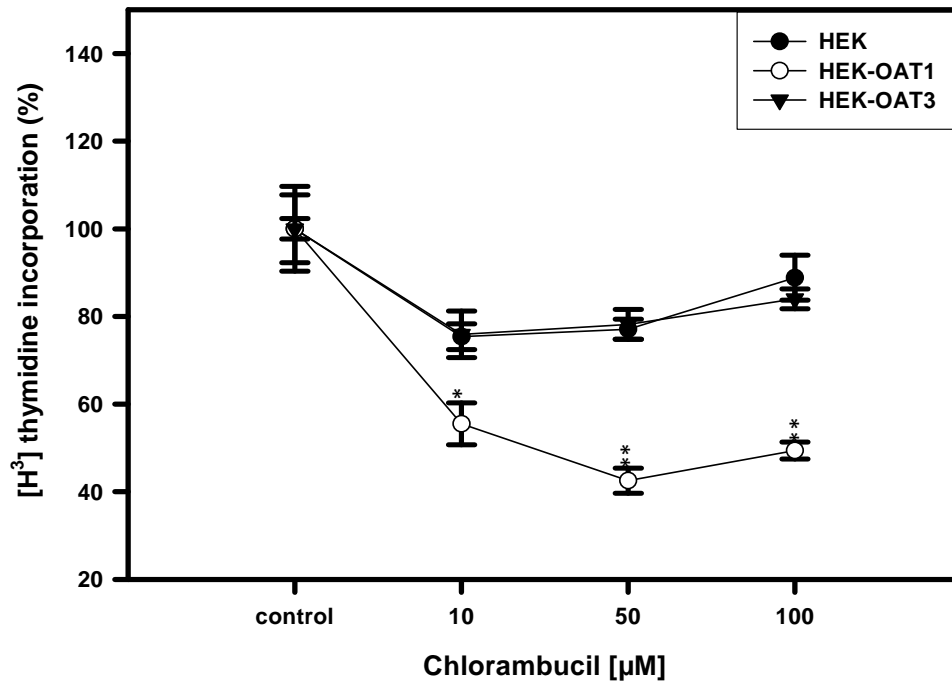


Figure 3.15 [<sup>3</sup>H]thymidine incorporation measurement after chlorambucil treatment. Cells were treated 30 min with various concentrations of chlorambucil, ● HEK 293 and ○ HEK-OAT1 cells, ▼ HEK-OAT3. All experiments were standardized by setting the control (without cytostatic) of each experiment to 100%. Data are means ± SEM of three repeats. \* P<0.05. \*\* P<0.01

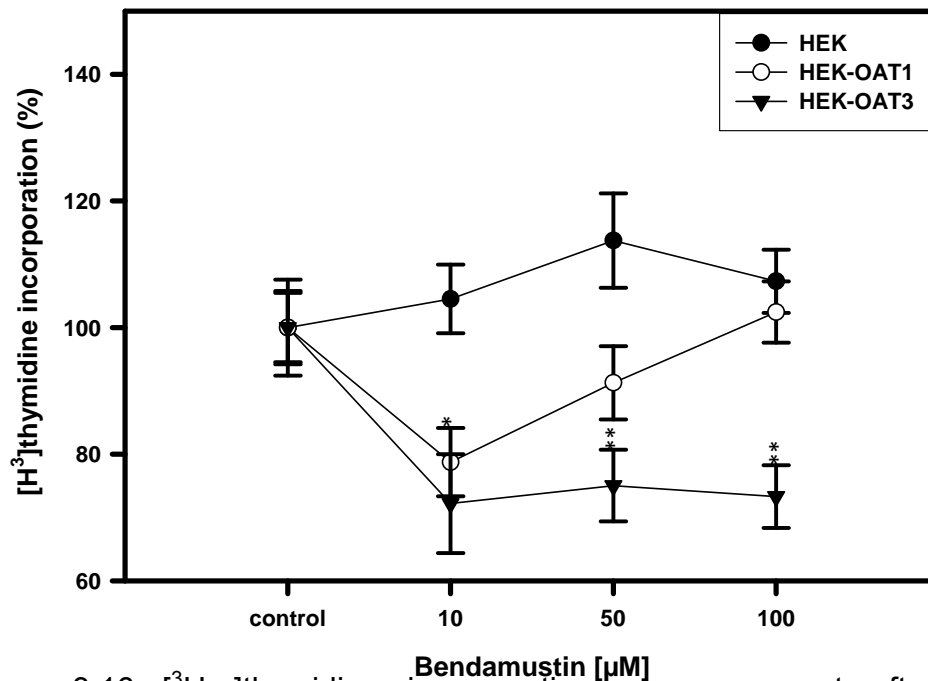


Figure 3.16 [<sup>3</sup>H]thymidine incorporation measurement after bendamustine treatment. Cells were treated 30 min with various concentrations of bendamustine, ● HEK 293 and ○ HEK-OAT1 cells, ▼ HEK-OAT3. All experiments were standardized by setting the control (without cytostatic) of each experiment to 100%. Data are means ± SEM of three repeats. \* P<0.05, \*\* P<0.01

After treatment of HEK-OAT3 cells by 50  $\mu\text{M}$  and 100  $\mu\text{M}$  bendamustine, [ $^3\text{H}$ ]thymidine incorporation was decreased to  $27 \pm 6\%$  ( $P < 0.05$ ) and  $29 \pm 5\%$  ( $P < 0.05$ ) compared to non-treated cells. HEK-OAT1 cells showed similar to HEK-OAT3 cells a higher sensitivity to bendamustine at a concentration by 10  $\mu\text{M}$ , [ $^3\text{H}$ ]thymidine incorporation was decreased to  $24 \pm 6\%$  in both HEK-OAT1 and HEK-OAT3 compared to non-treated. When HEK-OAT1 were treated with 50  $\mu\text{M}$  bendamustine, they showed increased [ $^3\text{H}$ ]thymidine incorporation in comparison to HEK-OAT3. Mock cells (non-transfected HEK-293) at all tested concentration were non-sensitive for bendamustine treatment.

#### *3.4.2 Evaluation of the cytostatic activity of melphalan by [ $^3\text{H}$ ]thymidine incorporation assay.*

As melphalan is a widely known DNA damaging agent, its cytotoxic activity was measured by [ $^3\text{H}$ ]thymidine incorporation assay. Cells were treated with different concentrations of melphalan and melphalan together with hOCT inhibitors. The results of melphalan treatment are summarized in Figure 3.17. We observed that after melphalan treatment [ $^3\text{H}$ ]thymidine incorporation with CHO-hOCT3 cells was decreased as compared to non-transfected CHO cells in a concentration dependent manner. In particular, [ $^3\text{H}$ ]thymidine incorporation was  $10 \pm 2\%$  ( $P < 0.05$ ) less upon 10  $\mu\text{M}$  melphalan treatment,  $20 \pm 6\%$  ( $P < 0.01$ ) less with 50  $\mu\text{M}$  melphalan and  $35 \pm 5\%$  ( $P < 0.01$ ) less with 100  $\mu\text{M}$  melphalan as compared to control CHO cells.

The inhibition of [ $^3\text{H}$ ]thymidine incorporation in A498 cells in comparison with ACHN cells demonstrated the following values:  $35 \pm 4\%$  ( $P < 0.01$ ) less [ $^3\text{H}$ ]thymidine incorporation with 10  $\mu\text{M}$  of melphalan,  $30\% \pm 5$  ( $P < 0.01$ ) less with 50  $\mu\text{M}$ , and 2% (not significant) less with 100  $\mu\text{M}$  (Figure 3.18). To prove hOCT3 mediated melphalan sensitivity both in CHO and RCC cells, we incubated them with TEA (Figure 3.19). As it was already demonstrated in

previous experiments, CHO-hOCT3 cells possessed more sensitivity to 50  $\mu\text{M}$  melphalan as compared to CHO cells. Interestingly, 50  $\mu\text{M}$  melphalan together with 2 mM TEA seemed to be more toxic than melphalan alone for CHO, but not for CHO-hOCT3 cells. The treatment of CHO-hOCT3 cells with melphalan together with TEA led to a recovery for  $12 \pm 4\%$  ( $P < 0.05$ ) in comparison with melphalan treated CHO-hOCT3 cells. Renal carcinoma cells A498 with high hOCT3 expression showed a higher sensitivity to melphalan compared to low hOCT3 expressing ACHN cells. However, the additional treatments of A498 with 2 mM TEA lead only to a 5% of recovery (Figure 3.20).

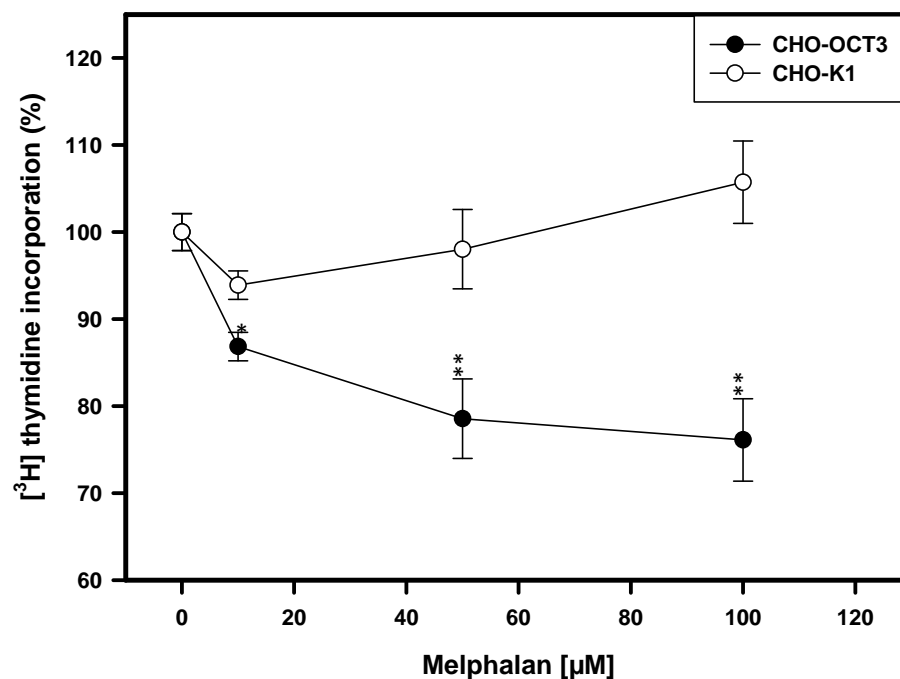


Figure 3.17 [ $^3\text{H}$ ]thymidine incorporation measurement after melphalan treatment of CHO cells. Cells were incubated for 30 min with various concentrations of melphalan, ● A498 and ○ ACHN cells. All experiments were standardized by setting the control (without melphalan) of each experiment to 100%. Data means  $\pm$  SEM of three repeats. \*  $P < 0.05$ , \*\*  $P < 0.01$

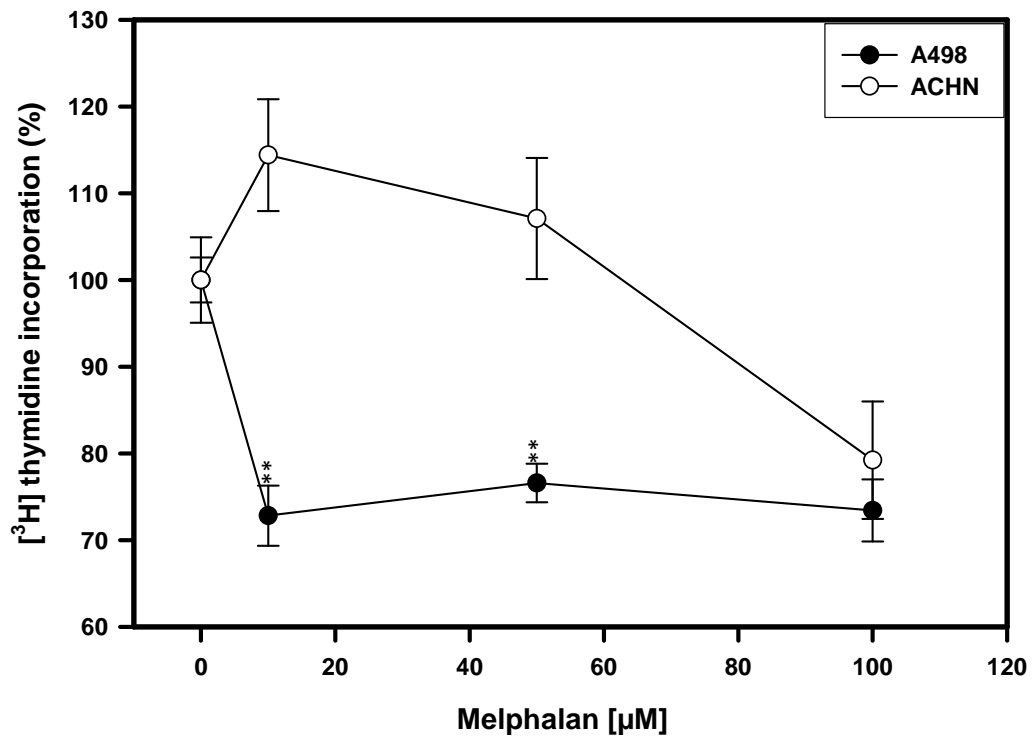


Figure 3.18 [ $^3\text{H}$ ]thymidine incorporation after melphalan treatment of RCC cells. The cells were incubated for 30 min with various concentrations of melphalan, ● CHO-hOCT3 and ○ CHO cells,. All experiments were standardized by setting the control (without melphalan) of each experiment to 100%. Data means  $\pm$ SEM of three repeats. \*  $P < 0.05$ , \*\*  $P < 0.01$

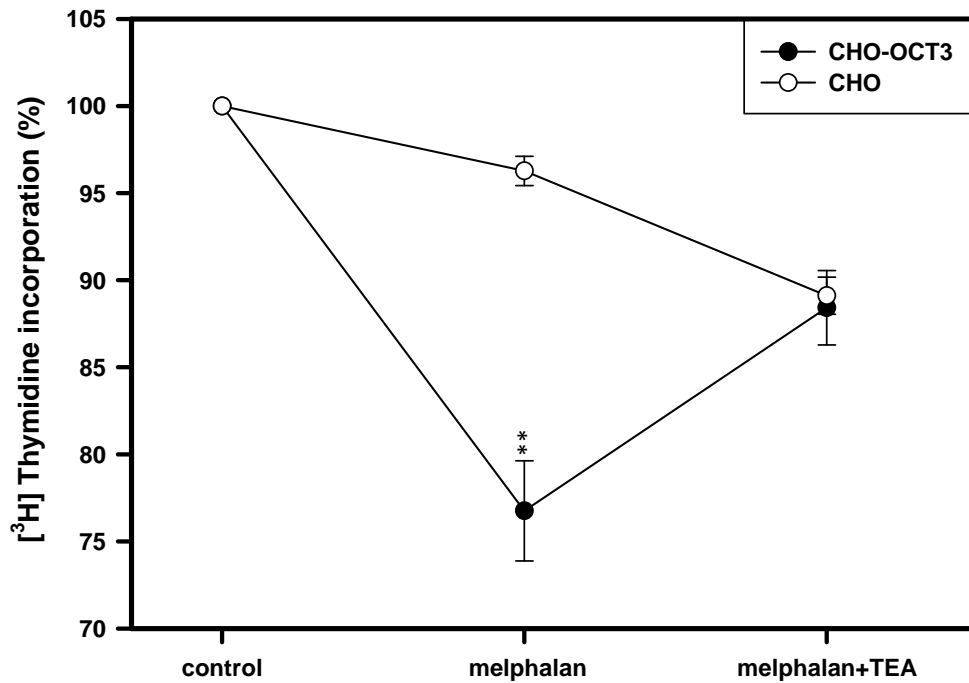


Figure 3.19 [<sup>3</sup>H]thymidine incorporation after melphalan/melphalan+TEA treatment in CHO cells. Cells were treated with 50 μM melphalan and 50 μM melphalan together with 2 mM TEA for 30 min, ● CHO-hOCT3 and ○ CHO cells. All experiments were standardized by setting the control (without melphalan) of each experiment to 100%. Data means ± SEM of three repeats. \*\* P<0.01

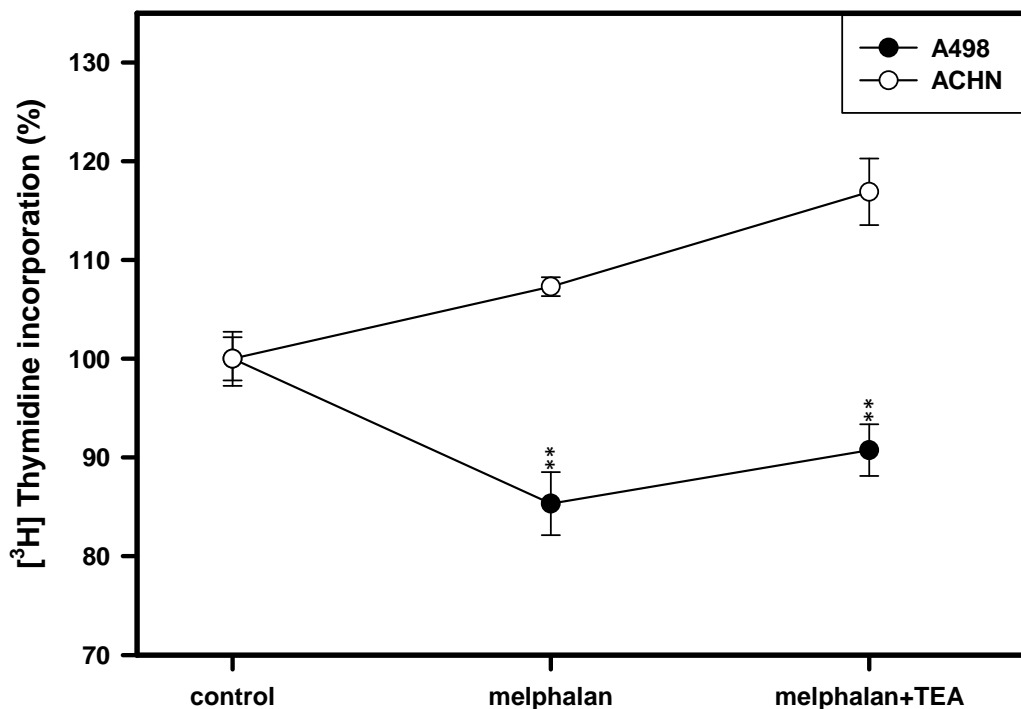


Figure 3.20 [<sup>3</sup>H]thymidine incorporation after melphalan/melphalan+TEA treatment in RCC cells. Cells were treated with 50  $\mu$ M melphalan and 50  $\mu$ M melphalan together with 2 mM TEA for 30 min, ● A498 and ○ ACHN cells. All experiments were standardized by setting the control (without melphalan) of each experiment to 100%. Data means  $\pm$  SEM of three repeats. \*\* P<0.01

### 3.4.3 Evaluation of cytostatic activity irinotecan and vincristine by the MTT assay.

For evaluation of the cytotoxic activity of irinotecan and vincristine we chose the MTT assay. The sensitivity of CHO-hOCT3 cells to irinotecan was not significantly higher compared to non transfected CHO. However, the irinotecan effect on CHO-OCT3 cells was elevated up to  $25 \pm 3\%$  (P<0.01) upon additional treatment with the MDR1-blockator verapamil (Figure 3.21). These decreased viability was reversed upon additional treatment of the cells with 500  $\mu$ M of MPP, 2 mM TEA (P<0.01). The decrease in viability in the presence of 500  $\mu$ M MPP, 2 mM TEA, 1  $\mu$ M verapamil on CHO-hOCT3 cells was less than 7-9% and not significant. The viability of CHO-hOCT3 treated by vincristine was



inhibited by  $40 \pm 2.5\%$  ( $P < 0.001$ ), and after verapamil treatment it decreased additionally by  $19 \pm 2.4\%$ . The cytotoxic effect of vincristine can be recovered for  $15 \pm 2.1\%$  ( $P < 0.01$ ) upon 2mM TEA treatment, however the treatment with 500  $\mu$ M MPP did not significantly recover viability of treated cells (Figure 3.22).

The sensitivity of RCC cells to irinotecan and vincristine was also tested by MTT assay (Figure 3.23, 3.24). But in contrast to OCT3 stably transfected CHO cells irinotecan did not demonstrate a significant difference in viability between A498 and ACHN cells (Figure 3.23). Renal cancer cells tested by vincristine showed a similar behavior as CHO-OCT3 cells. Vincristine treated A498 cells were 18% more sensitive to the cytostatic compared to ACHN cells. The effect of vincristine was elevated up to 25% by additional treatment with 1 $\mu$ M verapamil. The cytotoxic effect of vincristine was slightly rescued by the incubation with 500  $\mu$ M MPP, 2 mM TEA (Figure 3.22).

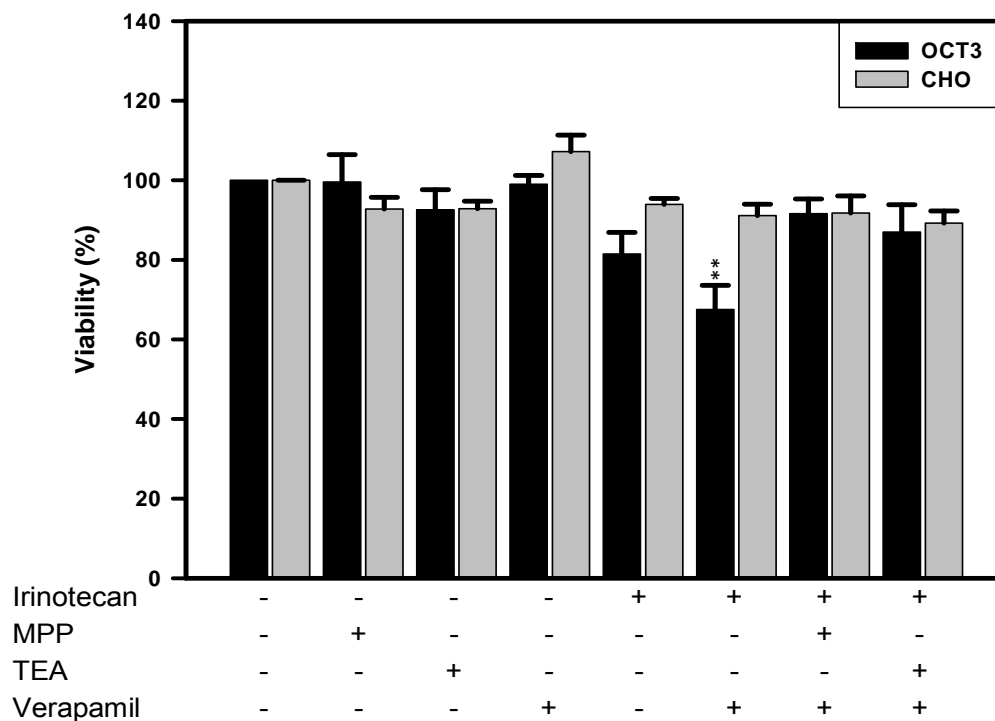


Figure 3.21. Viability test of CHO-hOCT3 cells after irinotecan treatment. The test was performed by MTT colorimetric assay. Cells were treated with 100  $\mu$ M of the cytostatic for 15 min, washed with PBS and left for additional 24h in the cell culture medium with or without 1  $\mu$ M verapamil. ■ CHO-hOCT3 and □ CHO cells; Data are means  $\pm$  SEM of three repeats. \*\*  $P < 0.01$ , \*\*\*  $P < 0.001$

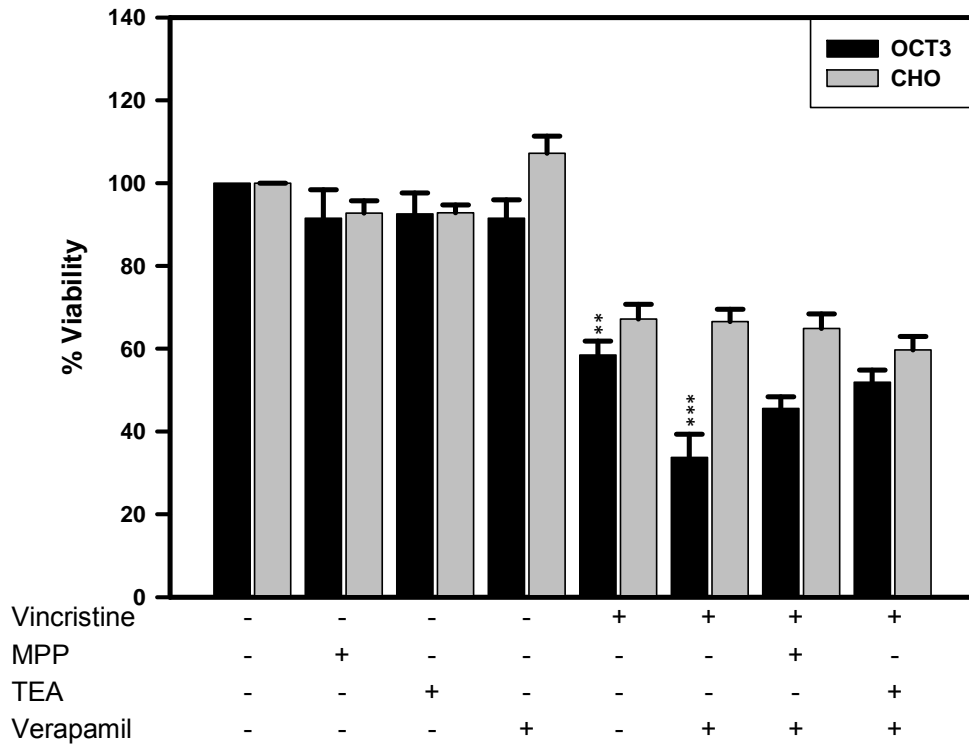


Figure 3.22. Viability test of CHO cells after vincristine treatment. The test was performed by MTT colorimetric assay. Cells were treated with 100  $\mu$ M of the cytostatic for 15 min, washed with PBS and left for additional 24h in cell culture medium with or without 1 $\mu$ M verapamil. ■ CHO-hOCT3 and □ CHO cells. Data are means  $\pm$  SEM of three repeats. \*\* P<0.01, \*\*\* P<0.001

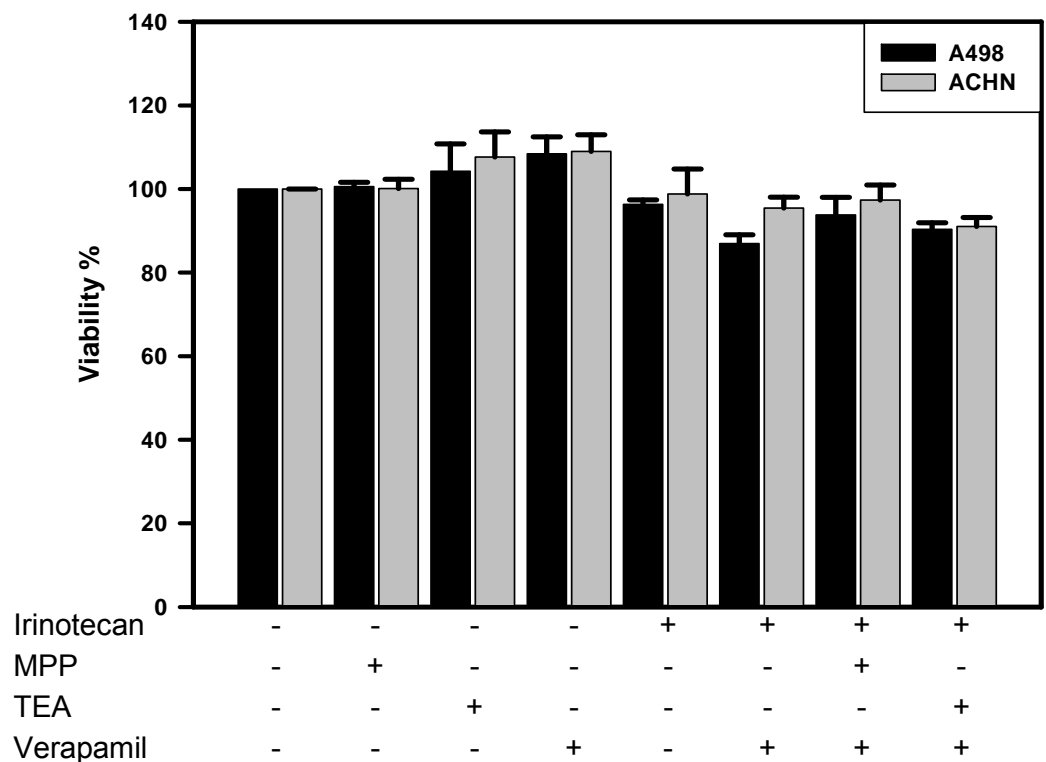


Figure 3.23. Viability test of RCC cells after irinotecan treatment. The test was performed by MTT colorimetric assay. Cells were treated with 100  $\mu$ M of the cytostatic for 15 min, washed with PBS and left for additional 24h in cell culture medium with or without 1  $\mu$ M verapamil. ■ A498 and □ ACHN cells. Data means  $\pm$  SEM of three repeats. \*\* P<0.01, \*\*\* P<0.001

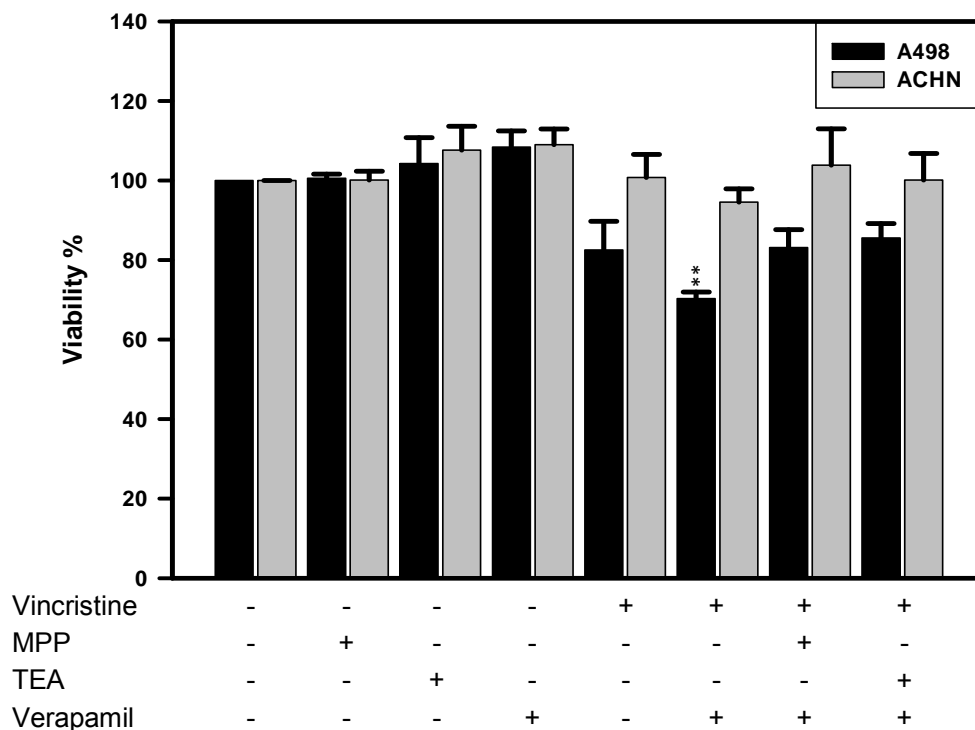


Figure 3.24. Viability test of RCC cells after vincristine treatment. The test was performed by MTT colorimetric assay. Cells were treated with 100  $\mu$ M of the cytostatic for 15 min, washed with PBS and left for additional 24 h in cell culture medium with or without 1  $\mu$ M verapamil. ■ A498 and □ ACHN cells. Data are means  $\pm$  SEM of three repeats. \*\* P<0.01, \*\*\* P<0.001

#### *3.4.4 Evaluation of the cytostatic activity of gemcitabine by MTT assay.*

To prove that cytotoxic sensitivity related to hENT1 and hENT2 activities we performed investigations on high expressing LN78 and low expressing A498 cells (data presented in figures 3.25). Cells were incubated with 100  $\mu$ M gemcitabine for 15 min and different combinations of ENT1 and 2 inhibitors. After incubation cells were washed and left for 24 h to maximize effects. The viability of LN78 cells were inhibited by gemcitabine to  $14.36 \pm 5.93\%$  as compared to non-treated cells. A498 cells were inhibited by gemcitabine to  $50.38 \pm 3.35\%$ . The gemcitabine effect was slightly reversed by addition of 1 mM thymidine or 1 mM cytidine to LN78 cells:  $28.99 \pm 2.25\%$  and  $31.14 \pm 4.91\%$ . A similar behavior was observed with A498 cells:  $40.19 \pm 2.73\%$  and  $39.46 \pm 2.60\%$ . The strongest reversal was obtained when cells were incubated with gemcitabine together with 500  $\mu$ M NBTI. Viability of LN78 cell line was  $77.90 \pm 6.71\%$  almost 5 times higher than cells incubated with gemcitabine incubation alone. The viability of A498 cells was decreased after incubation with gemcitabine together with 500  $\mu$ M NBTI to  $65.63 \pm 2.63\%$ . LN78 and A498 cell lines were incubated with 500  $\mu$ M NBTI alone. The viability of LN78 cells were inhibited to  $79.18 \pm 5.93\%$  and that of A498 cells to  $52.45 \pm 2.06\%$ .

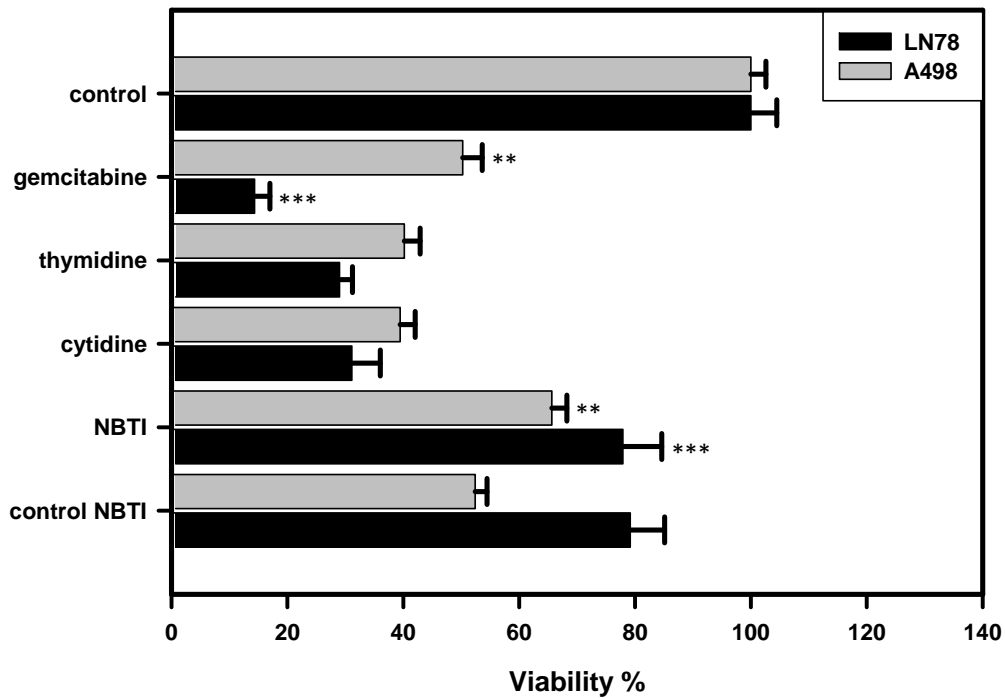


Figure 3.25. Viability test of RCC cells after gemcitabine treatment. The test was performed by MTT colorimetric assay. Cells were treated with 100  $\mu$ M of the cytostatic for 15 min, washed with PBS and left for additional 24h. ■ LN78 and □ A498 cells. Data are means  $\pm$  SEM of three repeats. \*\* P<0.01, \*\*\* P<0.001

## **4. Discussion**

The resistance of tumour cells to cytostatic drugs represents a large and unfortunately often insurmountable problem in the chemotherapy. The increased expression of cytostatic drug exporting transporters like the multidrug resistant transporter MDR and multidrug resistance related proteins (MRP) are considered a substantial cause for the cytostatic drug resistance. While these exporting transporters have been well examined over the last decade very little is known about transporters, which could lead to an increased uptake of cytostatic drugs in tumor cells. First of all, only to some extent it has been examined, which of the well-known, to the SLC (carrier solute) family belonging uptake transporters are expressed in kidney tumor cells. Second, the individual equipment of tumor cells with uptake transporters was so far not explored systematically. Third, little is known about the interaction of cytostatics with several uptake transporters of the SLC family. Therefore the aim of this study was firstly to examine the expression level of thirty well characterised uptake transporters of the SLC family in kidney tumour cells, secondly to investigate the interaction of transporter proteins with several clinical relevant cytostatics, and thirdly to find out the role of the uptake transporters in the cytostatic effect and the proliferation of the tumour cells.

### **4.1 Expression of uptake transporters of the SLC family in kidney tumour cells**

Initially several primers were designed on the base of the DNA sequence of the transporters from the NCBI Database. To consider the splice variants of each transporter by the selection of the primers we used the conserved regions of the DNA sequence. From 5 different kidney tumor cell lines the total RNA was purified and after reverse transcription were PCR-products generated which



observed a similar size (as indicated in the tables 2.1-2.8). The PCR-products were cloned and sequence verified. These clones were then used as a standard for the quantitative resolution of the expression level of each transporter by real-time PCR with SYBR Green I.

As a target for cytostatic drugs we examined the expression level of organic anion transporters in the kidney tumor cell lines 786-O, RCCNG1, A498, LN78, ACHN and tumor as well as normal tissue from the same patient. Organic anion transporters (OAT) are mainly expressed in the epithelial cells of kidney proximal tubules, but also in liver and blood-brain barrier. The substrates for these transporters include organic anions, such as p-aminohippurate (PAH) and estrone sulfate (ES) [8]. OAT family members (OAT1, OAT2, OAT3, OAT4, and URAT1) are very important for excretion of organic anions from blood to urine [106]. They are also involved in the reabsorption of endogenous organic anions like estrone sulfate, dehydroepiandrosterone sulfate (DHEAS) and urate from primary urine through the lumenally located OAT4 and URAT1 [106]. Nothing was known about the expression of OATs in kidney tumor cells and little about the interaction of cytostatics with organic anion transporters. Up to now only the interaction of methotrexate with organic anion transporters was reported [107]. There are some anionic cytostatics which are used in chemotherapy of cancer patients, e.g. chlorambucil and bendamustin. Unpublished studies in our department demonstrated the interaction of chlorambucil and bendamustin with OAT1, OAT3, and OAT4 (Dr. Yohannes Hagos personal communication). On the other hand, the use of cytostatics in the cancer treatment may cause an accumulation of these drugs in the kidney proximal tubule cells and result in complications like nephropathy [108]. Our study revealed unfortunately no or only little expression of organic anion transporters in kidney cancer cell lines and tumour tissue in comparison to a normal kidney tissue. Therefore organic anion transporters are not the appropriate target transporter protein for chemotherapy of RCC with anionic cytostatics.

Organic cation transporters (OCT) also belong to the SLC22 family. The OCT transporters are mostly expressed in kidney, liver and blood-brain barrier [68]. These transporters possess an affinity for positively charged endogenous (epinephrine, norepinephrine, carnitine etc.) and exogenous substances (MPP, TEA ) [68]. Also it was shown that OCTs play an important role in the drug distribution in the organism [9] and drug transport from blood to brain [109]. Concerning the cytostatic drug transport, it is known, that OCT2 is responsible for cisplatin accumulation inside the kidney and brain tissues [11]. Nephropathies and neuropathies have been observed after chemotherapy with cisplatin due to accumulation of this cytostatic [110, 111].

The results of this study show that OCT3 is the only OCT family member that was expressed in some kidney cancer cell lines. In the kidney tumor tissue from a patient OCT2 was also highly expressed. This fact renders OCT2 and OCT3 appropriate candidates to be considered in kidney tumor therapy. Kidney tumor as well as normal tissue and the cell lines A498 and ACHN exhibited a very low expression of OCT6. This transporter was previously described as a transporter of doxorubicin [12].

Taken together, OCTs expressed in renal tumor tissues may be used to target cationic cytostatics. Additional experiments were required to show an increased sensitivity of OCT-expressing cells to cytostatics.

The organic anion transporting polypeptides are highly present in the liver, but some of the OATP family members like OATP-A, OATP-D and OATP-E [9] are also expressed in kidneys. These proteins transport organic anions such as taurocholate, estrone sulfate, but possess additionally the affinity to bile acids [112, 113]. As previously described, several OATPs showed an interaction with cytostatics like bamet-UD2 (a cisplatin bile acid derivate) and irinotekan metabolites [9, 13, 17]. Therefore OATPs are further candidates to be included in our study as potential transporters for cytostatics in tumor cells. The results demonstrate a high expression of OATP-A and OATP-B in tumor kidney tissue

and in some of the kidney cancer cell lines. The presence of these transporters could be used to deliver special cytostatics to the tumor cells.

Nucleoside transport in humans is provided by concentrative and equilibrative nucleoside transporters. CNTs and ENTs are ubiquitously expressed in different parts of human body [18, 114]. These group of transporters possess a high affinity to nucleosides. Many of the new cytostatic drugs are nucleoside analogs, such as 5'-fluorouracil, uramustine and gemcitabine [20], [19]. These facts could be used to treat kidney cancer cells with nucleoside analogs like gemcitabine. In our study a clear cut expression profile was observed in the kidney tumor cell lines and tumor as well as normal tissue. In most of the examined cells the expression of ENTs was much higher than the expression of CNTs. That is why ENTs are very interesting transporters for the developing an ENT-based strategy of chemotherapy for kidney tumor cells.

The L-type amino acid transporters are ubiquitously expressed in human organism. Besides transporting L-type neutral amino acids, LATs handle melphalan, a frequently used cytostatic in chronic lymphatic leukemia [115, 116]. Previously it was reported that LAT1 is expressed in lymphoma cells [35]. Because of high expression of LATs in the kidney, it was important to observe the expression pattern of the malignantly transformed kidney cells. The RT-PCR analysis demonstrated that in the kidney tumor tissue the expression level of LATs was the same as in normal tissue. This suggests that renal cancer cells may be sensitive to cytostatic analogs of L-amino acids.

The sodium dicarboxylate transporter (NaDC3) is highly expressed in kidney, liver, brain and placenta. Nothing is known concerning its interaction with cytostatics and about the expression in tumor cells. The physiological function of NaDC3 is the supply of epithelial cells with Krebs-cycle metabolites such as succinate or  $\alpha$ -ketoglutarate [10, 68, 117]. In kidney cancer cell lines and in tumor tissue, the expression of NaDC3 was very high. Possibly, this transporter may have an important metabolic function in delivering in Krebs cycle

metabolites to cancer cells. Therefore it could be a very interesting target by the decreasing the supply of dicarboxylate delivery and limitation of the energy generation of the tumor cell.

Members of the monocarboxylate transporter (MCT) family are ubiquitously expressed in the human body [25, 26, 118, 119]. The most important function of MCTs is the distribution of monocarboxylate such as lactate, and pyruvate to the target cells [25-27, 120, 121]. Furthermore, members of the MCT family (MCT-2) showed an interaction with ifosfamide metabolites as demonstrated previously [27]. The specific cytostatic transport and the interaction of the MCTs with some of the cytostatics make them very important transporters to be considered in chemotherapy. However, our expression study revealed a very high expression of the MCTs in healthy tissue as well as in tumor tissue. This data suggest that MCT transporter is important for the survival of all cells. This fact makes it difficult to consider these transporters for tumor-specific chemotherapy.

The SLC19 is widely expressed in the human organism. This group of transporters which have affinity for reduced folate/thiamine, was interesting for us as a potent transporter of cytostatic drugs like methotrexate [122]. In kidney tumor cell lines and normal tissue the thiamine transporter ThTr as well as the reduced folate transporter (RFT) was observed middle expression level. In some RCC cells, RFT, as well as ThTr, showed lower expression levels compared to normal tissues. Thus, the choice of chemotherapy with folate-derived cytostatics in this case may rather result in major side effects, then in efficient anticancer treatment.

Nowadays a lot of attention is paid to efflux transporters from ABC family. The ABC transporters are widely distributed in human tissue. In the kidney a few members of the ABC family like MRP1, MRP2, MRP4, and MDR1 are highly expressed [123], 26]. They use ATP for pumping several chemicals such as cytostatics and other compounds out of the cell [25,124]. Physiologically these

transporters pump out endogenous “waste“, glutathione conjugates and glucuronides, and exogenous hydrophobic xenobiotic like benzopyrenes [125]. The functions of ABC transporters include of course the excretion of cytostatics from cancer cells [126], which renders tumor cells chemoresistant. We performed in kidney cancer cell lines and tumor tissues a screening of the ABC transporter family to compare the level of the expression with the expression of the SLC family members. Most of the tested ABC transporters were highly expressed. It will be very important in the planning of chemotherapy to consider the expression level of the ABC transporters, because as efflux transporters they counteract of the uptake transporter.

#### **4.2 Real-time PCR reinvestigation of SLC22 transporters in renal carcinoma cells**

As mentioned before the SLC22 transporters play an important role in transport organic anions and cations in human body. This makes the SLC22 group also important for transport of wide range of cytostatics. We showed previously the expression of OAT1 and OCT3 in our tested cell lines. To evaluate differences in expression we used the TaqMan real-time PCR method. We found that OAT transporters are present at low levels in comparison to OCT3. For further experiments we chose the OCT3 expressing cell line A498 and the non-expressing ACHN line.

A similar procedure we used for investigation of ENT transporters in kidney carcinoma cell lines. We tested by TaqMan real-time PCR the expression levels in LN78 and A498. For further experiments we used the high expressing LN78 cell line ENT1, 2 and the low expressing A498.

### 4.3 Investigation of OCT3 activity in renal carcinoma cell lines

Human OCT3 has a high affinity for cationic substrates such as MPP, histamine, cimetidine, and quinine. It was shown that OCT1, OCT2, and OCT3 were inhibitable by quinine. The  $IC_{50}$  value for quinine is 5 nM [53]. All members of the OCT family also transported TEA, but with different affinity. Data of the interaction of organic cation transporters with cationic substances are summarized in figure 4.1

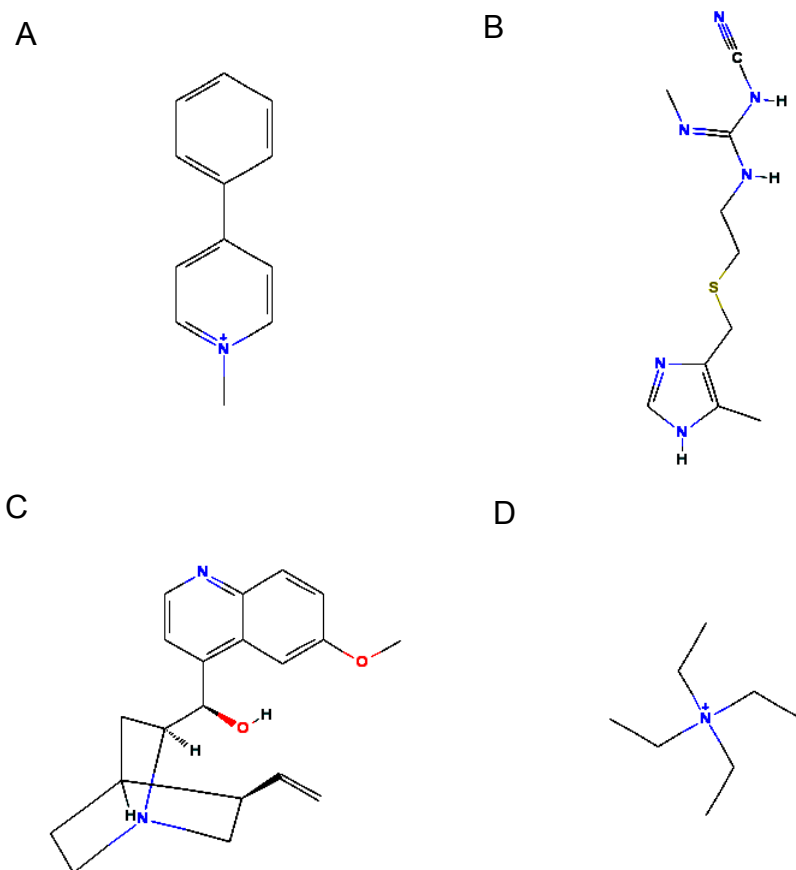


Figure 4.1 Structural formula of substrates transported by OCTs

A – MPP, B – cimetidine, C – quinine, D – TEA

To prove the presence of OCT3 in tumor cell membranes we performed a series of uptake experiments with known OCT3 substrates. We found that [<sup>3</sup>H]MPP was transported in high expressing A498 cells with a similar rate as in CHO cells stably transfected with OCT3. The ability to transport MPP with similar affinity was shown for OCT1, OCT2 and OCT3 [127]. To clarify the organic cation transport activity in renal carcinoma cells we inhibited [<sup>3</sup>H]MPP uptake by tetraethylammonium (TEA). Organic cation transporter 1 and 2 showed high affinity to TEA in comparison to organic cation transporter 3 [59]. The A498 cell line expressing high amounts of OCT3 showed a similar profile of [<sup>3</sup>H]MPP uptake inhibition by TEA as CHO cells stably transfected with OCT3. Therefore, we suggest is that organic cation transport in A498 cells is mediated by OCT3. The low expressing ACHN cells did not show significant uptake of [<sup>3</sup>H]MPP and no inhibition by TEA.

#### **4.4 Investigation the interaction of cytostatics with OCT3**

The main function of human OCT3 was connected with the transport of physiologically active substances such as adrenaline, noradrenaline, and histamine [128]. The impact of OCT3 on transport of cytostatics was not clear. It was shown that OCT3 can transport a number of platinum compounds such as carboplatin and oxaliplatin [54]. We performed a number of [<sup>3</sup>H]MPP uptake experiments to test for cytostatics which may be transported by OCT3. For our experiments we selected substances with structural similarity to OCT3 substrates. Among these compound, irinotecan, vincristine, and melphalan inhibited [<sup>3</sup>H]MPP uptake by more than 50%.

The inhibitory cytostatics were tested in competitive inhibition experiments to investigate their affinity and character of interaction with OCT3. After data analysis by Dixon plots it was found that irinotecan, vincristine and melphalan interact with OCT3 in a non-competitive manner. Dixon plots also provided the

possibility to calculate the affinity i.e. the  $K_i$  value of interaction. It was found that irinotecan and vincristine interacted with high affinity showing  $K_i$  value of 1.75  $\mu\text{M}$  and 17  $\mu\text{M}$ , respectively. Melphalan exhibited a medium affinity:  $K_i=366 \mu\text{M}$ . The obtained results suggest that the tested substances cannot occupy the substrate recognition centre and cannot be transported. However, deviations from the classical competitive type of inhibition were also observed for some pairs of substrate and inhibitors (Koepsell H., unpublished data) [59]. From this point of view we cannot exclude that the tested cytostatics are transported by OCT3.

#### **4.5 Investigation on the activity of ENTs in renal carcinoma cell lines**

Equilibrative nucleoside transporters are widely expressed in human body [21]. Special functions of ENTs are exchanges of nucleoside analogs. Renal carcinoma cell lines were found to have high expression levels of ENT 1 and 2 in comparison to concentrative nucleoside transporters (CNT). The expression profiles suggest that nucleoside transport is mainly dependent on ENT 1 and 2. It was shown that ENT1 prefers as substrates purine analogs such as guanine and adenosine [81]. ENT2 mainly transports pyrimidine analogs such as cytidine and thymidine [129]. Both transporters have high affinity to NBTI which is used as inhibitor for ENT transporters. Also both ENT1 and 2 interact with a number of cytostatics such as gemcitabine and cladribine [20]. Substrates which interact with ENT1 and 2 are shown in figure 4.2. To investigate the correlation between expression and activity of equilibrative nucleoside transporters we performed a series of uptake experiments with [ $^3\text{H}$ ]gemcitabine. For uptake experiments were chosen the LN78 cell line expressing high amounts of ENT1 and 2 and the A498 low expressing cell line. [ $^3\text{H}$ ]gemcitabine uptake was inhibited by thymidine, cytidine, and NBTI. The inhibition profile



suggested that nucleoside transport in LN78 cells is mediated by ENT1 and 2. Thus, renal carcinoma cells expressing high amounts of ENT1 and 2 may be susceptible to treatment with gemcitabine.

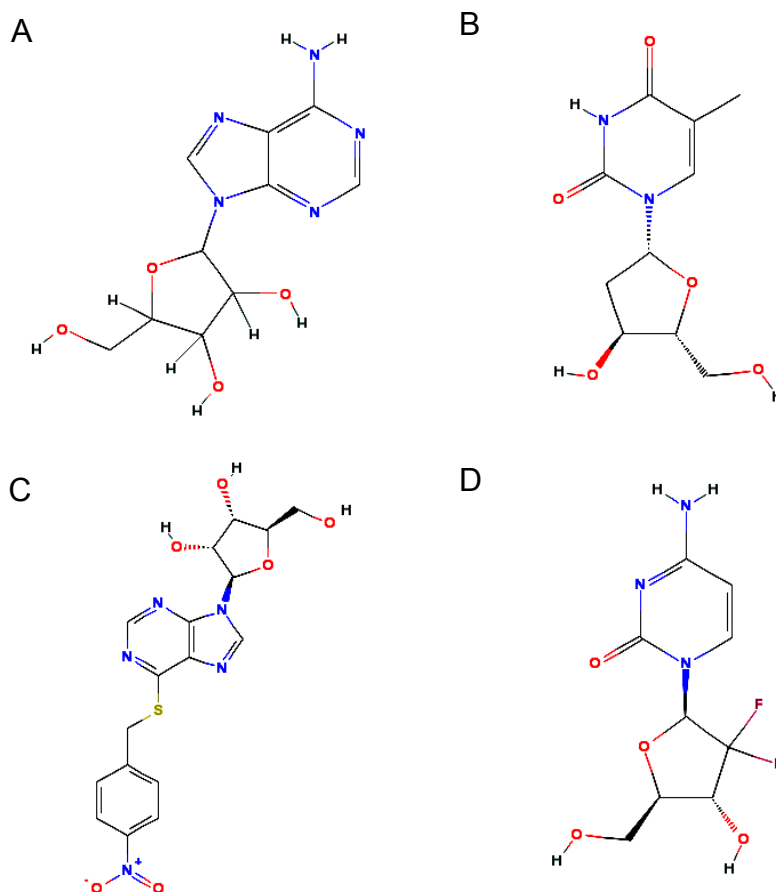


Figure 4.2 Substrates interacting with ENT1 and 2. A – adenosine, B – thymidine, C – NBTI, D - gemcitabine

#### 4.6 Transporter-mediated inhibition of thymidine incorporation by chlorambucil, bendamustin and melphalan

Finally, as a proof of principle, I tested whether the expression of a transporter influences cell growth in the presence of a cytostatic. [<sup>3</sup>H]thymidine incorporation was used as a rapid indicator for an inhibition of DNA synthesis by

cytostatics. The test was performed on HEK293 cells stably expressing either human OAT1 or human OAT3. Since these two transporters interact with organic anions, I chose the anionic cytostatics bendamustin and chlorambucil, both alkylating nitrogen mustard compounds. In OAT3-expressing cells the [<sup>3</sup>H]thymidine incorporation was somewhat more inhibited by bendamustin than in OAT1-expressing cells, and in both cells slightly more than in mock cells. These results suggest that the expression of OAT1 and OAT3 renders cells slightly more susceptible to bendamustine. Chlorambucil, on the other hand, inhibited [<sup>3</sup>H]thymidine incorporation considerably more in OAT1-expressing cells than in mock cells and OAT3-expressing cells. Thus, OAT1 makes cells more sensitive to chlorambucil.

To evaluate the cytotoxic effect of melphalan on OCT3 expressing cells we also chose [<sup>3</sup>H]thymidine incorporation as a method. After uptake of melphalan into cells it binds to –NH<sub>2</sub> and -SH groups of proteins or nucleic acids [130]. It was shown that the mustard residue interacts with the γ-phosphate group of nucleoside triphosphates and produces mustard-nucleoside derivatives with possess toxic effects [131]. OCT3 expressing CHO cells showed a correlation between melphalan concentration and the inhibition of [<sup>3</sup>H]thymidine incorporation. To prove that the cytotoxic effect of melphalan is dependent on OCT3 activity we inhibited melphalan uptake by 2 mM of TEA. OCT3 expressing cells which were treated by a combination of melphalan and TEA showed less inhibition of [<sup>3</sup>H]thymidine incorporation in comparison to those treated with only melphalan.

To test the possibility that melphalan can be used for treatment renal carcinomas expressing OCT3, we performed similar experiments with renal carcinoma cell lines. From my previous investigations on expression and function of OCT3 in RCC lines I selected A498 with high expression of OCT3 and ACHN as a non-expressing cell line. Both cell lines were also tested for the expression of the L-amino acid transporters 1 and 2 which mediate melphalan

uptake. A498 and ACHN cell lines showed high expression levels for LAT1 and low expression levels for LAT2.

Melphalan sensitivity tests revealed that A498 cells are more sensitive than ACHN, but sensitivity was observed for higher melphalan concentration. At high melphalan concentrations, both cell lines showed similar [<sup>3</sup>H]thymidine incorporation. We suggest that the sensitivity to melphalan is dependent on two transporter system, OCT3 and LAT1, which work independently. OCT3 can transport at low concentrations of melphalan with high efficiency, whereas LAT1 contributed at high concentrations of melphalan. The cytotoxic effect of melphalan was not significantly inhibited by TEA. This phenomenon can be explained by melphalan transport by LAT1 which is not inhibited by TEA.

#### **4.7 Transporter mediated-cytotoxic activity of irinotecan**

Irinotecan was obtained by modification of SN38 (camptotecin) which is a strong inhibitor of topoisomerase I. This cytostatic is used for the treatment of the colorectal cancer as part of the cytostatics combination FOLFIRI [132]. On the other hand it was shown that the expression of OCT3 is present in many tested colorectal cancer samples [11]. Topoisomerase I plays an important role in cell cycle and relaxed secondary structures of DNA [97]. In general, topoisomerase I activity is important for gene translation [133]. SN38 inactivates topoisomerase I and the enzyme is locked on DNA. [100]. The formed complexes are blocking DNA duplication and RNA translation. The SN38 treatment inhibits the expression of many genes and makes cells more sensitive to other cytostatics. Irinotecan is a positively charged substance which has a partial structural similarity to MPP. After transport into the cell, irinotecan is converted to SN38 by hydrolysis. SN38 is inactivated by glucuronidation [97]. Irinotecan cytotoxic activity is dependent on the concentration of the active SN38 product inside the cells. The concentration of SN38 is dependent on

activities of hydrolase, UDP-glucuronosyltransferase, and MDR1, which export SN38. I tried to investigate the role of OCT3 and MDR1 on irinotecan cytotoxicity and I used a combination of irinotecan with verapamil. Verapamil is a potent inhibitor of MDR1 [134]. MDR1 expression was detected in CHO cells. It was found that CHO stably expressing OCT3 cells treated irinotecan and verapamil had a lower viability in comparison to non-expressing CHO cells treated only with irinotecan. This proves the importance of MDR1 for chemoresistance to irinotecan [135]. But the renal carcinoma cell line A498 with high expression of OCT3 was not significantly inhibited by irinotecan in comparison to non-expressing ACHN cell line. As mentioned before, cytotoxic activity of irinotecan is dependent on three processes. Possibly, UDP-glucuronosyltransferase activity was higher in RCC lines in comparison to CHO cells.

#### **4.8 Transporter mediated cytotoxic activity of vincristine**

Vincristine is a potent cytostatic which is used for the treatment of blood cancers such as non Hodgkin's lymphoma, and lymphoblastic leukemia [136-138]. The main intracellular target for vincristine is the mitotic spindle included in their structure tubulin. Vincristine binds to tubulin molecules and prevents their polymerization. After vincristine treatment, cells cannot divide and this leads to cell death by apoptosis or to producing artificial caryotypes [139, 140]. Vincristine possesses a weak positive charge and can be transported by OCT3. From my data I suggest that vincristine is more toxic in comparison to irinotecan and melphalan. A possible reason is the high affinity to tubulin, the resulting complexes have a low constant of dissociation. After treatment, cells cannot excrete or metabolize bound to tubulin vincristine, one way for surviving is exchange of affected tubulin molecules by *de novo* protein synthesis. Additional treatment vincristine with verapamil amplified the cytotoxic effect of vincristine.

This cytostatic effect was only slightly reversed by inhibitors of OCT3. This finding suggests that even low amounts of vincristine disturb the microtubule net in an irreversible manner. One pronouncing side effect of vincristine is neuropathy [141]. This side effect could be due to OCT3 mediated transport, since OCT3 is expressed in the central neural system.

#### **4.9 Conclusions and outlook**

In the present study I investigate the dependence of cytostatic activities on influx transporters expressed in renal carcinoma cell lines. These cell lines exhibited a variable profile of influx and efflux transporters. For example I found that the expression of tissue-specific transporters such as OAT1, OAT2, OAT3, OCT1 and OCT2 was decreased. In three out of five tested RCC lines, a high expression of the organic cation transporter 3 was observed. These results allow for the following conclusions. First, we cannot treat renal carcinomas by cytostatics which interact with OATs such as chlorambucil, bendamustin and methotrexate. Second, expression of OCT3 gives the possibility to select specific cytostatics which are transported by OCT3. Third, I found an interaction of irinotecan, melphalan and vincristine with OCT3. These cytostatics can be used for the treatment of renal carcinomas. On the other hand, the presence of efflux transporters like MDR1 and MRPs make tumor cells chemoresistant. Inhibitors of multidrug transporters can be used to overcome chemoresistance. But this treatment may produce side effects in normal tissues.

Since under the therapy a selection pressure is produced, tumor cells with yet another set of transporters may arise and expand. Hence, a re-testing of transporter expression may be needed before applying cytostatic therapy.

Taken together I have provided evidence for the expression of a number of transporters in renal carcinoma cells. Some of these transporters may be used

to target cytostatic drugs to the cancer cells and to partially overcome the chemoresistance. The next experiments to be performed will therefore test of the influence of cytostatics selected on the basis of transporter expression. I hope that in the future a tailored therapy can be delineated from transporter expression in tumor cells.

## 5. References

1. Martel, C.L. and P.N. Lara, *Renal cell carcinoma: current status and future directions*. Crit Rev Oncol Hematol, 2003. **45**(2): p. 177-90.
2. Amato, R.J., *Chemotherapy for renal cell carcinoma*. Semin Oncol, 2000. **27**(2): p. 177-86.
3. Zambrano, N.R., et al., *Histopathology and molecular genetics of renal tumors toward unification of a classification system*. J Urol, 1999. **162**(4): p. 1246-58.
4. Weiss, R.H. and P.Y. Lin, *Kidney cancer: identification of novel targets for therapy*. Kidney Int, 2006. **69**(2): p. 224-32.
5. Wright, S.H. and W.H. Dantzler, *Molecular and cellular physiology of renal organic cation and anion transport*. Physiol Rev, 2004. **84**(3): p. 987-1049.
6. Koepsell, H., *Polyspecific organic cation transporters: their functions and interactions with drugs*. Trends Pharmacol Sci, 2004. **25**(7): p. 375-81.
7. Otsuka, M., et al., *A human transporter protein that mediates the final excretion step for toxic organic cations*. Proc Natl Acad Sci U S A, 2005. **102**(50): p. 17923-8.
8. Burckhardt, B.C. and G. Burckhardt, *Transport of organic anions across the basolateral membrane of proximal tubule cells*. Rev Physiol Biochem Pharmacol, 2003. **146**: p. 95-158.
9. van Montfoort, J.E., et al., *Drug uptake systems in liver and kidney*. Curr Drug Metab, 2003. **4**(3): p. 185-211.
10. Russel, F.G., R. Masereeuw, and R.A. van Aabel, *Molecular aspects of renal anionic drug transport*. Annu Rev Physiol, 2002. **64**: p. 563-94.
11. Ciarimboli, G., et al., *Cisplatin nephrotoxicity is critically mediated via the human organic cation transporter 2*. Am J Pathol, 2005. **167**(6): p. 1477-84.

12. Okabe, M., et al., *Characterization of the organic cation transporter SLC22A16: a doxorubicin importer*. *Biochem Biophys Res Commun*, 2005. **333**(3): p. 754-62.
13. Briz, O., et al., *Carriers involved in targeting the cytostatic bile acid-cisplatin derivatives cis-diammine-chloro-cholyglycinate-platinum(II) and cis-diammine-bisursodeoxycholate-platinum(II) toward liver cells*. *Mol Pharmacol*, 2002. **61**(4): p. 853-60.
14. Hagenbuch, B. and P.J. Meier, *The superfamily of organic anion transporting polypeptides*. *Biochim Biophys Acta*, 2003. **1609**(1): p. 1-18.
15. Nozawa, T., et al., *Role of organic anion transporter OATP1B1 (OATP-C) in hepatic uptake of irinotecan and its active metabolite, 7-ethyl-10-hydroxycamptothecin: in vitro evidence and effect of single nucleotide polymorphisms*. *Drug Metab Dispos*, 2005. **33**(3): p. 434-9.
16. Adachi, H., et al., *Molecular characterization of human and rat organic anion transporter OATP-D*. *Am J Physiol Renal Physiol*, 2003. **285**(6): p. F1188-97.
17. Aymerich, I., et al., *The concentrative nucleoside transporter family (SLC28): new roles beyond salvage?* *Biochem Soc Trans*, 2005. **33**(Pt 1): p. 216-9.
18. Pastor-Anglada, M., et al., *Nucleoside transporters in chronic lymphocytic leukaemia*. *Leukemia*, 2004. **18**(3): p. 385-93.
19. Nagai, K., K. Nagasawa, and S. Fujimoto, *Uptake of the anthracycline pirarubicin into mouse M5076 ovarian sarcoma cells via a sodium-dependent nucleoside transport system*. *Cancer Chemother Pharmacol*, 2005. **55**(3): p. 222-30.
20. Garcia-Manteiga, J., et al., *Nucleoside transporter profiles in human pancreatic cancer cells: role of hCNT1 in 2',2'-difluorodeoxycytidine-induced cytotoxicity*. *Clin Cancer Res*, 2003. **9**(13): p. 5000-8.
21. Baldwin, S.A., et al., *The equilibrative nucleoside transporter family, SLC29*. *Pflugers Arch*, 2004. **447**(5): p. 735-43.



22. Kanai, Y. and H. Endou, *Functional properties of multispecific amino acid transporters and their implications to transporter-mediated toxicity*. J Toxicol Sci, 2003. **28**(1): p. 1-17.
23. Wagner, C.A., F. Lang, and S. Broer, *Function and structure of heterodimeric amino acid transporters*. Am J Physiol Cell Physiol, 2001. **281**(4): p. C1077-93.
24. Uchino, H., et al., *Transport of amino acid-related compounds mediated by L-type amino acid transporter 1 (LAT1): insights into the mechanisms of substrate recognition*. Mol Pharmacol, 2002. **61**(4): p. 729-37.
25. Halestrap, A.P. and D. Meredith, *The SLC16 gene family-from monocarboxylate transporters (MCTs) to aromatic amino acid transporters and beyond*. Pflugers Arch, 2004. **447**(5): p. 619-28.
26. Pierre, K. and L. Pellerin, *Monocarboxylate transporters in the central nervous system: distribution, regulation and function*. J Neurochem, 2005. **94**(1): p. 1-14.
27. Chatton, J.Y., et al., *Insights into the mechanisms of ifosfamide encephalopathy: drug metabolites have agonistic effects on alpha-amino-3-hydroxy-5-methyl-4-isoxazolepropionic acid (AMPA)/kainate receptors and induce cellular acidification in mouse cortical neurons*. J Pharmacol Exp Ther, 2001. **299**(3): p. 1161-8.
28. Ganapathy, V., S.B. Smith, and P.D. Prasad, *SLC19: the folate/thiamine transporter family*. Pflugers Arch, 2004. **447**(5): p. 641-6.
29. Sirotnak, F.M. and B. Tolner, *Carrier-mediated membrane transport of folates in mammalian cells*. Annu Rev Nutr, 1999. **19**: p. 91-122.
30. Palacin, M. and Y. Kanai, *The ancillary proteins of HATs: SLC3 family of amino acid transporters*. Pflugers Arch, 2004. **447**(5): p. 490-4.
31. Bridges, C.C., et al., *Structure, function, and regulation of human cystine/glutamate transporter in retinal pigment epithelial cells*. Invest Ophthalmol Vis Sci, 2001. **42**(1): p. 47-54.
32. Closs, E.I., et al., *Structure and function of cationic amino acid transporters (CATs)*. J Membr Biol, 2006. **213**(2): p. 67-77.

33. Mann, G.E., D.L. Yudilevich, and L. Sobrevia, *Regulation of amino acid and glucose transporters in endothelial and smooth muscle cells*. *Physiol Rev*, 2003. **83**(1): p. 183-252.
34. Kizhatil, K. and L.M. Albritton, *System y<sup>+</sup> localizes to different membrane subdomains in the basolateral plasma membrane of epithelial cells*. *Am J Physiol Cell Physiol*, 2002. **283**(6): p. C1784-94.
35. Lin, J., et al., *L-type amino acid transporter-1 overexpression and melphalan sensitivity in Barrett's adenocarcinoma*. *Neoplasia*, 2004. **6**(1): p. 74-84.
36. Lee, A., P.A. Dawson, and D. Markovich, *NaSi-1 and Sat-1: structure, function and transcriptional regulation of two genes encoding renal proximal tubular sulfate transporters*. *Int J Biochem Cell Biol*, 2005. **37**(7): p. 1350-6.
37. Lee, H.J., et al., *Modulation of sulfate renal transport by alterations in cell membrane fluidity*. *J Pharm Sci*, 1999. **88**(10): p. 976-80.
38. Markovich, D. and P.S. Aronson, *Specificity and regulation of renal sulfate transporters*. *Annu Rev Physiol*, 2007. **69**: p. 361-75.
39. Peng, L.X., et al., *[Na<sup>+</sup>/dicarboxylate cotransporter expression changed with aging in basolateral membrane of the renal tubular epithelial cells]*. *Zhonghua Yi Xue Za Zhi*, 2003. **83**(2): p. 123-7.
40. Sepponen, K., et al., *Expression of CD147 and monocarboxylate transporters MCT1, MCT2 and MCT4 in porcine small intestine and colon*. *Vet J*, 2007. **174**(1): p. 122-8.
41. Gill, R.K., et al., *Expression and membrane localization of MCT isoforms along the length of the human intestine*. *Am J Physiol Cell Physiol*, 2005. **289**(4): p. C846-52.
42. Schron, C.M., C. Washington, Jr., and B.L. Blitzer, *The transmembrane pH gradient drives uphill folate transport in rabbit jejunum. Direct evidence for folate/hydroxyl exchange in brush border membrane vesicles*. *J Clin Invest*, 1985. **76**(5): p. 2030-3.

43. Moscow, J.A., et al., *Reduced folate carrier gene (RFC1) expression and anti-folate resistance in transfected and non-selected cell lines*. Int J Cancer, 1997. **72**(1): p. 184-90.
44. Takemura, Y., H. Kobayashi, and H. Miyachi, *Antifolate resistance and its circumvention by new analogues*. Hum Cell, 2001. **14**(3): p. 185-202.
45. Eudy, J.D., et al., *Identification and characterization of the human and mouse SLC19A3 gene: a novel member of the reduced folate family of micronutrient transporter genes*. Mol Genet Metab, 2000. **71**(4): p. 581-90.
46. Kullak-Ublick, G.A., et al., *Molecular and functional characterization of an organic anion transporting polypeptide cloned from human liver*. Gastroenterology, 1995. **109**(4): p. 1274-82.
47. Tamai, I., et al., *Molecular identification and characterization of novel members of the human organic anion transporter (OATP) family*. Biochem Biophys Res Commun, 2000. **273**(1): p. 251-60.
48. Marzolini, C., R.G. Tirona, and R.B. Kim, *Pharmacogenomics of the OATP and OAT families*. Pharmacogenomics, 2004. **5**(3): p. 273-82.
49. Choudhuri, S., et al., *Constitutive expression of various xenobiotic and endobiotic transporter mRNAs in the choroid plexus of rats*. Drug Metab Dispos, 2003. **31**(11): p. 1337-45.
50. Suzuki, T., et al., *Identification and characterization of novel rat and human gonad-specific organic anion transporters*. Mol Endocrinol, 2003. **17**(7): p. 1203-15.
51. Kawai, J., et al., *Functional annotation of a full-length mouse cDNA collection*. Nature, 2001. **409**(6821): p. 685-90.
52. Gorboulev, V., et al., *Cloning and characterization of two human polyspecific organic cation transporters*. DNA Cell Biol, 1997. **16**(7): p. 871-81.
53. Koepsell, H., B.M. Schmitt, and V. Gorboulev, *Organic cation transporters*. Rev Physiol Biochem Pharmacol, 2003. **150**: p. 36-90.

54. Zhang, S., et al., *Organic cation transporters are determinants of oxaliplatin cytotoxicity*. *Cancer Res*, 2006. **66**(17): p. 8847-57.
55. Asaka, J., et al., *Characterization of the Basal promoter element of human organic cation transporter 2 gene*. *J Pharmacol Exp Ther*, 2007. **321**(2): p. 684-9.
56. Karbach, U., et al., *Localization of organic cation transporters OCT1 and OCT2 in rat kidney*. *Am J Physiol Renal Physiol*, 2000. **279**(4): p. F679-87.
57. Horvath, G., et al., *Norepinephrine transport by the extraneuronal monoamine transporter in human bronchial arterial smooth muscle cells*. *Am J Physiol Lung Cell Mol Physiol*, 2003. **285**(4): p. L829-37.
58. Volk, C., et al., *Different affinities of inhibitors to the outwardly and inwardly directed substrate binding site of organic cation transporter 2*. *Mol Pharmacol*, 2003. **64**(5): p. 1037-47.
59. Koepsell, H., K. Lips, and C. Volk, *Polyspecific organic cation transporters: structure, function, physiological roles, and biopharmaceutical implications*. *Pharm Res*, 2007. **24**(7): p. 1227-51.
60. Yokoo, S., et al., *Differential contribution of organic cation transporters, OCT2 and MATE1, in platinum agent-induced nephrotoxicity*. *Biochem Pharmacol*, 2007. **74**(3): p. 477-87.
61. Lamhonwah, A.M., et al., *Expression patterns of the organic cation/carnitine transporter family in adult murine brain*. *Brain Dev*, 2008. **30**(1): p. 31-42.
62. Crljen, V., et al., *Immunocytochemical characterization of the incubated rat renal cortical slices*. *Pflugers Arch*, 2005. **450**(4): p. 269-79.
63. Hilgendorf, C., et al., *Expression of thirty-six drug transporter genes in human intestine, liver, kidney, and organotypic cell lines*. *Drug Metab Dispos*, 2007. **35**(8): p. 1333-40.
64. Nozaki, Y., et al., *Characterization of the uptake of organic anion transporter (OAT) 1 and OAT3 substrates by human kidney slices*. *J Pharmacol Exp Ther*, 2007. **321**(1): p. 362-9.

65. Miller, D.S., *Nucleoside phosphonate interactions with multiple organic anion transporters in renal proximal tubule*. J Pharmacol Exp Ther, 2001. **299**(2): p. 567-74.
66. Simonson, G.D., et al., *Molecular cloning and characterization of a novel liver-specific transport protein*. J Cell Sci, 1994. **107 ( Pt 4)**: p. 1065-72.
67. Sekine, T., et al., *Identification of multispecific organic anion transporter 2 expressed predominantly in the liver*. FEBS Lett, 1998. **429**(2): p. 179-82.
68. Burckhardt, G. and N.A. Wolff, *Structure of renal organic anion and cation transporters*. Am J Physiol Renal Physiol, 2000. **278**(6): p. F853-66.
69. Kusuhara, H., et al., *Molecular cloning and characterization of a new multispecific organic anion transporter from rat brain*. J Biol Chem, 1999. **274**(19): p. 13675-80.
70. Cha, S.H., et al., *Molecular cloning and characterization of multispecific organic anion transporter 4 expressed in the placenta*. J Biol Chem, 2000. **275**(6): p. 4507-12.
71. Pastor-Anglada, M., et al., *Concentrative nucleoside transporters (CNTs) in epithelia: from absorption to cell signaling*. J Physiol Biochem, 2007. **63**(1): p. 97-110.
72. Duflot, S., et al., *Concentrative nucleoside transporter (rCNT1) is targeted to the apical membrane through the hepatic transcytotic pathway*. Exp Cell Res, 2002. **281**(1): p. 77-85.
73. Dresser, M.J., et al., *Electrophysiological analysis of the substrate selectivity of a sodium-coupled nucleoside transporter (rCNT1) expressed in Xenopus laevis oocytes*. Drug Metab Dispos, 2000. **28**(9): p. 1135-40.
74. Wang, J., et al., *Na(+)-dependent purine nucleoside transporter from human kidney: cloning and functional characterization*. Am J Physiol, 1997. **273**(6 Pt 2): p. F1058-65.

75. Fernandez-Veledo, S., et al., *Bile acids alter the subcellular localization of CNT2 (concentrative nucleoside cotransporter) and increase CNT2-related transport activity in liver parenchymal cells*. *Biochem J*, 2006. **395**(2): p. 337-44.
76. Ritzel, M.W., et al., *Molecular identification and characterization of novel human and mouse concentrative Na<sup>+</sup>-nucleoside cotransporter proteins (hCNT3 and mCNT3) broadly selective for purine and pyrimidine nucleosides (system cib)*. *J Biol Chem*, 2001. **276**(4): p. 2914-27.
77. Griffiths, M., et al., *Cloning of a human nucleoside transporter implicated in the cellular uptake of adenosine and chemotherapeutic drugs*. *Nat Med*, 1997. **3**(1): p. 89-93.
78. Handa, M., et al., *Cloning of a novel isoform of the mouse NBMPR-sensitive equilibrative nucleoside transporter (ENT1) lacking a putative phosphorylation site*. *Gene*, 2001. **262**(1-2): p. 301-7.
79. Choi, D.S., et al., *Genomic organization and expression of the mouse equilibrative, nitrobenzylthioinosine-sensitive nucleoside transporter 1 (ENT1) gene*. *Biochem Biophys Res Commun*, 2000. **277**(1): p. 200-8.
80. Griffiths, M., et al., *Molecular cloning and characterization of a nitrobenzylthioinosine-insensitive (ei) equilibrative nucleoside transporter from human placenta*. *Biochem J*, 1997. **328 ( Pt 3)**: p. 739-43.
81. Ward, J.L., et al., *Kinetic and pharmacological properties of cloned human equilibrative nucleoside transporters, ENT1 and ENT2, stably expressed in nucleoside transporter-deficient PK15 cells. Ent2 exhibits a low affinity for guanosine and cytidine but a high affinity for inosine*. *J Biol Chem*, 2000. **275**(12): p. 8375-81.
82. Clarke, M.L., et al., *The role of membrane transporters in cellular resistance to anticancer nucleoside drugs*. *Cancer Treat Res*, 2002. **112**: p. 27-47.
83. Crawford, C.R., et al., *Cloning of the human equilibrative, nitrobenzylmercaptapurine riboside (NBMPR)-insensitive nucleoside*

- transporter ei by functional expression in a transport-deficient cell line. J Biol Chem*, 1998. **273**(9): p. 5288-93.
84. Williams, J.B. and A.A. Lanahan, *A mammalian delayed-early response gene encodes HNP36, a novel, conserved nucleolar protein. Biochem Biophys Res Commun*, 1995. **213**(1): p. 325-33.
  85. Mangravite, L.M., G. Xiao, and K.M. Giacomini, *Localization of human equilibrative nucleoside transporters, hENT1 and hENT2, in renal epithelial cells. Am J Physiol Renal Physiol*, 2003. **284**(5): p. F902-10.
  86. Hyde, R.J., et al., *The ENT family of eukaryote nucleoside and nucleobase transporters: recent advances in the investigation of structure/function relationships and the identification of novel isoforms. Mol Membr Biol*, 2001. **18**(1): p. 53-63.
  87. Dean, M., A. Rzhetsky, and R. Allikmets, *The human ATP-binding cassette (ABC) transporter superfamily. Genome Res*, 2001. **11**(7): p. 1156-66.
  88. Chen, J. and J. Stubbe, *Bleomycins: towards better therapeutics. Nat Rev Cancer*, 2005. **5**(2): p. 102-12.
  89. Dedon, P.C., *The chemical toxicology of 2-deoxyribose oxidation in DNA. Chem Res Toxicol*, 2008. **21**(1): p. 206-19.
  90. Harrap, K.R., *Anti-folate toxicity and its reversal. Biochem Soc Trans*, 1976. **4**(5): p. 856-9.
  91. Gisondi, P., et al., *Folic acid in general medicine and dermatology. J Dermatolog Treat*, 2007. **18**(3): p. 138-46.
  92. Bonomi, P.D., *Therapeutic advances in second-line treatment of advanced non-small-cell lung cancer. Clin Lung Cancer*, 2004. **6**(3): p. 154-61.
  93. Dumez, H., et al., *Human red blood cells: rheological aspects, uptake, and release of cytotoxic drugs. Crit Rev Clin Lab Sci*, 2004. **41**(2): p. 159-88.

94. Liao, Z., et al., *Reduced expression of DNA topoisomerase I in SF295 human glioblastoma cells selected for resistance to homocamptothecin and diflomotecan*. Mol Pharmacol, 2008. **73**(2): p. 490-7.
95. Marsh, S., *Pharmacogenetics of colorectal cancer*. Expert Opin Pharmacother, 2005. **6**(15): p. 2607-16.
96. Engel, R., et al., *The cytoplasmic trafficking of DNA topoisomerase IIalpha correlates with etoposide resistance in human myeloma cells*. Exp Cell Res, 2004. **295**(2): p. 421-31.
97. Stewart, C.F., *Topoisomerase I interactive agents*. Cancer Chemother Biol Response Modif, 2001. **19**: p. 85-128.
98. Anyanwutaku, I.O., et al., *Activities of novel nonglycosidic epipodophyllotoxins in etoposide-sensitive and -resistant variants of human KB cells, P-388 cells, and in vivo multidrug-resistant murine leukemia cells*. Mol Pharmacol, 1996. **49**(4): p. 721-6.
99. Coiffier, B., *New treatment strategies in lymphomas: aggressive lymphomas*. Ann Hematol, 2004. **83 Suppl 1**: p. S73-4.
100. Mizutani, H., *[Mechanism of DNA damage and apoptosis induced by anticancer drugs through generation of reactive oxygen species]*. Yakugaku Zasshi, 2007. **127**(11): p. 1837-42.
101. Marsh, S. and H.L. McLeod, *Pharmacogenetics and oncology treatment for breast cancer*. Expert Opin Pharmacother, 2007. **8**(2): p. 119-27.
102. Sugimoto, Y., et al., *Breast cancer resistance protein: molecular target for anticancer drug resistance and pharmacokinetics/pharmacodynamics*. Cancer Sci, 2005. **96**(8): p. 457-65.
103. Kim, D.W., *[Real time quantitative PCR]*. Exp Mol Med, 2001. **33**(1 Suppl): p. 101-9.
104. Muller, P.Y., et al., *Processing of gene expression data generated by quantitative real-time RT-PCR*. Biotechniques, 2002. **32**(6): p. 1372-4, 1376, 1378-9.



105. Ramakers, C., et al., *Assumption-free analysis of quantitative real-time polymerase chain reaction (PCR) data*. *Neurosci Lett*, 2003. **339**(1): p. 62-6.
106. Enomoto, A., et al., *Interaction of human organic anion transporters 2 and 4 with organic anion transport inhibitors*. *J Pharmacol Exp Ther*, 2002. **301**(3): p. 797-802.
107. Dresser, M.J., M.K. Leabman, and K.M. Giacomini, *Transporters involved in the elimination of drugs in the kidney: organic anion transporters and organic cation transporters*. *J Pharm Sci*, 2001. **90**(4): p. 397-421.
108. Ferrari, S., et al., *Prospective evaluation of renal function in pediatric and adult patients treated with high-dose ifosfamide, cisplatin and high-dose methotrexate*. *Anticancer Drugs*, 2005. **16**(7): p. 733-8.
109. Shang, T., et al., *1-Methyl-4-phenylpyridinium accumulates in cerebellar granule neurons via organic cation transporter 3*. *J Neurochem*, 2003. **85**(2): p. 358-67.
110. Ludwig, T. and H. Oberleithner, *Platinum complex toxicity in cultured renal epithelia*. *Cell Physiol Biochem*, 2004. **14**(4-6): p. 431-40.
111. Arany, I. and R.L. Safirstein, *Cisplatin nephrotoxicity*. *Semin Nephrol*, 2003. **23**(5): p. 460-4.
112. Mikkaichi, T., et al., *The organic anion transporter (OATP) family*. *Drug Metab Pharmacokinet*, 2004. **19**(3): p. 171-9.
113. Hagenbuch, B. and P. Dawson, *The sodium bile salt cotransport family SLC10*. *Pflugers Arch*, 2004. **447**(5): p. 566-70.
114. Podgorska, M., K. Kocbuch, and T. Pawelczyk, *Recent advances in studies on biochemical and structural properties of equilibrative and concentrative nucleoside transporters*. *Acta Biochim Pol*, 2005. **52**(4): p. 749-58.
115. Segawa, H., et al., *Identification and functional characterization of a Na<sup>+</sup>-independent neutral amino acid transporter with broad substrate selectivity*. *J Biol Chem*, 1999. **274**(28): p. 19745-51.

116. Killian, D.M. and P.J. Chikhale, *A bioreversible prodrug approach designed to shift mechanism of brain uptake for amino-acid-containing anticancer agents*. J Neurochem, 2001. **76**(4): p. 966-74.
117. Fei, Y.J., K. Inoue, and V. Ganapathy, *Structural and functional characteristics of two sodium-coupled dicarboxylate transporters (ceNaDC1 and ceNaDC2) from Caenorhabditis elegans and their relevance to life span*. J Biol Chem, 2003. **278**(8): p. 6136-44.
118. Bonen, A., M. Heynen, and H. Hatta, *Distribution of monocarboxylate transporters MCT1-MCT8 in rat tissues and human skeletal muscle*. Appl Physiol Nutr Metab, 2006. **31**(1): p. 31-9.
119. Soares-da-Silva, P. and M.P. Serrao, *Apical and basolateral 4F2hc and the amino acid exchange of L-DOPA in renal LLC-PK1 cells*. Amino Acids, 2005. **29**(3): p. 213-9.
120. Halestrap, A.P. and N.T. Price, *The proton-linked monocarboxylate transporter (MCT) family: structure, function and regulation*. Biochem J, 1999. **343 Pt 2**: p. 281-99.
121. Eladari, D., et al., *Polarized expression of different monocarboxylate transporters in rat medullary thick limbs of Henle*. J Biol Chem, 1999. **274**(40): p. 28420-6.
122. Chiao, J.H., et al., *Ligand-directed immunoaffinity purification and properties of the one-carbon, reduced folate transporter. Interspecies immuno-cross-reactivity and expression of the native transporter in murine and human tumor cells and their transport-altered variants*. J Biol Chem, 1995. **270**(50): p. 29698-704.
123. Nishimura, M. and S. Naito, *Tissue-specific mRNA expression profiles of human ATP-binding cassette and solute carrier transporter superfamilies*. Drug Metab Pharmacokinet, 2005. **20**(6): p. 452-77.
124. Smith, P.C., et al., *ATP binding to the motor domain from an ABC transporter drives formation of a nucleotide sandwich dimer*. Mol Cell, 2002. **10**(1): p. 139-49.

125. Han, B. and J.T. Zhang, *Multidrug resistance in cancer chemotherapy and xenobiotic protection mediated by the half ATP-binding cassette transporter ABCG2*. *Curr Med Chem Anticancer Agents*, 2004. **4**(1): p. 31-42.
126. Suzuki, T., K. Nishio, and S. Tanabe, *The MRP family and anticancer drug metabolism*. *Curr Drug Metab*, 2001. **2**(4): p. 367-77.
127. Hayer-Zillgen, M., M. Bruss, and H. Bonisch, *Expression and pharmacological profile of the human organic cation transporters hOCT1, hOCT2 and hOCT3*. *Br J Pharmacol*, 2002. **136**(6): p. 829-36.
128. Zhang, X., et al., *Relative contribution of OAT and OCT transporters to organic electrolyte transport in rabbit proximal tubule*. *Am J Physiol Renal Physiol*, 2004. **287**(5): p. F999-1010.
129. Yao, S.Y., et al., *Transport of antiviral 3'-deoxy-nucleoside drugs by recombinant human and rat equilibrative, nitrobenzylthioinosine (NBMPR)-insensitive (ENT2) nucleoside transporter proteins produced in Xenopus oocytes*. *Mol Membr Biol*, 2001. **18**(2): p. 161-7.
130. Sunters, A., et al., *The cytotoxicity, DNA crosslinking ability and DNA sequence selectivity of the aniline mustards melphalan, chlorambucil and 4-[bis(2-chloroethyl)amino] benzoic acid*. *Biochem Pharmacol*, 1992. **44**(1): p. 59-64.
131. Grachev, M.A., A.A. Mustaev, and S.I. Oshevski, *A route to RNA with an alkylating group at the 5'-triphosphate residue*. *Nucleic Acids Res*, 1980. **8**(15): p. 3413-26.
132. Lee, M.A., et al., *Irinotecan, continuous 5-fluorouracil, and low dose of leucovorin (modified FOLFIRI) as first line of therapy in recurrent or metastatic colorectal cancer*. *Korean J Intern Med*, 2005. **20**(3): p. 205-9.
133. Li, S.J. and J. Gu, *[DNA topoisomerase and telomerase activity with relation to multi-drug resistance in leukemia--review]*. *Zhongguo Shi Yan Xue Ye Xue Za Zhi*, 2007. **15**(1): p. 207-10.
134. Perez-Tomas, R., *Multidrug resistance: retrospect and prospects in anti-cancer drug treatment*. *Curr Med Chem*, 2006. **13**(16): p. 1859-76.

135. Toffoli, G., et al., *Pharmacogenetics of irinotecan*. *Curr Med Chem Anticancer Agents*, 2003. **3**(3): p. 225-37.
136. Marcus, R. and A. Hagenbeek, *The therapeutic use of rituximab in non-Hodgkin's lymphoma*. *Eur J Haematol Suppl*, 2007(67): p. 5-14.
137. Coiffier, B., *Rituximab therapy in malignant lymphoma*. *Oncogene*, 2007. **26**(25): p. 3603-13.
138. Ng, A.K., *Diffuse large B-cell lymphoma*. *Semin Radiat Oncol*, 2007. **17**(3): p. 169-75.
139. Islam, M.N. and M.N. Iskander, *Microtubulin binding sites as target for developing anticancer agents*. *Mini Rev Med Chem*, 2004. **4**(10): p. 1077-104.
140. Zhou, X.J. and R. Rahmani, *Preclinical and clinical pharmacology of vinca alkaloids*. *Drugs*, 1992. **44 Suppl 4**: p. 1-16; discussion 66-9.
141. McGuire, S.A., S.M. Gospe, Jr., and G. Dahl, *Acute vincristine neurotoxicity in the presence of hereditary motor and sensory neuropathy type I*. *Med Pediatr Oncol*, 1989. **17**(6): p. 520-3.

## Addition 1

Symbol		Alias	Function	Expression	Mendelian disease
ABCA	ABCA1	ABC1	Cholesterol efflux into HDL	ubiquitous	Tangier disease, FHDLD
	ABCA2	ABC2	Drug resistance	Brain	
	ABCA3	ABC3, ABCC	Surfactant Excretion?	Lung	
	ABCA4	ABCR	N-retinylidene-PE efflux	photoreceptors	Stargardt/FFM, RP, CRD, CD
	ABCA5			Muscle, heart, testes	
	ABCA6			Liver	
	ABCA7			Spleen, thymus	
	ABCA8			Ovary	
	ABCA9			Heart	
	ABCA10			Muscle, heart	
	ABCA12			Stomach	
	ABCA 13			Ovary, kidney, thymus	
	ABCA17P			ubiquitous	
ABCB	ABCB1	PGY1, MDR	Multidrug resistance	Adrenal, kidney, brain	Ivermectine susceptibility
	ABCB2	TAP1	Peptide transport	All cells	Immune deficiency
	ABCB3	TAP2	Peptide transport	All cells	Immune deficiency
	ABCB4	PGY3	PC transport	Liver	PFIC3

	ABCB5			ubiquitous	
	ABCB6	MTABC3	Iron transport, Fe/S transport	Mitochondria	
	ABCB7	ABC7		Mitochondria	XLSA/A
	ABCB8	MABC1		Mitochondria	
	ABCB9			Heart, brain	
	ABCB10	MTABC2		Mitochondria	
	ABCB11	SPGP	Bile salt transport	Liver	PFIC2
ABCC	ABCC1	MRP1	Drug resistance	Lung, testes	
	ABCC2	MRP2	Organic anion efflux	Liver	Dubin-Jonson syndrom
	ABCC3	MRP3	Drug resistance	Lung, intestine, liver	
	ABCC4	MRP4	Nucleoside transport	Prostate	
	ABCC5	MRP5	Nucleoside transport	Ubiquitous	
	ABCC6	MRP6		Kidney, liver	Pseudoxantoma elasticum
	ABCC7	CFTR	Chloride ion channel	Exocrine tissue	Cystic Fibrosis, CBAVD
	ABCC8	SUR	Sulphonylurea receptor	Pancreas	FPHHI
	ABCC9	SUR2	K(ATP)channel regulation	Heart, muscle	
	ABCC10	MRP7		Low in all tissues	
	ABCC11			Low in all tissues	
	ABCC12			Low in all tissues	

ABCD	ABCD1	ALD	VLCFA transport regulation	Peroxisomes	
	ABCD2	ALD1, ALDR		Peroxisomes	
	ABCD3	PXMP1, PMP70		Peroxisomes	
	ABCD4	PMP69, P70R		Peroxisomes	
ABCE	ABCE1	OABP, RNS4I	Oligoadenylate binding protein	Ovary, testis, spleen	
ABCF	ABCF1	ABC50		Ubiquitous	
	ABCF2			Ubiquitous	
	ABCF3			Ubiquitous	
ABCG	ABCG1	ABC8, White, ABCP, MXP	Cholesterol transport	Ubiquitous	
	ABCG2	BCRP	Toxin efflux, drug resistance	Placenta, intestine	
	ABCG4	White2		Liver	
	ABCG5	White3	Sterol transport	Liver, intestine	Sitosterolemia
	ABCG8		Sterol transport	Liver, intestine	Sitosterolemia

Table 1.2 ABC transporter superfamily characteristics

## **Acknowledgments**

This work was supported by the Deutsche Forschungsgemeinschaft, GRK 1034.

I would like to express my gratitude to following people

Professor Burckhardt, head of the department, and my Ph.D. adviser, for support and direction

My supervisor Dr. Yohannes Hagos for her professional and personal help and care

Dr. W.Kramer and Prof. Dr.S.Hoyer-Fender for acting as Referent and Korreferent, respectively.

All my colleagues in the Abteilung Vegetative Physiologie und Pathophysiologie for their assistance and nice attitude, specially to Sören Petzke and Shivangi Gupta who have been always helpful and kind to me.

My wife Irina for love and personal support, and help with preparing thesis.

And I am always grateful to my parents for their love and support



## Lebenslauf

---

Name	Shnitsar
Vorname	Volodymyr
Geburtsdatum	18.03.1979
Geburtsort	Mostys'ka, Lviv region, Ukraine
Staatsangehörigkeit	Ukrainisch
Anschrift	Georg-August-Universität Abteilung Vegetative Physiologie und Pathophysiologie, Bereich Humanmedizin, Humboldtallee 23 D-37073 Göttingen, Germany
E-mail	shnitsar@gmail.com

### Schulbildung

1994-1996	Biological Kolledge, Tvirzha, Lviv region, Ukraine
-----------	--

### Studium

1996-2001	Specialist in Biochemistry (equivalent to Master)  Lviv national university, biological faculty
-----------	---

Jun 2005- Mar 2008	Doktorarbeit in der Abteilung Vegetative Physiologie, Zentrum Physiologie und Pathophysiologie, Georg-August- Universität Göttingen Title der Doktorarbeit: „Expression von polyspezifischen Transportern in renalen Tumoren und ihre Bedeutung für die Chemotherapie
--------------------	--

“

Jun 2005 – May 2008	Mitglied des Graduiertenkolleg 1034 (“The impact of inherited polymorphisms in oncology: from basic science to clinical application“)
---------------------	---

April 29 2008	Abgabe der vorliegenden Dissertation
---------------	--------------------------------------

Volodymyr Shnitsar

Göttingen 18.03.2008